Technische Universität München

Max-Planck-Institut für Quantenoptik

Quantum Information Processing with Atomic Ensembles and Light

Klemens Hammerer

Vollständiger Abdruck der von der Fakultät für Physik
der Technischen Universität München
zur Erlangung des akademischen Grades eines

Doktors der Naturwissenschaften (Dr. rer. nat.)

genehmigten Dissertation.

Vorsitzender :		Univ.-Prof. Dr. Dr.h.c. A. Laubereau
Prüfer der Dissertation :	1.	Hon.-Prof. I. Cirac, Ph. D.
	2.	Univ.-Prof. Dr. M. Kleber

Die Dissertation wurde am 31.01.06 bei der
Technischen Universität München eingereicht und
durch die Fakultät für Physik am 20.4.06 angenommen.

Abstract

This thesis contributes to the theory of a light-matter quantum interface based on the Kerr-effect arising in the dispersive interaction of pulsed laser light with a spin-polarized atomic ensemble. The scattering process can be described on the basis of a simple, yet fully quantum mechanical model involving only a small number of bosonic modes referring to transverse spin components and quadratures of forward scattered light. Based on this model we derive protocols for the creation of entangled states of light and atoms and the teleportation of quantum states of light onto atoms employing this entanglement. Furthermore we present a protocol, which allows one to exchange the state of light and atoms and thus provides a quantum memory for states of the light field. For both, the storage and the teleportation of coherent states we prove a benchmark on the average fidelity, which is achievable by purely classical protocols. Both protocols allow one to significantly surpass this threshold and to demonstrate thereby a gain in employing quantum strategies. Under common experimental conditions the initial state of light and atoms is Gaussian and the given interaction preserves this property. Motivated by this observation, we examine in this context, how a given interaction can be used to simulate others and how it can be employed to create entanglement at optimal rates. The results are applied to construct protocols based on several passes of light through an atomic ensemble.

Acknowledgements

First and foremost I would like to thank my thesis advisor and teacher Ignacio J. Cirac for the guidance and support he has provided throughout the course of this work. Starting already with his lectures on Quantum Optics and Quantum Information Theory back in the Innsbruck days he continuously conveyed to me his fascination for and joy in doing physics. Among the many things for which I am in debt to him, it is this, for which I am most grateful.

I am deeply thankful to Eugene S. Polzik for his valuable advice concerning many parts of this thesis and for generous hospitality during several visits at the Aarhus University and the Niels-Bohr Institute in Copenhagen. I thank him and all other members of his group, especially Brian Julsgaard, Jacob Sherson and Jörg H. Müller for stimulating and instructive discussions.

I gratefully acknowledge kind hospitality of Klaus Mølmer during two visits at the Aarhus University and thank him for many productive discussions.

Many thanks go to Barbara Kraus, Geza Giedke, Michael Wolf and Christine Muschik, the most enthusiastic and diligent Master student ever, for the fruitful collaboration on important parts of this thesis.

My regards extend to all my colleagues and friends at the Max-Planck Institute, especially to Christian Schön, Toby Cubitt, Markus Popp, Henning Christ, Michael Geissler, Silke Weinfurtner, Enrique Solano, Diego Porras, Juan Jose Garcia-Ripoll and Belen Paredes.

I also thank my girlfriend Theresa for her support and patience and for sweetening so much the last months here in Munich.

Finally, I wish to express my warmest thanks to my family, my brothers, my sister and my dear parents, on whose support, encouragement and love I have relied throughout my time in Munich. It is to them that I dedicate this work.

I thankfully acknowledge funding of the Max-Planck Society and the European Union under project COVAQIAL.

Contents

1 Introduction **9**

2 Interaction of light with an atomic ensemble **13**
2.1 Physical system 13
2.2 Effective Hamiltonian 16
2.3 Atomic polarizability 21
2.4 One dimensional model 23
2.5 Atomic decay 26
2.6 Linearization of equations of motion 27
2.7 Solutions for various setups and applications 31

3 Teleportation of quantum states from light onto atoms **37**
3.1 Single sample in a magnetic field 38
3.2 Teleportation of light onto atoms 41
3.3 Spin squeezing and state read-out 48
3.4 Feedback in systems of continuous variables 51

4 Quantum benchmark for transmission and storage of states **55**
4.1 Quantum benchmark for transmission and storage 56
4.2 Proof of quantum benchmark for coherent states 58

5 Quantum memory and entanglement of light with atoms **63**
5.1 Basic idea and central results 65
5.2 Quantum memory 68
5.3 Two mode squeezing 77
5.4 Consideration of noise 81

6 Simulation of interactions and creation entanglement **93**
6.1 Overview 94
6.2 Simulation of interactions 101
6.3 Entanglement and Squeezing 109

7 Protocols using multiple passes **123**
7.1 Single pass 125
7.2 Multiple passes 126
7.3 Disentangling pass and spin squeezing 128

A Effective interaction **133**
A.1 Step up and down components of the dipole operator 133
A.2 Elimination of spontaneous emission modes 134
A.3 Decomposition of atomic polarizability operator 136

Bibliography **139**

Chapter 1

Introduction

Quantum Information Theory (QIT) is based upon the fundamental observation that the ultimate rules at which information can be transmitted, stored and processed are given by the laws of quantum mechanics [1]. This is not a mere restriction. Central results in QIT show, that it is in fact possible to take advantage of these laws in order to accomplish tasks, which are untractable by classical means, that is, with devices operating on the basis of classical physics. At the moment, there are two major concepts, which demonstrate such a quantum gain in Information Theory: These are quantum computation and quantum communication [2]. A quantum computer would allow to solve problems – such as factoring of large numbers [3] or simulation of quantum systems [4] – for which there exist no efficient classical algorithms. In quantum communication the most striking example is quantum cryptography [5]. It allows two parties to establish a secret key, whose secrecy is guaranteed by the laws of quantum mechanics and not just by the computational complexity of certain mathematical problems, as it is the case for classical key distribution protocols. Pilot applications of quantum cryptographic systems are already commercially available. The same techniques, which are developed in the context of quantum communication, also hold the promise to achieve the first loophole-free violation of a Bell inequality.

The implementation of quantum communication protocols requires the reliable distribution of quantum states and, in particular, entangled states over large distances. For this task the natural carrier of quantum states is light, sent through optical fibers or free space. With present technology the bridgeable distance will be on the order of hundred kilometers, the absorption length of silica fibers. To overcome this limitation the concept of a quantum repeater has been devised [6]. The basic idea is to split a larger distance into parts, which can be bridged by direct communication, and to connect them in

relay stations exploiting entanglement swapping and quantum teleportation. In these relay stations decoherence effects can be compensated by means of purification and entanglement distillation protocols [7]. An essential prerequisite for such a quantum repeater is the possibility to transfer a quantum state from light, its traveling carrier, to a stationary medium, where it can be stored, eventually processed and converted back to light on demand. Directly storing and processing quantum states carried by light is not an option as it would require vast delay lines and enormous optical nonlinearities. The natural choice for the storage medium are long lived atomic ground states. In order to interface the electromagnetic quantum field with internal degrees of freedom of atoms strong coupling is required, which can be achieved either with single atoms in high quality cavities [8, 9] or with optically dense clouds of atoms interacting with light in a ring cavity or in free space.

This thesis contributes to the theory of a quantum interface for light and atomic ensembles. The questions investigated in the following six chapters are to a large extent motivated by experiments [10, 11] performed with a spin-polarized Cesium vapor dispersively interacting with pulsed light, giving rise to what is known in the literature as the Kerr- or Faraday-effect [12]. It is possible to give a remarkably simple, yet rather precise description of the resulting dynamics in this many particle system in terms of only a few bosonic modes, referring to well defined forward scattering modes for light and certain collective spin variables of atoms [13, 14]. Under certain conditions it is even possible to restrict the description to Gaussian quantum states of these modes. This motivated to investigate also more general questions concerning Gaussian states and interactions, irrespective of their physical carrier. Two chapters correspondingly contain general results in QIT of systems of continuous variables and are thus of relevance not only in the context of a quantum interface of light and atoms. They are however of immediate significance in the other chapters, where concrete protocols are presented, which directly apply to the system discussed above.

In the following we will give an overview of the content of this thesis. In chapter 2 we derive the model for the ensemble of atoms interacting with light, already mentioned above. The model itself is not new and can be found in the literature [13, 14]. We chose to include its derivation here in order of have a firm ground for what follows and introduce the notation used throughout this thesis. The starting point of the derivation is the standard Hamiltonian in quantum optics for the interaction of light with atoms. Pointing out the central approximations, we reduce the description to the relevant quantum degrees of freedom. Their evolution is given by Maxwell-Bloch equations, which are the central result of this chapter. The resulting model still allows one to keep track of quantum correlations of light and

atoms, which is essential for the following chapters. In chapter 3 we present a protocol for the teleportation of quantum states of light onto atoms. We examine its performance for coherent states in terms of the fidelity between input state and teleported state. We show, that it is possible to achieve higher fidelities, than can be attained by classical means. Beating this quantum benchmark demonstrates entanglement of light and atoms. We note, that this protocol is under experimental investigation at the moment of writing this thesis. In chapter 4 we prove the quantum benchmark, which was relevant in the preceding chapter. This classical bound on the fidelity was conjectured some time ago and served as the central criterion for success in several seminal experiments, but its prove remained an open question. Here we give its solution. We emphasize, that this result is relevant for all experiments on the transmission and storage of coherent states. In chapter 5 we present two protocols. One is for a full quantum memory for light including mapping of the state onto atoms and releasing it again into light. The other one allows one to create a two mode squeezed state of light and atoms, exhibiting significant amount of entanglement. Remarkably, both tasks can be achieved with basically the same simple setup. It requires two passes of light through an atomic ensemble, which is placed in an external magnetic field. For the memory of coherent states, the quantum benchmark of the preceding chapter is again relevant and we show that it can be beaten under realistic experimental conditions. We also show, that single photons can be successfully stored. Chapter 6 analyzes the general questions of how repeated application of a given interaction of two systems described by continuous variables can be used to simulate another interaction and how entanglement and squeezing of Gaussian states can be created at optimal rates. We answer these questions for general quadratic interaction and discuss the results for the given interaction of light and an atomic ensemble. Finally, in chapter 7 we examine the performance of the multipass protocols for the generation of entanglement and squeezing, derived in the preceding chapter, under realistic conditions. We include noise effects and determine optimal regimes for central experimental parameters. The results presented in chapters 3 to 7 are published in [15], [16], [17], [18] and [19] respectively.

Chapter 2

Interaction of light with an atomic ensemble

2.1 Physical system

In this section we will introduce the physical system and some of its basic properties, which will allow us to derive in the following sections a fully quantum mechanical description in terms of only a few relevant degrees of freedom. We are interested here in the off-resonant interaction of pulsed laser light with an atomic ensemble, as schematically shown in figure 2.1. It will be convenient to list here a couple of observations for each of the components making up the system, the collection of atoms, the coherent pulse, forward scattered light and light scattered into other directions. In the same course we will also introduce some notation, which will be used throughout the thesis.

Atoms: The atomic ensemble consists of N_{at} alkaline-earth atoms, having a single electron outside a closed shell. The ensemble is contained in a glass cell of size $V = L^3$ where L is on the order of cm. The number density of atoms $n = N_{\mathrm{at}}/V$ is assumed to be such, that there is not more than a single atom per cubic wavelength,

$$n\lambda_c^3 \lesssim 1, \tag{2.1}$$

where λ_c is the central wavelength of light irradiating the atoms. For the most part of this thesis we will think of the ensemble being at room-temperature and atoms undergoing thermal motion. Positions of atoms can then be treated as classical random variables. Concerning the internal structure of atoms, we assume a level scheme as shown in figure 2.2a, that is, each atom carries a ground state spin $J = 1/2$ and has an optical, dipole allowed tran-

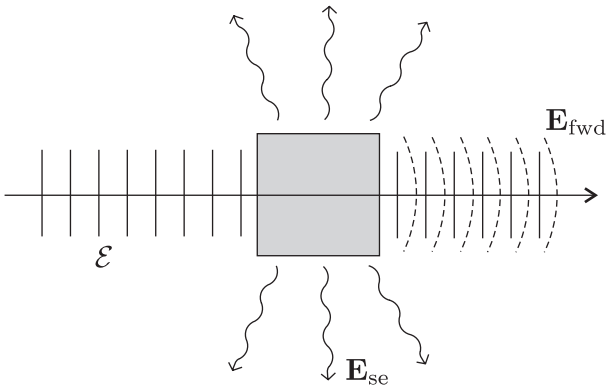

Figure 2.1: The physical system under consideration consists of the atomic ensemble, a coherent pulse $\boldsymbol{\mathcal{E}}$ irradiating it, forward scattered light $\mathbf{E}_{\mathrm{fwd}}$ and spontaneously emitted light $\mathbf{E}_{\mathrm{se}}$ scattered into different directions.

sition of frequency ω_0 to an excited states' manifold of spin $J' = 1/2$. The oscillator strength of this transition is determined by its reduced matrix element

$$d = \langle J||d||J'\rangle, \tag{2.2}$$

which we take to be real. This configuration is the simplest one, which leads to a possible birefringence of the atomic medium, a property which builds the very basis of the effect we are interested in. In this respect, our model grasps the main properties of any real Hydrogen like atom such as Cesium with a level scheme as shown in figure 2.2b, where hyperfine splitting has to be taken into account. The validity of our simple model will be discussed in section 2.3 in more detail.

Coherent field: The coherent pulse of light is described by a $\mathbb{C}$-number field $\boldsymbol{\mathcal{E}} = \boldsymbol{\mathcal{E}}^- + \boldsymbol{\mathcal{E}}^+$ with positive frequency component

$$\boldsymbol{\mathcal{E}}^-(\mathbf{r}, t) = \mathcal{E}(t)u(\mathbf{r})e^{-i(\mathbf{k_c}\mathbf{r}-\omega_c t)}\boldsymbol{\epsilon}, \tag{2.3}$$

where $\boldsymbol{\epsilon}$ is the pulse's polarization, $u(\mathbf{r})$ its profile in the plane transverse to the direction of propagation $\mathbf{k}_c$ and $\mathcal{E}(t)$ is a slowly varying amplitude. We assume that the transverse cross section is such that the pulse covers most of the ensemble, that is the beam diameter $l \lesssim L$. For beams of this size the form (2.3) is certainly a good approximation. The driving field will give rise to a Rabbi frequency which will be on the order of,

$$\Omega = \frac{d\mathcal{E}_0}{\hbar}$$

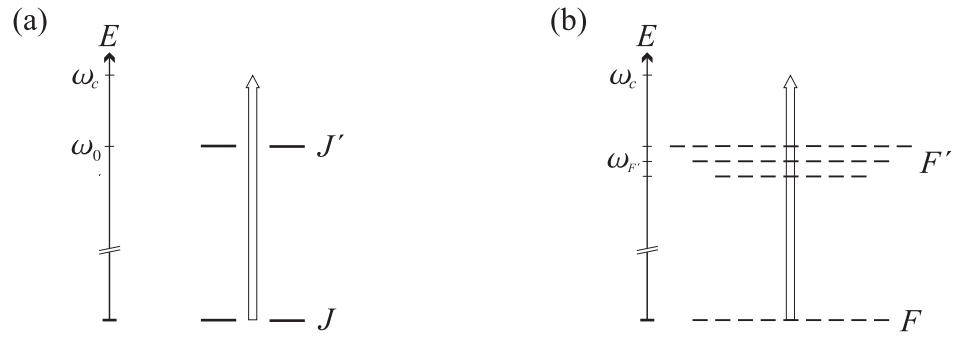

Figure 2.2: (a) Internal structure of atoms with ground state spin $J = 1/2$ and excited state manifold of spin $J' = 1/2$. The transition frequency is ω_0 and light is blue detuned with frequency ω_c. (b) Level scheme for the D_2 transition of Cesium at $F = 4 \rightarrow F' = 3, 4, 5$. Due to hyperfine splitting there are three optical transitions with respective frequencies $\omega_{F'}$.

times a Clebsch Gordan coefficient, where $\mathcal{E}_0$ is the maximum of the pulse envelope. The central frequency ω_c of the pulse is blue detuned from the atomic transition with a detuning

$$\Delta = \omega_0 - \omega_c.$$

The length T of the pulse is assumed to be such that the Fourier limited bandwidth is much smaller than the detuning, $\Delta \gg T^{-1}$. We further assume that

$$\Delta \gg \Omega, \tag{2.4}$$

in which case each atomic dipole will adiabatically follow the applied driving force.

Forward scattered light: We will be particularly interested in the light, which is scattered into the forward direction. As we will show, this component of the field will be strongly correlated to a certain collective mode of the atomic spin. In order to describe this effect, it is of course necessary to retain a full quantum mechanical treatment for this field. The operator for the (positive frequency part of the) forward scattered field is

$$\mathbf{E}^{-}_{\mathrm{fwd}}(\mathbf{r}, t) \;=\; \sum_{\lambda} \int_b d^3k\rho \; a^{\dagger}_{\mathbf{k}\lambda} e^{-i\mathbf{kr}} \boldsymbol{\epsilon}_{\mathbf{k}\lambda}, \tag{2.5}$$

where the sum is over polarizations λ and the domain of integration over wave vectors $\mathbf{k}$ is defined as $b = \{\mathbf{k} : (1 - \mathbf{k}\mathbf{k}_c/k_c^2) < \theta\}$, that is it includes

only wave vectors which enclose at most an angle $\theta \ll 1$ with $\mathbf{k}_c$. We also used $\rho = \sqrt{\hbar\omega/2\epsilon_0(2\pi)^3}$. Finally, $a_{\mathbf{k}\lambda}$ is the destruction operator for photons of wave vector $\mathbf{k}$ and polarization λ and obeys the bosonic commutation relation

$$[a_{\mathbf{k}\lambda}, a^\dagger_{\mathbf{k}'\lambda'}] = \delta_{\lambda\lambda'}\delta^3(\mathbf{k}-\mathbf{k}').$$

Spontaneously emitted light: Apart from forward scattering, there will inevitably be light scattered also into different directions than that of $\mathbf{k}_c$. We will take this component of the field into account in the standard way spontaneous emission is treated, that is, we will eliminate in a Born-Markov approximation all but the forward scattering modes of the electromagnetic field and keep only the resulting decohering effect on the state of atoms. At first we will include the spontaneous emission field as

$$\mathbf{E}^-_{\mathrm{se}}(\mathbf{r},t) \;=\; \sum_\lambda \int_{\bar{b}} d^3k\rho \; a^\dagger_{\mathbf{k}\lambda} e^{-i\mathbf{kr}} \boldsymbol{\epsilon}_{\mathbf{k}\lambda}, \tag{2.6}$$

where the domain of integration $\bar{b}$ denotes the complement of b.

2.2 Effective Hamiltonian

With the notation introduced in the previous section, the standard Hamiltonian for this system in the dipole, rotating wave and long wavelength approximation is given by

$$H = H_{\mathrm{at}} + H_{\mathrm{li}} + H_{\mathrm{int}}, \tag{2.7a}$$

$$H_{\mathrm{at}} = \sum_{j=1}^{N_{\mathrm{at}}} \hbar\omega_0 \pi_j^{J'}, \tag{2.7b}$$

$$H_{\mathrm{li}} = \sum_\lambda \int d^3k\, \hbar\omega a^\dagger_{\mathbf{k}\lambda} a_{\mathbf{k}\lambda}, \tag{2.7c}$$

$$H_{\mathrm{int}} = \sum_j \left[\boldsymbol{\mathcal{E}}^-(\mathbf{r}_j,t) + \mathbf{E}^-_{\mathrm{fwd}}(\mathbf{r}_j) + \mathbf{E}^-_{\mathrm{se}}(\mathbf{r}_j)\right]\cdot\mathbf{d}_j^- + \mathrm{h.c.}\,. \tag{2.7d}$$

The full Hamiltonian (2.7a), consists of the internal energy of all atoms (2.7b), the energy of the free electromagnetic field (2.7c) and the dipole interaction of the field and atoms (2.7d). In Equ. (2.7b) $\pi_j^{J'}$ denotes the projector onto the excited manifold of atom j, defined as

$$\pi_j^{J'} = \sum_{m'=-J'}^{J'} |J'm'\rangle_j\langle J'm'|.$$

The symbol π_j^J will be used for the projector onto the ground state manifold. In Equ. (2.7d) we introduced the step down component of the dipole operator for the jth atom

$$\mathbf{d}_j^- = \pi_j^J \mathbf{d}_j \pi_j^{J'} \tag{2.8}$$

where $\mathbf{d}_j$ is the dipole moment of atom j.

The aim in this section is to derive from the full Hamiltonian (2.7a) an effective one taking into account the adiabatic evolution of atomic dipoles under condition (2.4) and the fact that light is scattered in the forward direction. The final Hamiltonian will thus include only ground state levels and the forward scattered field but will, of course, be non-hermitian, as it includes decoherence effects due to spontaneous emission. The resulting equations of motion will therefore also include Langevin noise terms.

To start with it, will be useful to define the dimensionless operator

$$\boldsymbol{\sigma}_j^- = \frac{1}{d}\mathbf{d}_j^-$$

and its adjoint $\boldsymbol{\sigma}_j^+ = (\boldsymbol{\sigma}_j^-)^\dagger$, where d is the reduced matrix element for the $J \to J'$ transition, c.f. (2.2). In appendix A we show that one can express $\boldsymbol{\sigma}_j^-$ by means of the Wigner Eckart as

$$\boldsymbol{\sigma}_j^- = \sum_{m=-J}^{J} \sum_{m'=-J'}^{J'} \sum_{q=-1}^{1} \langle 1q\, Jm | J'm' \rangle |J'm'\rangle\langle Jm| \boldsymbol{\epsilon}_q^*, \tag{2.9}$$

where $\langle 1q\, Jm|J'm'\rangle$ is a Clebsch-Gordan coefficient and $\boldsymbol{\epsilon}_q^*$ is a unit vector of the spherical basis. See the appendix for the definition of this basis. Note that the definition of $\boldsymbol{\sigma}_j^-$ applies to any value of the spins J, J'. The explicit form of $\boldsymbol{\sigma}_j^-$ is given here just for completeness and we will not resort to it in the following calculations. Instead, we will frequently make use of the properties,

$$\boldsymbol{\sigma}_j^- \pi_j^J = \pi_j^{J'} \boldsymbol{\sigma}_j^- = 0, \qquad \boldsymbol{\sigma}_j^+ \pi_j^{J'} = \pi_j^J \boldsymbol{\sigma}_j^+ = 0, \qquad \boldsymbol{\sigma}_j^+ \cdot \boldsymbol{\sigma}_j^- = \pi_j^{J'}. \tag{2.10}$$

The first two equations are trivial and the last one is derived in Appendix A. With this definition the Heisenberg equation of motion of an arbitrary atomic observable A is given by[1]

$$\dot{A} = i\omega_0 \sum_j [\pi_j^{J'}, A] + \frac{id}{\hbar} \sum_j \Big(\big\{ \boldsymbol{\mathcal{E}}^-(\mathbf{r}_j) + \mathbf{E}_{\text{fwd}}^-(\mathbf{r}_j) + \mathbf{E}_{\text{se}}^-(\mathbf{r}_j) \big\} \cdot [\boldsymbol{\sigma}_j^-, A] + [\boldsymbol{\sigma}_j^+, A] \cdot \big\{ \boldsymbol{\mathcal{E}}^+(\mathbf{r}_j) + \mathbf{E}_{\text{fwd}}^+(\mathbf{r}_j) + \mathbf{E}_{\text{se}}^+(\mathbf{r}_j) \big\} \Big), \tag{2.11}$$

[1] In (2.11) and all following equations operators have to be understood to depend on time, $\boldsymbol{\sigma}_j^+ = \boldsymbol{\sigma}_j^+(t)$ etc. The argument is t everywhere, unless in cases where it is written explicitly.

where the commutators in the last two terms have to be taken componentwise.

In the next step we will eliminate the spontaneous emission modes from this equation. In appendix A.2 we show, that in a standard Markov approximation and under the assumption that each atom couples to an independent reservoir, which is equivalent to assumption (2.1), we can identify

$$\mathbf{E}^-_{\rm se}(\mathbf{r}_j,t)=\frac{\hbar\sqrt{\gamma}}{d}\mathbf{f}^-_j(t)+\frac{i\hbar\gamma}{2d}\widetilde{\boldsymbol{\sigma}}^+_j(t), \tag{2.12}$$

where we introduced the decay rate

$$\gamma=\frac{d^2\omega_c^3}{6\pi\hbar\epsilon_0 c^3} \tag{2.13}$$

and vectors $\mathbf{f}^-_j(t)$ of Langevin noise operators. The latter are - up to a normalization - identical to the free evolving vacuum field at the positions r_j of atoms (see appendix A.2), have zero mean and are delta correlated componentwise, such that

$$\begin{aligned}\langle\mathbf{f}^+_j(t)\rangle=\langle\mathbf{f}^-_j(t)\rangle &= 0, &(2.14a)\\ \langle f^-_{i,\alpha}(t)f^+_{j,\beta}(t')\rangle &= 0, &(2.14b)\\ \langle f^+_{i,\alpha}(t)f^-_{j,\beta}(t')\rangle &\simeq \delta_{\alpha\beta}\delta_{ij}\delta(t-t') &(2.14c)\end{aligned}$$

for $\alpha,\beta=x,y,z$. If we insert now (2.12) into (2.11) we arrive at a quantum Langevin equation for atomic observables

$$\begin{aligned}\dot{A}=\;& i\omega_0\sum_j[\pi_j^{J'},A]\\ &+\frac{id}{\hbar}\sum_j\Big(\big\{\boldsymbol{\mathcal{E}}^-(\mathbf{r}_j)+\mathbf{E}^-_{\rm fwd}(\mathbf{r}_j)\big\}\cdot[\boldsymbol{\sigma}^-_j,A]+[\boldsymbol{\sigma}^+_j,A]\cdot\big\{\boldsymbol{\mathcal{E}}^+(\mathbf{r}_j)+\mathbf{E}^+_{\rm fwd}(\mathbf{r}_j)\big\}\Big),\\ &+\sum_j\Big(\Big\{i\sqrt{\gamma}\,\mathbf{f}^-_j-\frac{\gamma}{2}\widetilde{\boldsymbol{\sigma}}^+_j\Big\}\cdot[\boldsymbol{\sigma}^-_j,A]+[\boldsymbol{\sigma}^+_j,A]\cdot\Big\{i\sqrt{\gamma}\,\mathbf{f}^+_j+\frac{\gamma}{2}\widetilde{\boldsymbol{\sigma}}^-_j\Big\}\Big).\end{aligned} \tag{2.15}$$

In order to eliminate the excited levels, it is convenient to move to a frame rotating at the central frequency ω_c, in which all operators and the coherent field are slowly varying[2],

$$\widetilde{\boldsymbol{\sigma}}^+_j=\boldsymbol{\sigma}^+_j e^{-i\omega_c t},\quad \widetilde{\mathbf{E}}^-(\mathbf{r})=\mathbf{E}^-(\mathbf{r})e^{-i\omega_c t},\quad \widetilde{\boldsymbol{\mathcal{E}}}^-(\mathbf{r})=\boldsymbol{\mathcal{E}}^-(\mathbf{r})e^{-i\omega_c t}.$$

[2]In principle we should also introduce slowly varying Langevin noise operators $\widetilde{\mathbf{f}}^-_j$ etc. However, given that these operators have zero mean and are delta correlated in time, operators $\widetilde{\mathbf{f}}^-_j$ will behave just the same way as $\mathbf{f}^-_j$. We will therefore not distinguish between them and omit the tilde.

The evolution of slowly varying coherences between ground and excited states is given by (2.15) with $\widetilde{\boldsymbol{\sigma}}_j^+$ substituted for A, which yields

$$\dot{\widetilde{\boldsymbol{\sigma}}}_j^+ \;=\; \Big(i\Delta - \frac{\gamma}{2}\Big)\,\widetilde{\boldsymbol{\sigma}}_j^+ + \frac{id}{\hbar}\left\{\widetilde{\boldsymbol{\mathcal{E}}}^-(\mathbf{r}_j) + \widetilde{\mathbf{E}}^-_{\mathrm{fwd}}(\mathbf{r}_j)\right\}\cdot \widetilde{\boldsymbol{\sigma}}_j^-\,\widetilde{\boldsymbol{\sigma}}_j^+ + i\sqrt{\gamma}\,\mathbf{f}_j^-\cdot\,\widetilde{\boldsymbol{\sigma}}_j^-\,\widetilde{\boldsymbol{\sigma}}_j^+, \tag{2.16}$$

where we made use of (2.10) and skipped terms, which are proportional to $\widetilde{\sigma}^+_{j,\alpha}\widetilde{\sigma}^-_{j,\beta}$. The latter describe populations of and coherences between excited states' levels and therefore are in the dispersive limit (2.4) smaller than the last two terms in (2.16) by a factor $s = \Omega^2/\Delta^2 \ll 1$, the saturation parameter. The adiabatic solution to the last equation is

$$\begin{aligned}\widetilde{\boldsymbol{\sigma}}_j^+ &= -\frac{d}{\hbar(\Delta + i\gamma/2)}\left\{\widetilde{\boldsymbol{\mathcal{E}}}^-(\mathbf{r}_j) + \widetilde{\mathbf{E}}^-_{\mathrm{fwd}}(\mathbf{r}_j)\right\}\cdot \widetilde{\boldsymbol{\sigma}}_j^-\,\widetilde{\boldsymbol{\sigma}}_j^+ - \frac{\sqrt{\gamma}}{(\Delta + i\gamma/2)}\,\mathbf{f}_j^-\cdot\,\widetilde{\boldsymbol{\sigma}}_j^-\,\widetilde{\boldsymbol{\sigma}}_j^+ \\ &\simeq -\frac{d}{\hbar\Delta}\left\{\widetilde{\boldsymbol{\mathcal{E}}}^-(\mathbf{r}_j) + \widetilde{\mathbf{E}}^-_{\mathrm{fwd}}(\mathbf{r}_j)\right\}\cdot \widetilde{\boldsymbol{\sigma}}_j^-\,\widetilde{\boldsymbol{\sigma}}_j^+ + \frac{id\gamma}{2\hbar\Delta^2}\widetilde{\boldsymbol{\mathcal{E}}}^-(\mathbf{r}_j)\cdot\,\widetilde{\boldsymbol{\sigma}}_j^-\,\widetilde{\boldsymbol{\sigma}}_j^+ - \frac{\sqrt{\gamma}}{\Delta}\,\mathbf{f}_j^-\cdot\,\widetilde{\boldsymbol{\sigma}}_j^-\,\widetilde{\boldsymbol{\sigma}}_j^+.\end{aligned} \tag{2.17}$$

where in the last step we assumed $\Delta \gg \gamma$ and neglected the contribution of the quantum field in forward direction $\widetilde{\mathbf{E}}^-_{\mathrm{fwd}}$ in the damping term proportional to γ. This is justified given that these modes will contain only a small population as compared to the driving field $\widetilde{\boldsymbol{\mathcal{E}}}^-$. In the adiabatic limit the evolution of $\widetilde{\boldsymbol{\sigma}}_j^+$ is thus entirely determined by the one of ground state operators of the form $\sigma^-_{j,\alpha}\,\sigma^+_{j,\beta}$ and the fields propagating along $\mathbf{k}_c$.

This can be used to derive the desired effective evolution of ground state observables, such as the collective ground state spin. Let $A = \sum_j A_j$ now be any such observable, where A_j acts only on ground state levels of atom j. According to (2.15) it evolves as

$$\begin{aligned}\dot{A} = \frac{id}{\hbar}\sum_j \Big(-A_j\,\left\{\widetilde{\boldsymbol{\mathcal{E}}}^-(\mathbf{r}_j) + \widetilde{\mathbf{E}}^-_{\mathrm{fwd}}(\mathbf{r}_j)\right\}\cdot\,\widetilde{\boldsymbol{\sigma}}_j^- + \widetilde{\boldsymbol{\sigma}}_j^+\cdot\left\{\widetilde{\boldsymbol{\mathcal{E}}}^+(\mathbf{r}_j) + \widetilde{\mathbf{E}}^+_{\mathrm{fwd}}(\mathbf{r}_j)\right\}\,A_j\Big) \\ + \sum_j\sum_\alpha\left\{\gamma\,\widetilde{\sigma}^+_{j,\alpha}\,A_j\widetilde{\sigma}^-_{j,\alpha} - i\sqrt{\gamma}\,f^-_{j,\alpha}\,A_j\widetilde{\sigma}^-_{j,\alpha} + i\sqrt{\gamma}\,\widetilde{\sigma}^+_{j,\alpha}A_j f^+_{j,\alpha}\right\},\end{aligned}$$

where α labels any convenient basis in $\mathbb{R}^3$. We now substitute the adiabatic solution (2.17) as well as its adjoint into the last equation and skip all terms of order $\gamma^{3/2}$ and γ^2. It can be easily checked that these terms can in deed be neglected under the assumptions used so far. The effective evolution is

then given by

$$\dot{A} = \frac{i}{\hbar}\left[-\sum_j \frac{d^2}{\hbar\Delta}\left(\widetilde{\boldsymbol{\mathcal{E}}}^-(\mathbf{r}_j)+\widetilde{\mathbf{E}}^-_{\mathrm{fwd}}(\mathbf{r}_j)\right)\cdot\widetilde{\boldsymbol{\sigma}}_j^-\widetilde{\boldsymbol{\sigma}}_j^+\cdot\left(\widetilde{\boldsymbol{\mathcal{E}}}^+(\mathbf{r}_j)+\widetilde{\mathbf{E}}^+_{\mathrm{fwd}}(\mathbf{r}_j)\right), A\right] + \sum_j \mathcal{L}_j(A_j) \quad (2.18)$$

where we defined a superoperator $\mathcal{L}_j$ describing losses due to spontaneous emission of atom j

$$\begin{aligned}\mathcal{L}_j(A_j) = \frac{d^2\gamma}{2\hbar^2\Delta^2}\Bigg\{&2\sum_\alpha \widetilde{\boldsymbol{\mathcal{E}}}^-(\mathbf{r}_j)\cdot\widetilde{\boldsymbol{\sigma}}_j^-\widetilde{\sigma}^+_{j,\alpha}A_j\widetilde{\sigma}^-_{j,\alpha}\,\widetilde{\boldsymbol{\sigma}}_j^+\cdot\widetilde{\boldsymbol{\mathcal{E}}}^+(\mathbf{r}_j)\\ &-\left[\widetilde{\boldsymbol{\mathcal{E}}}^-(\mathbf{r}_j)\cdot\widetilde{\boldsymbol{\sigma}}_j^-\widetilde{\boldsymbol{\sigma}}_j^+\cdot\widetilde{\boldsymbol{\mathcal{E}}}^+(\mathbf{r}_j), A_j\right]_+\Bigg\}\\ &-i\frac{d\sqrt{\gamma}}{\hbar\Delta}\left\{\mathbf{f}_j^-\cdot[\widetilde{\boldsymbol{\sigma}}_j^-\widetilde{\boldsymbol{\sigma}}_j^+\cdot\widetilde{\boldsymbol{\mathcal{E}}}^+(\mathbf{r}_j), A_j] + [\widetilde{\boldsymbol{\mathcal{E}}}^-(\mathbf{r}_j)\cdot\widetilde{\boldsymbol{\sigma}}_j^-\widetilde{\boldsymbol{\sigma}}_j^+, A_j]\cdot\mathbf{f}_j^+\right\}. \quad (2.19)\end{aligned}$$

The symbol $[.,.]_+$ denotes an anticommutator. The evolution of O thus contains a coherent dynamics, governed by an effective Hamiltonian, which can be read off from the commutator in (2.18), and an incoherent one, described by the action of the superoperators $\mathcal{L}_j$. We would like to postpone the discussion of the latter terms to section 2.5 and focus instead on the effective Hamiltonian in the next section.

Before going into detail, we will show, that the same effective Hamiltonian governs also the evolution of forward scattering modes. This is easily seen by looking at the evolution equation of the slowly varying operator $\widetilde{a}_{\mathbf{k}\lambda} = a_{\mathbf{k}\lambda}\exp(i\omega_c t)$ of one of the forward scattering modes following from the original Hamiltonian (2.7a),

$$\begin{aligned}\dot{\widetilde{a}}_{\mathbf{k}\lambda} =& i\omega_c\widetilde{a}_{\mathbf{k}\lambda} + \frac{i}{\hbar}[H_{\mathrm{li}}, \widetilde{a}_{\mathbf{k}\lambda}] + \frac{i}{\hbar}\sum_j[\widetilde{\mathbf{E}}^-_{\mathrm{fwd}}(\mathbf{r}_j)\cdot\widetilde{\boldsymbol{\sigma}}^-, \widetilde{a}_{\mathbf{k}\lambda}]\\ =& -i(\omega-\omega_c)\widetilde{a}_{\mathbf{k}\lambda}\\ &+\frac{i}{\hbar}\left[\sum_j -\frac{d^2}{\hbar\Delta}\,\widetilde{\mathbf{E}}^-_{\mathrm{fwd}}(\mathbf{r}_j)\cdot\widetilde{\boldsymbol{\sigma}}_j^-\widetilde{\boldsymbol{\sigma}}_j^+\cdot\left(\widetilde{\boldsymbol{\mathcal{E}}}^+(\mathbf{r}_j)+\widetilde{\mathbf{E}}^+_{\mathrm{fwd}}(\mathbf{r}_j)\right), \widetilde{a}_{\mathbf{k}\lambda}\right], \quad (2.20)\end{aligned}$$

where we again substituted the (adjoint of the) adiabatic solution (2.17) and neglected spontaneous emission terms, which would give rise to light scattering out of the forward direction. We neglect this effect, because light losses are dominated by reflections at the walls of the glass cell, which we will

take into account separately. Note however, that it is perfectly possible to derive Langevin terms along the same way, as it was done above for atomic observables and that the resulting terms would take on a form, which is familiar from the description of lossy cavities coupled to the vacuum field.

What is here important to us, is that the coherent evolution of both, ground state observables and forward scattering modes, is governed by the same effective interaction Hamiltonian

$$H_{\rm int}^{\rm eff} = -\sum_j \left(\widetilde{\boldsymbol{\mathcal{E}}}^-(\mathbf{r}_j) + \widetilde{\mathbf{E}}^-_{\rm fwd}(\mathbf{r}_j)\right) \overleftrightarrow{\alpha} \left(\widetilde{\boldsymbol{\mathcal{E}}}^+(\mathbf{r}_j) + \widetilde{\mathbf{E}}^+_{\rm fwd}(\mathbf{r}_j)\right), \tag{2.21}$$

where

$$\overleftrightarrow{\alpha}_j = \frac{d^2}{\hbar\Delta}\, \boldsymbol{\sigma}_j^- \otimes \boldsymbol{\sigma}_j^+, \tag{2.22}$$

as can be seen by comparing equations (2.18) and (2.20). In the last line we used the notation $\mathbf{w}\cdot\mathbf{x}\,\mathbf{y}\cdot\mathbf{z} = \mathbf{w}\,\mathbf{x}\otimes\mathbf{y}\,\mathbf{z}$ for the Cartesian tensor product of vectors.

This Hamiltonian describes - loosely speaking - the Stark shift of atomic levels caused by off resonant light. In the context of cooling and trapping of atoms it was therefore termed *level shift Hamiltonian*. While there the accent was on the internal and motional quantum dynamics of atoms in the potential created by light, treated as a reservoir, we are here interested in the quantum state of both, internal degrees of freedom of atoms and forward scattered light.

2.3 Atomic polarizability

In this section we will focus on the atomic operator appearing in the level shift Hamiltonian, (2.22), commonly termed *atomic polarizability tensor operator*. It is well known that this operator can always be decomposed into a scalar, vector and tensor component [12]. For the case of a $J = 1/2 \rightarrow J' = 1/2$ transition one can show by means of the definition of $\boldsymbol{\sigma}_j^-$ in (2.9) and elementary tensor calculus (see appendix A.3) that

$$\overleftrightarrow{\alpha}_j = \frac{d^2}{\hbar\Delta}\left(a_0 \mathbb{1}_j + i a_1 \mathbf{J}_j \times\right), \tag{2.23}$$

where $\mathbb{1}$ is the 3×3 matrix of operator identities and $\mathbf{J}\times$ has to be understood to give the Cartesian vector product of the ground state spin vector, $\mathbf{J} = (\sigma_x, \sigma_y, \sigma_z)/2$, with the vector to the right. The coefficients are given by $a_0 = 1/3$, $a_1 = -2/3$. Note that there appears no tensor component for the case of a spin 1/2 ground state.

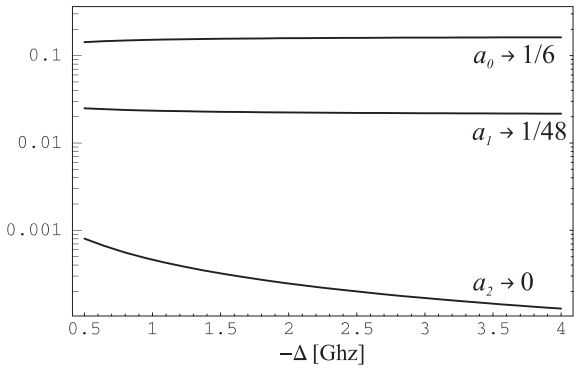

Figure 2.3: Dependence of coefficients of scaler, vector and tensor polarizability, a_0, a_1 and a_2 respectively, on the (blue) detuning Δ for the special case of the cesium D_2 line at $F = 4 \to F' = 3, 4, 5$. The weight of the tensor polarizability is always at least an order of magnitude smaller than the one of the vector polarizability and tends to vanish for large detuning.

For more complex level structures, such as the one shown in figure 2.2b, things will be slightly different [14]. With a little effort in notation a calculation analogous to the one in the preceding section, but taking into account all possible transitions $F \to F'$, shows that the effective Hamiltonian will be still of the form (2.21) while the atomic polarizability follows from a sum over all contributions of the various transitions. That is,

$$\overleftrightarrow{\alpha} = \sum_{F'=F-1}^{F+1} \frac{d_{F'}^2}{\hbar \Delta_{F'}} \boldsymbol{\sigma}^-_{j,FF'} \otimes \boldsymbol{\sigma}^+_{j,F'F}, \tag{2.24}$$

where $d_{F'}$, $\Delta_{F'}$, $\boldsymbol{\sigma}^-_{j,FF'}$ are the reduced matrix element, the detuning and the step down operator for the $F \to F'$ transition respectively. The decomposition of this operator is given in detail in appendix A.3, where we show that

$$\overleftrightarrow{\alpha}_j = \frac{d^2}{\hbar \Delta} \left(a_0(\Delta) \mathbb{1}_j + i a_1(\Delta) \mathbf{F}_j \times + a_2(\Delta) \overleftrightarrow{T}_j \right),$$

where d is again the reduced matrix element for the underlying $J \to J'$ transition and the detuning $\Delta = \omega_{F'=F+1} - \omega_c$ is taken with respect to the uppermost level (see figure 2.2b). Note that the coefficients a_k now depend on the detuning and there is a non-vanishing contribution of the tensor polarizability $\overleftrightarrow{T}$. The dependence of a_k on the detuning is shown for the example of Cesium in figure 2.3. The explicit formula is given in formula (A.10) of the appendix. For a detuning larger than the typical hyperfine splitting of excited states' manifolds all coefficients tend to an asymptotic

value. In particular the coefficient a_2 for the tensor polarizability vanishes in this limit. Note that this is a general feature of all hydrogen like atoms. We conclude that it is precisely the condition that the detuning is larger than the excited states' hyperfine splitting, which justifies to use the simple model atom shown in figure 2.2a.

In the following we will assume that this condition is fulfilled and work with an atomic polarizability as given in (2.23). For a discussion of the effects of the second order, tensor polarizability we refer to [14]. In the approximation used here, the resulting effective interaction will contain two contributions. The one proportional to a_0 does not depend on the internal states of atoms but on their number density and describes the index of refraction of the atomic medium. One can think of it as giving rise to a global phase shift of the wave function of atomic internal states and forward scattered photons. In this sense it is irrelevant and can be dropped. The second one, proportional to a_1, depends on populations and coherences of ground state levels, and is the one we are interested here. By means of expression (2.23) for the atomic polarizability it will be straight forward to evaluate the evolution of atomic ground state spins.

2.4 One dimensional model

In the previous sections we eliminated all but a small number of forward scattering modes of the electromagnetic field, based upon the observation that only these will be populated considerably. In the present section we will reduce the description further to a simple one dimensional model. For work treating the three-dimensional aspects of light scattering in the regime we are interested here we refer to [20, 21]. Adopting a one dimensional model can be justified by noting, that in the end we will be interested in the homodyne signal of the scattered field arising in a measurement, where the laser pulse triggering also the interaction is taken as a local oscillator. Thus, the only signal, which will be relevant is the one, which comes from light scattered into the laser mode. Light, which is scattered into other forward scattering modes, will not produce a signal.

The reduction to one dimension can be performed along the lines of [22]. We assume without loss of generality that light propagates along z and that the coherent pulse is linearly polarized along x. For the quantum field in turn we will keep only the polarization component along y. Remember that we are interested here in the birefringence associated with the vector polarizability of the atomic medium, which will lead to scattering of photons out of the x polarized pulse into the y polarized modes. It is the quantum field in this

component, which is relevant to us. In a one dimensional theory we thus take for the coherent pulse $\widetilde{\boldsymbol{\mathcal{E}}}^-(z) = \widetilde{\mathcal{E}}^-(z)\boldsymbol{\epsilon}_x$, where

$$\widetilde{\mathcal{E}}^-(z) = \rho\sqrt{\frac{2\pi N_{ph}}{T}}e^{-ik_c z}. \tag{2.25}$$

We use here $\rho(\omega) \simeq \rho(\omega_c) = \sqrt{\hbar\omega_c/4\pi\epsilon_0 Ac}$, which is an excellent approximation for optical frequencies, and A to denote the cross section of the pulse. The square root factor in (2.25) is the amplitude of the pulse, whose envelope we take to be box shaped, dropping to zero at time T. The amplitude is chosen such that the power P of the pulse is $P = 2c\epsilon_0 A|\widetilde{\boldsymbol{\mathcal{E}}}^-\widetilde{\boldsymbol{\mathcal{E}}}^+| = N_{\rm ph}\hbar\omega_c/T$, where $N_{\rm ph}$ is the number of photons in the pulse (and T its duration). Similarly, we have for the quantum field $\widetilde{\mathbf{E}}^-(z) = \widetilde{E}^-(z)\boldsymbol{\epsilon}_y$, where

$$\widetilde{E}^-(z) = \rho\int_b \mathrm{d}\omega a^\dagger_\omega e^{-i(kz-\omega_c t)} \tag{2.26}$$

and $[a_\omega, a^\dagger_{\omega'}] = \delta(\omega-\omega')$. The Hamiltonian for the free electromagnetic field in this one dimensional model is given by

$$H_{\rm li} = \int d\omega\hbar\omega a^\dagger_\omega a_\omega \tag{2.27}$$

If we insert the expression for $\widetilde{\boldsymbol{\mathcal{E}}}^-(z)$ and $\widetilde{\mathbf{E}}^-(z)$ into (2.21) and evaluate the vector products taking into account that we need to keep only the vector part of the atomic polarizability (2.23), the interaction is given by

$$H^{\rm eff}_{\rm int} = \frac{id^2 a_1}{\hbar\Delta}\sum_j J^j_z\left[\widetilde{\mathcal{E}}^-(z_j)\widetilde{E}^+(z_j) - \widetilde{\mathcal{E}}^+(z_j)\widetilde{E}^-(z_j)\right]. \tag{2.28}$$

In principle each term in this sum contains a weighting factor $u(\mathbf{r}^j_\perp)$, which can even be zero, if the atom is outside the volume covered by the light beam. However, if atoms move at a thermal velocity $v_{\rm th}$ such that they enter leave this volume several times during the pulse length T, each atom will see on average the same, constant potential. This is what we assumed in the last equation. The corresponding condition is

$$\frac{v_{\rm th}T}{L} \gg 1.$$

We would like to remark, that the term in square brackets is proportional to the z component of the Stokes vector. That is, it is proportional to the difference of the number of photons of left and right circular polarization

in the beam and thus measures its angular momentum projection along the propagation direction. The interaction (2.28) therefore describes exchange of angular momentum between atoms and light under conservation of the total z component. For a formulation of the dynamics in this language emphasizing this view, we refer to [14].

Here we would like to use instead a formulation in terms of light quadratures. Using (2.25) and (2.26) we have

$$\widetilde{\mathcal{E}}^{-}(z)\widetilde{E}^{+}(z) - \widetilde{\mathcal{E}}^{+}(z)\widetilde{E}^{-}(z) = \\ = \rho^2\sqrt{\frac{2\pi N_{ph}}{T}}\int_b \mathrm{d}\omega \left(a_\omega e^{i[(k-k_c)z-\omega_c t)} - a_\omega^\dagger e^{-i[(k-k_c)z-\omega_c t)}\right). \quad (2.29)$$

This can obviously be expressed as a quadrature of the y polarized quantum field,

$$p(z) = -\frac{i}{\sqrt{4\pi}}\int d\omega \left(a_\omega e^{i([k-k_c]z-\omega_c t)} - \text{h.c.}\right), \quad (2.30a)$$

whose conjugate variable is

$$x(z) = \frac{1}{\sqrt{4\pi}}\int d\omega \left(a_\omega e^{i([k-k_c]z-\omega_c t)} + \text{h.c.}\right). \quad (2.30b)$$

The integration runs over positive frequencies, corresponding to forward scattered light, and over a certain bandwidth $\delta\omega$ around ω_c, for which assume $\delta\omega \ll c/L$, where L is the extension of the sample along z. The commutator is then $[x(z), p(z')] = ic\delta(z-z')$, where the delta function has to be understood to have a width $c/\delta\omega$. The mode functions we are going to use here thus have a spatial extension, which is larger than the linear extension of the sample. In this case the effective Hamiltonian (2.28) can be written as

$$H_{\text{int}}^{\text{eff}} = -\frac{\hbar\chi}{\sqrt{T}}\sum_j J_z^j p(0), \quad (2.31)$$

where we defined a dimensionless parameter

$$\chi = \frac{d^2 a_1 \omega_c}{\hbar\Delta\epsilon_0 A c}\sqrt{\frac{N_{\text{ph}}}{2}} \quad (2.32)$$

and neglected the spatial extension of the sample by replacing in (2.31) the argument of the light quadrature by $z = 0$ for all atoms. Note that the effective Hamiltonian basically depends only on the collective atomic spin $\mathbf{J} = \sum_j \mathbf{J}^j$. Next, before studying the resulting equations of motion, we will take a closer look at the loss terms in equation (2.18).

2.5 Atomic decay

In this section we will study in more detail the loss terms given in equation (2.19). In the approximations we have adopted here, each atom will couple to its own, independent bath, such that it is enough to study these terms on the single atom level. For a ground state observable O of atom j, losses are described by

$$\mathcal{L}(A) = \frac{d^2\gamma}{2\hbar^2\Delta^2}\left\{2\,\widetilde{\boldsymbol{\mathcal{E}}}^-(\mathbf{r})\widetilde{\boldsymbol{\sigma}}^-\otimes\widetilde{\boldsymbol{\sigma}}^+ A\,\widetilde{\boldsymbol{\sigma}}^-\otimes\widetilde{\boldsymbol{\sigma}}^+\widetilde{\boldsymbol{\mathcal{E}}}^+ - \left[\widetilde{\boldsymbol{\mathcal{E}}}^-\widetilde{\boldsymbol{\sigma}}^-\otimes\widetilde{\boldsymbol{\sigma}}^+\cdot\widetilde{\boldsymbol{\mathcal{E}}}^+, A\right]_+\right\}$$
$$- i\frac{d\sqrt{\gamma}}{\hbar\Delta}\left\{\mathbf{f}^-\cdot[\widetilde{\boldsymbol{\sigma}}^-\otimes\widetilde{\boldsymbol{\sigma}}^+\widetilde{\boldsymbol{\mathcal{E}}}^+, A] + [\widetilde{\boldsymbol{\mathcal{E}}}^-\,\widetilde{\boldsymbol{\sigma}}^-\otimes\widetilde{\boldsymbol{\sigma}}^+, A]\cdot\mathbf{f}^+\right\}. \quad (2.33)$$

In order to bring out the structure of this expression more clearly, we suppressed all indices j as well as the arguments r_j of the coherent field amplitude.

It is instructive and a good test to cross check the validity of the present approach, to derive from equation (2.33) a master equation for the atomic density operator $\hat{\rho}$. Neglecting coherent evolution for the moment, the average of any observable A will evolve as

$$\mathrm{tr}\left\{A\dot{\hat{\rho}}\right\} = \mathrm{tr}\left\{\dot{A}\hat{\rho}\right\} = \mathrm{tr}\{\mathcal{L}(A)\hat{\rho}\}$$
$$= \mathrm{tr}\left\{A\frac{d^2\gamma}{2\hbar^2\Delta^2}\left(2\,\mathrm{Sp}\left\{\widetilde{\boldsymbol{\sigma}}^-\otimes\widetilde{\boldsymbol{\sigma}}^+\widetilde{\boldsymbol{\mathcal{E}}}^+\hat{\rho}\widetilde{\boldsymbol{\mathcal{E}}}^-(\mathbf{r})\widetilde{\boldsymbol{\sigma}}^-\otimes\widetilde{\boldsymbol{\sigma}}^+\right\}\right.\right.$$
$$\left.\left. - \left[\widetilde{\boldsymbol{\mathcal{E}}}^-\widetilde{\boldsymbol{\sigma}}^-\otimes\widetilde{\boldsymbol{\sigma}}^+\cdot\widetilde{\boldsymbol{\mathcal{E}}}^+, \hat{\rho}\right]_+\right)\right\},$$

where we used the cyclic property of the trace and the fact that Langevin noise operators have zero mean. The symbol $\mathrm{Sp}\{M\}$ denotes the trace of the 3×3 matrix M. This equation holds for arbitrary observables and therefore as an operator identity for the density matrix itself, that is

$$\dot{\hat{\rho}} = \frac{d^2\gamma}{2\hbar^2\Delta^2}\left(2\,\mathrm{Sp}\left\{\widetilde{\boldsymbol{\sigma}}^-\otimes\widetilde{\boldsymbol{\sigma}}^+\widetilde{\boldsymbol{\mathcal{E}}}^+\hat{\rho}\widetilde{\boldsymbol{\mathcal{E}}}^-(\mathbf{r})\widetilde{\boldsymbol{\sigma}}^-\otimes\widetilde{\boldsymbol{\sigma}}^+\right\} - \left[\widetilde{\boldsymbol{\mathcal{E}}}^-\widetilde{\boldsymbol{\sigma}}^-\otimes\widetilde{\boldsymbol{\sigma}}^+\cdot\widetilde{\boldsymbol{\mathcal{E}}}^+, \hat{\rho}\right]_+\right).$$

This master equation is identical to the one, which was derived in [23] in the context of sisyphus cooling under the same approximations that we have adopted here. We refer to [23] for an alternative derivation in the Schrödinger picture and for further remarks.

Next we will use the results of the preceding sections to specialize equation (2.33) to our one dimensional model. Taking into account the decomposition of the ground state polarizability equations, (2.22) and (2.23), as well as

the explicit form of the x-polarized coherent amplitude (2.25), we find for equation (2.33)

$$\mathcal{L}^j(A) = \frac{\eta}{T}\left\{J_z^j A J_z^j + J_y^j A J_y^j - \frac{1}{2}A\right\} \tag{2.34}$$
$$+ \sqrt{\frac{\eta}{T}}\Big\{f_y^-[J_z^j, A] - [J_z^j, A]f_y^+ - f_z^-[J_y^j, A] + [J_y^j, A]f_z^+\Big\},$$

where we defined a dimensionless decay parameter

$$\eta = \frac{d^2\gamma\omega N_{\rm ph}a_1^2}{2\hbar\Delta^2\epsilon_0 Ac}. \tag{2.35}$$

Remember that T is the pulse length, which naturally determines not only the duration of the interaction but also of atomic decay[3].

On the basis of the same reasoning as above we can read off the corresponding master equation for the density operator $\hat{\rho}$, which reads

$$\begin{aligned}\mathcal{L}(\hat{\rho}) &= \frac{\eta}{T}\left\{J_z\hat{\rho}J_z + J_y\hat{\rho}J_y - \frac{1}{2}\hat{\rho}\right\} \\ &= \frac{\eta}{T}\left\{J_z\hat{\rho}J_z - \frac{1}{4}\hat{\rho}\right\} + \frac{\eta}{T}\left\{J_y\hat{\rho}J_y - \frac{1}{4}\hat{\rho}\right\}.\end{aligned} \tag{2.36}$$

In the second line we wrote the decay of ρ in the form of a sum of two decay terms, whose form is familiar from the description of collisional dephasing. Spontaneous emission obviously leads to simultaneous dephasing in both, the y and z basis. In the next section, where we finally evaluate the equations of motion, we will see that this leads to decay of the y and z component of the atomic spin at a rate $\eta/2T$, while the x component decays at twice this rate, as is to be expected, since both decay processes contribute here. Note also, that the fixed point of the map, defined by (2.36), is the identity. That is, each atom will decay to the completely mixed, unpolarized state.

2.6 Linearization of equations of motion

In this section we will evaluate the Heisenberg equations of motion for the relevant degrees of freedom, that is the collective spin,

$$\mathbf{J} = \sum_j \mathbf{J}^j,$$

[3]We prefer to keep T explicitly in equation (2.34), because we are in the end interested in input-output relations describing the scattering process, in which η and not the rate η/T will be the relevant parameter.

and quadratures of y polarized light propagating along z, $x(z), p(z)$ introduced in (2.30). Any of these observables will evolve as

$$\dot{A} = \frac{i}{\hbar}[H_{\rm li} + H_{\rm int}^{\rm eff}, A] + \sum_j \mathcal{L}_j(A),$$

where $H_{\rm li}$ is given in equation (2.27), $H_{\rm int}^{\rm eff}$ in equation (2.31) and the superoperator $\mathcal{L}_j$ in (2.34). Evaluating this equation we arrive at Maxwell-Bloch equations, which read for spin degrees of freedom

$$\frac{d}{dt}J_x = -\frac{\eta}{T}J_x + \frac{\chi}{\sqrt{T}}J_y p(0,t) + i\sqrt{\frac{\eta}{T}}\sum_j \left(f_{j,y}^- J_y^j - J_y^j f_{j,y}^+ + f_{j,z}^- J_z^j - J_z^j f_{j,z}^+\right), \tag{2.37a}$$

$$\frac{d}{dt}J_y = -\frac{\eta}{2T}J_y - \frac{\chi}{\sqrt{T}}J_x p(0,t) - i\sqrt{\frac{\eta}{T}}\sum_j \left(f_{j,y}^- J_x^j - J_x^j f_{j,y}^+\right), \tag{2.37b}$$

$$\frac{d}{dt}J_z = -\frac{\eta}{2T}J_z - i\sqrt{\frac{\eta}{T}}\sum_j \left(f_{j,z}^- J_x^j - J_x^j f_{j,z}^+\right), \tag{2.37c}$$

and for light variables

$$\left(\frac{\partial}{\partial t} + c\frac{\partial}{\partial z}\right)x(z,t) = -\frac{\chi c}{\sqrt{T}}J_z(t)\delta(z), \tag{2.38a}$$

$$\left(\frac{\partial}{\partial t} + c\frac{\partial}{\partial z}\right)p(z,t) = 0. \tag{2.38b}$$

The physical meaning of these equations is quite clear: The second terms in equations (2.37a) and (2.37b) describe rotation of the collective spin about the z axis by an angle, which is determined by the p-quadrature of y polarized light. The first and last terms in the Bloch equations (2.37) describe decay and Langevin noise forces due to spontaneous emission. The Maxwell equations in turn show, that the x quadrature, that is the component of y polarized light which oscillates in phase with the coherent x polarized pulse, acquires a signal proportional to the z component of the collective spin. The p quadrature (out-of-phase component) is conserved.

Note that the noise terms in the Bloch equations do depend on system operators. This is in fact essential to preserve the angular momentum commutation relations $[J_x, J_y] = iJ_z$ etc., as can be easily checked by solving the equations to first order in η and taking commutators.

These equations have to be integrated up to a time T, when the pulse leaves the sample. As initial conditions we assume, that the quantum field

is in vacuum and that the atomic sample is in a coherent spin state with maximal polarization along x, that is

$$\begin{aligned} \langle J_x(0)\rangle &= N_{\mathrm{at}}/2 \\ \Delta J_y^2(0) &= \Delta J_y^2(0) = N_{\mathrm{at}}/4. \end{aligned} \tag{2.39}$$

The variance of observable A is as usually defined by $\Delta A^2 = \langle A^2\rangle - \langle A\rangle^2$.

We assume furthermore that losses are small, that is

$$\eta \ll 1.$$

It is important to note here that this assumption in fact implies $\chi \ll 1$, as follows from equations (2.32) and (2.35), from which one can conclude

$$\chi^2 = \eta\frac{\sigma_{\mathrm{res}}}{A}, \tag{2.40}$$

where $\sigma_{\mathrm{res}} = 3\lambda_0^2/2\pi$ is the scattering cross section on resonance of the probed transition (and, as before, A is the cross section of the beam).

For the given initial conditions and with the assumptions stated above, it is possible to linearize the equations of motion for the collective atomic spin. The central idea is, that the mean polarization along x can be treated as a classical variable, while only transverse spin components are relevant quantum degrees of freedom. This approximation can be formalized by means of a method known as group contraction, introduced by Wigner [24, 25], or by means of a technique known as Holstein-Primakoff transformation and approximation [26]. Here we will use the latter method. We point out, that this approximation does not rely on the exact initial conditions stated above, but give good results also for situation, where the initial state is close to the coherent spin state and the quantum field contains few photons. In the following we will thus not use explicitly the fact that the transverse spin components and light quadratures have zero mean.

Let us first examine the evolution of the mean polarization along x. Solving equation (2.37a) to first order in η and χ and taking into account that $p(z,t) = p(z-ct,0)$ we find for the mean of J_x

$$\langle J_x(T)\rangle = (1-\eta)\langle J_x(0)\rangle - \chi\langle J_y(0)\rangle\langle p(0)\rangle, \tag{2.41}$$

where we introduced the normalized light quadrature for the entire pulse $p(0) = 1/\sqrt{T}\int_0^T dt p(-ct,0)$. We see, that the mean polarization along x will only be slightly rotated away from x and suffer small decay, such that after the interaction we still have a large polarization along x.

Keeping this in mind, let us now make use of the Holstein-Primakoff transformation, which consists in expressing the collective step up/down operators (along x), $J_\pm = J_y \pm i J_z$ in terms of bosonic creation and annihilation operators, $[b, b^\dagger] = \mathbb{1}$, as

$$J_+ = \sqrt{N_{\rm at}}\sqrt{\mathbb{1} - b^\dagger b/N_{\rm at}}\; b, \qquad J_- = \sqrt{N_{\rm at}}\; b^\dagger\sqrt{\mathbb{1} - b^\dagger b/N_{\rm at}}.$$

It is easily checked that these operators satisfy the correct commutation relations $[J_+, J_-] = 2J_x$ if one identifies $J_x = N_{\rm at}/2 - b^\dagger b$. The fully polarized initial state thus corresponds to the ground state of a fictitious harmonic oscillator. Note that this mapping is exact. Now, under the condition that $\langle b^\dagger b\rangle \ll N_{\rm at}$, which is here guaranteed by (2.41), one can approximate $J_+ \simeq \sqrt{N_{\rm at}}\, b$ and $J_- \simeq \sqrt{N_{\rm at}}\, b^\dagger$ or, for the transverse spin components,

$$J_y = \sqrt{N_{\rm at}/2}\, X, \qquad J_z = \sqrt{N_{\rm at}/2}\, P,$$

where $X = (b + b^\dagger)/\sqrt{2}$ and $P = -i(b - b^\dagger)/\sqrt{2}$. In terms of these canonical operators the initial conditions in (2.39) read

$$\langle X(0)\rangle = \langle P(0)\rangle = 0, \qquad \Delta X^2(0) = \Delta P^2(0) = 1/2.$$

The corresponding Maxwell-Bloch equations in terms of these operators follow from (2.37b), (2.37c) and (2.38),

$$\frac{d}{dt}X = -\frac{\eta}{2T}X + \frac{\kappa}{\sqrt{T}}p(0,t) + \sqrt{\frac{\eta}{T}}f_X(t), \tag{2.42a}$$

$$\frac{d}{dt}P = -\frac{\eta}{2T}P + \sqrt{\frac{\eta}{T}}f_P(t), \tag{2.42b}$$

$$\left(\frac{\partial}{\partial t} + c\frac{\partial}{\partial z}\right)x(z,t) = \frac{\kappa c}{\sqrt{T}}P(t)\delta(z), \tag{2.42c}$$

$$\left(\frac{\partial}{\partial t} + c\frac{\partial}{\partial z}\right)p(z,t) = 0. \tag{2.42d}$$

where we defined the effective coupling strength

$$\kappa = -\chi\sqrt{N_{\rm at}/2}. \tag{2.43}$$

We introduced here new Langevin noise operators

$$f_X(t) = -i\sqrt{2/N_{\rm at}}\sum_j \left(f^-_{j,y}J^j_x - J^j_x f^+_{j,y}\right), \tag{2.44a}$$

$$f_P(t) = -i\sqrt{2/N_{\rm at}}\sum_j \left(f^-_{j,z}J^j_x - J^j_x f^+_{j,z}\right), \tag{2.44b}$$

which are still of zero mean and have variances,

$$\langle f_X(t) f_X(t') \rangle = \langle f_P(t) f_P(t') \rangle = \delta(t - t')/2.$$

However, as mentioned before, they have the unpleasant property of not commuting with the system operators X, P. Since this property assures the preservation of commutation relations, it is not possible to merely replace $J_x^j \to 1/2$ in (2.44), as would be suggested by the Holstein-Primakoff approximation. If this is done, then one has to compensate by imposing the commutation relations

$$[f_X(t), f_P(t')] = i\delta(t - t') \tag{2.45}$$

for the Langevin operators, since this will again preserve the canonical commutation relations $[X, P] = i$. In the following, we will adopt this condition.

Equations (2.42) are the central result of this chapter. There are two points, which should be remarked here:

Note first that the coupling of light and atoms is collectively enhanced by a factor of $\sqrt{N_{\rm at}/2}$, as is evident from (2.43), while the decay of the collective atomic spin happens still at the rate η/T of the decay of a single spin. Thus, it is possible to have $\eta \ll 1$ and at the same time a large coupling $\kappa \gtrsim 1$.

Second, the coherent part of the interaction is generated by the Hamiltonian

$$H = H_{\rm li} + \frac{\kappa}{\sqrt{T}} P p(0), \tag{2.46}$$

where $H_{\rm li}$ is given in (2.27). Note in particular that this Hamiltonian is quadratic in the canonical operators X, P and $x(z), p(z)$. If the initial states of light and atoms is a Gaussian state, as is the case if atoms are prepared in a coherent spin state and light is in vacuum or in some coherent state, then the Gaussian character is preserved in the interaction. This implies, that the state is entirely determined by the first and second moments of the canonical operators.

2.7 Solutions for various setups and applications

In this section we will solve the Maxwell-Bloch equations (2.42) for two setups corresponding to recent experiments. The first scenario corresponds exactly to the setup considered so far, and was used in [27] to perform a quantum non demolition measurement of a collective atomic spin, as was originally proposed by Kuzmich et.al. in [28]. The second setup consists of two samples

placed in oppositely oriented magnetic fields, or equivalently, to two samples in the same field but with oppositely oriented spins. This setup was used in [10] to create entanglement between the two collective spins, as was originally proposed by Duan et.al. in [13]. In order to bring out the basic ideas of these experiments more clearly, we will focus here on the coherent interaction and neglect losses for the moment taking $\eta = 0$.

Quantum non demolition measurement and spin squeezing

This section concerns the most simple case of a single collective spin interacting with light in the one way as was considered in the preceding sections. In order to integrate the Maxwell-Bloch equations (2.42) it is convenient to introduce a new position variable $\xi = ct - z$ to eliminate the z dependence. New light quadratures defined by $\bar{x}(\xi, t) = x(ct - \xi, t)$, $\bar{p}(\xi, t) = p(ct - \xi, t)$ also have a simple interpretation: ξ labels the slices of the pulse moving in and out of the ensemble one after the other, starting with $\xi = 0$ and terminating at $\xi = cT$. The Maxwell equations now read

$$\frac{\partial}{\partial t}\bar{p}(\xi, t) = 0, \quad \frac{\partial}{\partial t}\bar{x}(\xi, t) = \frac{\kappa c}{\sqrt{T}} P(t)\delta(ct - \xi). \tag{2.47}$$

These equations together with (2.42a) and (2.42b) have to be integrated form t=0 at which the classical pulse is assumed to enter the sample up to time T when the pulse terminates. Integrating the Maxwell-Bloch equation causes no problems and the well known solutions are given by

$$X^{\,\mathrm{out}} = X^{\,\mathrm{in}} + \kappa p^{\,\mathrm{in}}, \quad P^{\,\mathrm{out}} = P^{\,\mathrm{in}}, \tag{2.48a}$$

$$x^{\,\mathrm{out}} = x^{\,\mathrm{in}} + \kappa P^{\,\mathrm{in}}, \quad p^{\,\mathrm{out}} = p^{\,\mathrm{in}}. \tag{2.48b}$$

where we defined input/output operators as

$$X^{\,\mathrm{in}} = X(0) \qquad X^{\,\mathrm{out}} = X(T)$$

$$x^{\,\mathrm{in}} = \frac{1}{\sqrt{T}} \int_0^T \mathrm{d}\tau \bar{x}(c\tau, 0) \qquad x^{\,\mathrm{out}} = \frac{1}{\sqrt{T}} \int_0^T \mathrm{d}\tau \bar{x}(c\tau, T)$$

and the same for P and p.

We see that x quadratures of both systems acquire signals of the p quadratures of the other system, while preserving them. The interaction thus fulfills the criteria for a quantum non demolition measurement [29]. The measurement of $x^{\,\mathrm{out}}$ can be performed in a standard polarimetric measurement of Stokes vector components [14] and the result will given an estimate of P.

Conditioned on the measurement outcome, the variance of a subsequent measurement of P will then be altered. The classical formula for conditional variances of a Gaussian random variable still applies and yields

$$(\Delta P)^2|_{x^{\rm out}} = (\Delta P^{\rm out})^2 - \frac{\langle P^{\rm out} x^{\rm out}\rangle}{2\langle (x^{\rm out})^2\rangle} = \frac{1}{2}\frac{1}{1+\kappa^2}.$$

As compared to a coherent spin state, the variance will be reduced by a factor $1/(1+\kappa^2)$. The measurement thus leaves the atomic spin in a squeezed state, conditioned on the measurement result. By means of a subsequent feedback process, the squeezing can be prepared unconditional. The most advanced experiment along this line, using continuous feedback, is [27] and demonstrated squeezing of about one order of magnitude.

Entanglement of two collective spins

If two samples, described by two pairs of canonical conjugate operators $[X_k, P_k] = i\delta_{kl}$, $k,l = 1,2$, are placed in two oppositely oriented magnetic fields aligned along x, the direction of polarization, the full Hamiltonian of the system is given by

$$\begin{aligned} H &= H_{\rm at} + H_{\rm li} + H_{\rm int}, \\ H_{\rm at} &= \frac{\hbar\Omega}{2}(X_1^2 + P_1^2) - \frac{\hbar\Omega}{2}(X_2^2 + P_2^2), \\ H_{\rm int} &= \frac{\hbar\kappa}{\sqrt{T}}(P_1 + P_2)p(0) \end{aligned} \tag{2.49}$$

The magnetic fields can be safely added like this under the condition that the Larmor frequency Ω is much smaller than any other time scale in the problem, which is well fulfilled for frequencies up to several 100 kHz.

In $H_{\rm int}$ we have neglected the distance between the two samples and placed them formally both at $z = 0$. Note that this assumption can easily be dropped and the results below still hold in exactly the same form.

It is convenient to change in the atomic subsystem to EPR modes defined by $X_\pm = (X_1 \pm X_2)/\sqrt{2}$, $P_\pm = (P_1 \pm P_2)/\sqrt{2}$ in terms of which the free atomic Hamiltonian becomes $H_{\rm at} = \Omega(X_+X_- + P_+P_-)$. Changing to an interaction picture with respect to $H_{\rm at}$ and evaluating the Heisenberg equations

yields the Maxwell-Bloch equations

$$\begin{aligned}
\frac{\partial}{\partial t}X_+(t) &= \kappa\sqrt{\frac{2}{T}}\cos(\Omega t)p(0,t), \quad \frac{\partial}{\partial t}P_+(t) = 0,\\
\frac{\partial}{\partial t}P_-(t) &= -\kappa\sqrt{\frac{2}{T}}\sin(\Omega t)p(0,t), \quad \frac{\partial}{\partial t}X_-(t) = 0,\\
\frac{\partial}{\partial t}\bar{x}(\xi,t) &= \kappa c\sqrt{\frac{2}{T}}\left[\cos(\Omega t)P_+(t) + \sin(\Omega t)X_-(t)\right]\delta(ct-\xi),\\
\frac{\partial}{\partial t}\bar{p}(\xi,t) &= 0.
\end{aligned}$$

The integration is again straight forward and one arrives at the input/output relations

$$X_+^{\rm out} = X_+^{\rm in} + \kappa p_{\rm c}^{\rm in} \qquad x_{\rm c}^{\rm out} = x_{\rm c}^{\rm in} + \kappa P_+^{\rm in} \tag{2.50a}$$

$$P_+^{\rm out} = P_+^{\rm in} \qquad p_{\rm c}^{\rm out} = p_{\rm c}^{\rm in} \tag{2.50b}$$

$$X_-^{\rm out} = X_-^{\rm in} \qquad x_{\rm s}^{\rm out} = x_{\rm s}^{\rm in} + \kappa X_-^{\rm in} \tag{2.50c}$$

$$P_-^{\rm out} = P_-^{\rm in} - \kappa p_{\rm s}^{\rm in} \qquad p_{\rm s}^{\rm out} = p_{\rm s}^{\rm in} \tag{2.50d}$$

where we defined input output operators of a cosine modulation mode as

$$p_{\rm c}^{\rm in[out]} = \sqrt{\frac{2}{T}}\int_0^T {\rm d}\tau\cos(\Omega\tau)\bar{p}(c\tau, 0[T]), \tag{2.51a}$$

$$x_{\rm c}^{\rm in[out]} = \sqrt{\frac{2}{T}}\int_0^T {\rm d}\tau\cos(\Omega\tau)\bar{x}(c\tau, 0[T]) \tag{2.51b}$$

and the same for the pairs $x_{\rm s}^{\rm in[out]}$, $p_{\rm s}^{\rm in[out]}$ with $\cos(\Omega\tau)$ replaced by $\sin(\Omega\tau)$. In deriving the second equations in (2.50a) and (2.50c) we made use of $\int_0^T {\rm d}\tau\cos(\Omega\tau)\sin(\Omega\tau) = \mathcal{O}(n_0^{-1}) \simeq 0$. In frequency space these modes consist of spectral components at sidebands $\omega_c \pm \Omega$ and are in fact closely related to the sideband modulation modes introduced in [30, 31] for the description of two photon processes. It is easily checked that these modes are asymptotically canonical, $[x_{\rm c}^{\rm in}, p_{\rm c}^{\rm in}] = [x_{\rm s}^{\rm in}, p_{\rm s}^{\rm in}] = i[1 + \mathcal{O}(n_0^{-1})] \simeq i$, and independent, $[x_{\rm c}^{\rm in}, p_{\rm s}^{\rm in}] = \mathcal{O}(n_0^{-1}) \simeq 0$, if we assume $n_0 \gg 1$ for $n_0 = \Omega T$, the pulse length measured in periods of Larmor precession.

Note that the solution (2.50) falls naturally into two groups (2.50a),(2.50b) and (2.50c),(2.50d) which have each, up to a phase difference, the same structure as the solution (2.48) in the last section. Thus, by means of a measurement of $x_{\rm s}^{\rm out}$ and $x_{\rm c}^{\rm out}$ the two commuting observables X_- and P_+ will be squeezed by a factor $1/(1+\kappa^2)$, just as in the preceding section. This implies

in particular, that the state of the two atomic spins is entangled, as follows from the criterion for entanglement of symmetric Gaussian states [32],

$$1 > \Delta EPR = \left(\Delta X_-^2 + P_+^2\right) = \frac{1}{1+\kappa^2}.$$

In experiment [10] entanglement of two macroscopic objects – each sample contained about 10^{12} atoms - was demonstrated along these lines.

Chapter 3

Teleportation of quantum states from light onto atoms

Quantum teleportation - the disembodied transport of quantum states - has been demonstrated so far in several seminal experiments dealing with purely photonic [33, 34, 35, 36, 37, 38, 39, 40, 41, 42, 43, 44] or atomic [45, 46] systems. Here we propose a protocol for the teleportation of a coherent state carried initially by a pulse of light onto the collective spin state of atoms. This protocol - just as the recently demonstrated direct transfer of a quantum state of light onto atoms [11] - is particularly relevant for long distance entanglement distribution, a key resource in quantum communication networks [47].

Our scheme can be implemented with just coherent light and room-temperature atoms in a *single* vapor cell placed in a homogeneous magnetic field. Existing protocols in Quantum Information (QI) with continuous variables of atomic ensembles and light [47] are commonly designed for setups where no external magnetic field is applied such that the interaction of light with atoms meets the Quantum non-demolition (QND) criteria [48, 49], as was discussed in section 2.7. In contrast, in all experiments dealing with vapor cells at room-temperature [11, 10] it is, for technical reasons, absolutely essential to employ magnetic fields. In experiments [11, 10] two cells with counter-rotating atomic spins were used to comply with both, the need for an external magnetic field and the one for an interaction of QND character, as was also explained in section 2.7. So far it was believed to be impossible to use a single cell in a magnetic field to implement QI protocols, since in this case - due to the Larmor precession - scattered light simultaneously reads out two non-commuting spin components such that the interaction is not of QND type.

In this chapter we do not only show that it is well possible to make use

of the quantum state of light and atoms created in this setup but we demonstrate that - for the purpose of teleportation [50, 51] - it is in fact better to do so. As compared to the state resulting from the common QND interaction the application of an external magnetic field enhances the creation of correlations between atoms and light, generating more and qualitatively new, multimode type of entanglement. The results of the chapter can be summarized as follows:
(*i*) Larmor precession in an external magnetic field enhances the creation of entanglement when a collective atomic spin is probed with off-resonant light. The resulting entanglement involves multiple modes and is stronger as compared to what can be achieved in a comparable QND interaction.
(*ii*) This type of entangled state can be used as a resource in a teleportation protocol, which is a simple generalization of the standard protocol [50, 51] based on Einstein-Podolsky-Rosen (EPR) type of entanglement. For the experimentally accessible parameter regime the teleportation fidelity is close to optimal. The protocol is robust against imperfections and can be implemented with state of the art technique.
(*iii*) Homodyne detection of appropriate scattering modes of light leaves the atomic state in a spin squeezed state. The squeezing can be the same as attained from a comparable QND measurement of the atomic spin [52, 27]. The same scheme can be used for atomic state read-out of the Larmor precessing spin, necessary to verify successful teleportation.

We would like to note that it was shown recently in [53] that the effect of a magnetic field can enhance the capacity of a quantum memory in the setup of two cells. Teleportation in the setup of a single cell without magnetic field was addressed in [54].

3.1 Single sample in a magnetic field

As follows from chapter 2 the Hamiltonian is in this case given by

$$\begin{aligned} H &= H_{at} + H_{li} + V, \\ H_{at} &= \frac{\hbar\Omega}{2}(X^2 + P^2), \\ V &= \frac{\hbar\kappa}{\sqrt{T}} P p(0). \end{aligned} \tag{3.1}$$

Changing to a rotating frame with respect to H_{at} by defining $X_I(t) = \exp(-iH_{at}t)X\exp(iH_{at}t)$ and evaluating the Heisenberg equations for these

operators yields the following Maxwell-Bloch equations

$$\begin{aligned}
\frac{\partial}{\partial t}X_I(t) &= \frac{\kappa}{\sqrt{T}}\cos(\Omega t)p(0,t), && \text{(3.2a)}\\
\frac{\partial}{\partial t}P_I(t) &= \frac{\kappa}{\sqrt{T}}\sin(\Omega t)p(0,t), && \text{(3.2b)}\\
\left(\frac{\partial}{\partial t}+c\frac{\partial}{\partial z}\right)x(z,t) &= \frac{\kappa c}{\sqrt{T}}\left[\cos(\Omega t)P_I(t)-\sin(\Omega t)X_I(t)\right]\delta(z),\\
\left(\frac{\partial}{\partial t}+c\frac{\partial}{\partial z}\right)p(z,t) &= 0.
\end{aligned}$$

These equations have a clear interpretation. Light noise coming from the field in quadrature with the classical probe piles up in both, the X and P spin quadrature, but it alternately affects only one or the other, changing with a period of $1/\Omega$. Conversely atomic noise adds to the in phase field quadrature only and the signal comes alternately from the X and P spin quadrature. The out of phase field quadrature is conserved in the interaction.

It will again be convenient to introduce the position variable, $\xi = ct - z$, to eliminate the z dependence and to define new light quadratures by $\bar{x}(\xi,t) = x(ct-\xi,t)$, $\bar{p}(\xi,t) = p(ct-\xi,t)$. The Maxwell equations now read

$$\frac{\partial}{\partial t}\bar{p}(\xi,t) = 0, \qquad \text{(3.2c)}$$

$$\frac{\partial}{\partial t}\bar{x}(\xi,t) = \frac{\kappa c}{\sqrt{T}}\left[\cos(\Omega t)P_I(t)-\sin(\Omega t)X_I(t)\right]\delta(ct-\xi). \qquad \text{(3.2d)}$$

The solutions to equations (3.2a, 3.2b, 3.2c) are

$$X_I(t) = X_I(0) + \frac{\kappa}{\sqrt{T}}\int_0^t \mathrm{d}\tau\cos(\Omega\tau)\bar{p}(c\tau,0), \qquad \text{(3.3a)}$$

$$P_I(t) = P_I(0) + \frac{\kappa}{\sqrt{T}}\int_0^t \mathrm{d}\tau\sin(\Omega\tau)\bar{p}(c\tau,0), \qquad \text{(3.3b)}$$

$$\bar{p}(\xi,t) = \bar{p}(\xi,0) \qquad \text{(3.3c)}$$

and the formal solution to (3.2d) is

$$\bar{x}(\xi,t) = \bar{x}(\xi,0) + + \frac{\kappa}{\sqrt{T}}\left[\cos(\Omega\xi/c)P_I(\xi/c)-\sin(\Omega\xi/c)X_I(\xi/c)\right]. \qquad \text{(3.3d)}$$

As mentioned before, both atomic spin quadratures are affected by light but, as is evident from the solutions for $X(t)$, $P(t)$, they receive contributions from different and, in fact, orthogonal projections of the out-of-phase field. As we

will show in the following, the corresponding projections of the in-phase field carry in turn the signal of atomic quadratures after the interaction. In terms of cosine and sine modulation modes introduced in Eq. (2.51) the atomic state after the interaction $X^{\,\mathrm{out}} = X_I(T)$, $P^{\,\mathrm{out}} = P_I(T)$ is given by

$$X^{\,\mathrm{out}} = X^{\,\mathrm{in}} + \frac{\kappa}{\sqrt{2}} p_{\mathrm{c}}^{\mathrm{in}}, \quad P^{\,\mathrm{out}} = P^{\,\mathrm{in}} + \frac{\kappa}{\sqrt{2}} p_{\mathrm{s}}^{\mathrm{in}}. \tag{3.4a}$$

The final state of cosine (sine) modes is described by $x_{\mathrm{c(s)}}^{\mathrm{out}}$, $p_{\mathrm{c(s)}}^{\mathrm{out}}$, defined by equations (2.51) with $\bar{x}(c\tau, 0)$, $\bar{p}(c\tau, 0)$ replaced by $\bar{x}(c\tau, T)$, $\bar{p}(c\tau, T)$ respectively. Since the out-of-phase field is conserved we trivially have

$$p_{\mathrm{c}}^{\mathrm{out}} = p_{\mathrm{c}}^{\mathrm{in}}, \quad p_{\mathrm{s}}^{\mathrm{out}} = p_{\mathrm{s}}^{\mathrm{in}}. \tag{3.4b}$$

Deriving the corresponding expressions for the cosine and sine components of the field in phase, $x_{\mathrm{c}}^{\mathrm{out}}$, $x_{\mathrm{s}}^{\mathrm{out}}$, raises some difficulties connected to the back action of light onto itself. This effect can be understood by noting that a slice ξ of the pulse receives a signal of atoms at a time ξ/c [see equation (3.3d)] which, regarding equations (3.3a, 3.3b), in turn carry already the integrated signal of all slices up to ξ. Thus, mediated by the atoms, light acts back on itself. In order to evaluate the input/output relations for the cosine and sine components of the in-phase field we take equation (3.3d) at $\xi = c\tau$, $t = T$, multiply by $\sqrt{2/T}\,\cos(\Omega\tau)$ and integrate over τ from 0 to T. Using equations (3.3a, 3.3b) and the approximate orthogonality of $\cos(\Omega\tau)$ and $\sin(\Omega\tau)$ one finds

$$\begin{aligned} x_{\mathrm{c}}^{\mathrm{out}} = x_{\mathrm{c}}^{\mathrm{in}} + \frac{\kappa}{\sqrt{2}} P^{\,\mathrm{in}} + \\ + \frac{\sqrt{2}\kappa^2}{T^{3/2}} \int_0^T \mathrm{d}\tau \int_0^\tau \mathrm{d}\tau' [\cos(\Omega\tau)^2 \sin(\Omega\tau') \bar{p}(c\tau', 0) - \\ - \cos(\Omega\tau)\sin(\Omega\tau)\cos(\Omega\tau')\bar{p}(c\tau', 0)]. \end{aligned}$$

After interchanging the order of integration, $\int_0^T \mathrm{d}\tau \int_0^\tau \mathrm{d}\tau' \to \int_0^T \mathrm{d}\tau' \int_{\tau'}^T \mathrm{d}\tau$ one can perform the integration over τ. Neglecting all terms of order n_0^{-1} or less where $n_0 = \Omega T \gg 1$ one finds

$$x_{\mathrm{c}}^{\mathrm{out}} = x_{\mathrm{c}}^{\mathrm{in}} + \frac{\kappa}{\sqrt{2}} P^{\,\mathrm{in}} + \frac{\sqrt{2}\kappa^2}{T^{3/2}} \int_0^T \mathrm{d}\tau \frac{T-\tau}{2} \sin(\Omega\tau)\bar{p}(c\tau, 0).$$

The last term represents back action of light onto itself. It can be expressed as a sum of two terms, one proportional to $p_{\mathrm{s}}^{\mathrm{in}}$ and another one proportional to

$$p_{\mathrm{s},1}^{\mathrm{in}} = \sqrt{3}\left(\frac{2}{T}\right)^{3/2} \int_0^T \mathrm{d}\tau \left(\frac{T}{2} - \tau\right) \sin(\Omega\tau)\bar{p}(c\tau, 0). \tag{3.4c}$$

It is easily verified that the back action mode defined by this equation and the corresponding expression for $x_{\mathrm{s}}^{\mathrm{back}}$ is canonical $[x_{\mathrm{s},1}^{\mathrm{in}}, p_{\mathrm{s},1}^{\mathrm{in}}] = i[1-\mathcal{O}(n_0^{-2})] \simeq i$ and independent from all the other modes introduced so far, f.e. $[x_{\mathrm{s}}^{\mathrm{in}}, p_{\mathrm{s},1}^{\mathrm{in}}] = \mathcal{O}(n_0^{-2}) \simeq 0$. The variance is thus $(\Delta p_{\mathrm{s},1}^{\mathrm{in}})^2 = 1/2$. Repeating the calculation for $x_{\mathrm{s}}^{\mathrm{out}}$ with appropriate replacements and a definition of $p_{\mathrm{c},1}^{\mathrm{in}}$ analogous to equation (3.4c) finally yields

$$x_{\mathrm{c}}^{\mathrm{out}} = x_{\mathrm{c}}^{\mathrm{in}} + \frac{\kappa}{\sqrt{2}} P^{\mathrm{in}} + \left(\frac{\kappa}{2}\right)^2 p_{\mathrm{s}}^{\mathrm{in}} + \frac{1}{\sqrt{3}} \left(\frac{\kappa}{2}\right)^2 p_{\mathrm{s},1}^{\mathrm{in}}, \tag{3.4d}$$

$$x_{\mathrm{s}}^{\mathrm{out}} = x_{\mathrm{s}}^{\mathrm{in}} - \frac{\kappa}{\sqrt{2}} X^{\mathrm{in}} - \left(\frac{\kappa}{2}\right)^2 p_{\mathrm{c}}^{\mathrm{in}} - \frac{1}{\sqrt{3}} \left(\frac{\kappa}{2}\right)^2 p_{\mathrm{c},1}^{\mathrm{in}}. \tag{3.4e}$$

The last two terms in both lines represent the effect of back action, part of which involves the already defined cosine and sine components of the field in quadrature. The remaining part is subsumed in the back action modes which are again canonical and independent from all other modes.

Equations (3.4) describe the final state of atoms and the relevant part of scattered light after the pulse has passed the atomic ensemble and are the central result of this section. Treating the last terms in equations (3.4d,3.4e) as noise terms, it is readily checked by means of the separability criteria in [55] that this state is fully inseparable, *i.e.* it is inseparable with respect to all splittings between the three modes. For the following teleportation protocol the relevant entanglement is the one between atoms and the two light modes. Figure 3.2b shows the von Neumann entropy E_{vN} of the reduced state of atoms in its dependence on the coupling strength κ.

3.2 Teleportation of light onto atoms

In this section we will show how the multimode entanglement between light and atoms generated in the scattering process can be employed in a teleportation protocol which is a simple generalization of the standard protocol for continuous variable teleportation using EPR-type entangled states [50, 51]. We first present the protocol and evaluate its fidelity and then analyze its performance under realistic experimental conditions.

Basic protocol

Figure 3.1 depicts the basic scheme which, as usually, consists of a Bell measurement and a feedback operation.

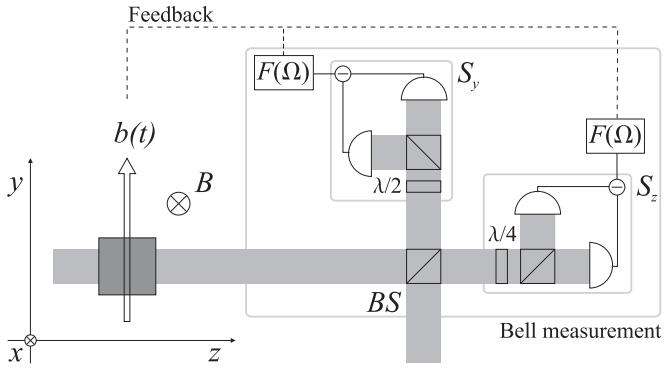

Figure 3.1: Scheme for teleportation of light onto atoms: As described in section 3.1, a classical pulse (linearly polarized along x) propagating along the positive z direction is scattered off an atomic ensemble contained in a glass cell and placed in a constant magnetic field B along x. Classical pulse and scattered light (linearly polarized along y) are overlapped with a with a coherent pulse (linearly polarized along z) at beam splitter BS. By means of standard polarization measurements Stokes vector components S_y and S_z are measured at one and the other port respectively, realizing the Bell measurement. The Fourier components at Larmor frequency Ω of the corresponding photocurrents determine the amount of conditional displacement of the atomic spin which can be achieved by applying a properly timed transverse magnetic field $b(t)$. See section 3.2 for details.

Input The coherent state to be teleported is encoded in a pulse which is linearly polarized orthogonal to the classical driving pulse and whose carrier frequency lies at the upper sideband, i.e. at $\omega_c + \Omega$. The pulse envelope has to match the one of the classical pulse. As we will show below, canonical operators y, q with $[y, q] = i$ describing this mode can conveniently be expressed in terms of cosine and sine modulation modes, analogous to equations (2.51), defined with respect to the carrier frequency, as

$$y = \frac{1}{\sqrt{2}} \left(y_{\mathrm{s}} + q_{\mathrm{c}} \right), \quad q = -\frac{1}{\sqrt{2}} \left(y_{\mathrm{c}} - q_{\mathrm{s}} \right). \tag{3.5}$$

A coherent input amounts to having initially $\Delta y^2 = \Delta q^2 = 1/2$ and an amplitude $\langle y \rangle$, $\langle q \rangle$ with mean photon number $n_{ph} = (\langle y \rangle^2 + \langle q \rangle^2)/2$.

In order to see, that the mode defined in (3.5) in deed corresponds to the upper sideband, we proceed as follows: The input field, propagating along the positive y direction and polarized along z (see figure 3.1), is described by operators $[b(\omega), b^\dagger(\omega')] = \delta(\omega - \omega')$ in frequency space and $[\hat{y}(y), \hat{q}(y')] =$

$ic\delta(y-y')$ in real space. ($\hat{y}$ is the quadrature operator for the field in-phase and y on the other hand is the position along the y-direction.) In analogy to equation (2.30) these bases are connected via

$$\begin{aligned}\hat{y}(y) &= \frac{1}{\sqrt{4\pi}}\int_b \mathrm{d}\omega \left(b(\omega)e^{-i(k_c-k)y} + h.c.\right),\\ \hat{q}(y) &= -\frac{i}{\sqrt{4\pi}}\int_b \mathrm{d}\omega \left(b(\omega)e^{-i(k_c-k)y} - h.c.\right).\end{aligned}$$

Using the definitions of cosine and sine modes (2.51) as well as $\hat{\tilde{y}}(c\tau,0) = \hat{y}(-c\tau,0)$ and the same for $\hat{q}(y)$ we have

$$\begin{aligned}y &= \frac{1}{\sqrt{T}}\int_0^T \mathrm{d}\tau \left[\sin(\Omega\tau)\hat{\tilde{y}}(c\tau,o) + \cos(\Omega\tau)\hat{\tilde{q}}(c\tau,0)\right]\\ &= \frac{-i}{\sqrt{4\pi T}}\int_0^T \mathrm{d}\tau \int_b \mathrm{d}\omega\Big[b(\omega)e^{i(\omega_c+\Omega-\omega)\tau} - h.c.\Big]\\ q &= -\frac{1}{\sqrt{T}}\int_0^T \mathrm{d}\tau \left[\cos(\Omega\tau)\hat{\tilde{y}}(c\tau,o) - \sin(\Omega\tau)\hat{\tilde{q}}(c\tau,0)\right]\\ &= \frac{-1}{\sqrt{4\pi T}}\int_0^T \mathrm{d}\tau \int_b \mathrm{d}\omega\Big[b(\omega)e^{i(\omega_c+\Omega-\omega)\tau} + h.c.\Big].\end{aligned}$$

To explicitly see that this corresponds to a pulse centered at the upper sideband it is convenient to change to a more precise model by replacing the $1/\sqrt{T}$ factor, which is just the pulse's slowly varying amplitude function in a simple square well approximation, by a function $A(\tau)$ of dimension $s^{-1/2}$ normalized such that $\int_0^T \mathrm{d}\tau |A(\tau)|^2 = 1$. Its Fourier transform $A(\omega) = \frac{1}{\sqrt{2\pi}}\int_0^T \mathrm{d}\tau A(\tau)\exp(i\omega\tau)$ is centered at zero and has a width $1/T = \Delta\omega \ll \Omega$ in accord with our condition $1 \ll \Omega T$. Replacing now $1/\sqrt{T}$ by $A(\tau)$ (of course inside the integral over τ) in the expressions for y and q yields

$$\begin{aligned}y &= \frac{-i}{\sqrt{4\pi}}\int_0^T \mathrm{d}\tau A(\tau) \int_b \mathrm{d}\omega\Big[b(\omega)e^{i(\omega_c+\Omega-\omega)\tau} - h.c.\Big]\\ &= \frac{-i}{\sqrt{2}}\int_b \mathrm{d}\omega\Big[A(\omega_c+\Omega-\omega)b(\omega) - h.c.\Big],\\ q &= \frac{-1}{\sqrt{2}}\int_b \mathrm{d}\omega\Big[A(\omega_c+\Omega-\omega)b(\omega) + h.c.\Big].\end{aligned}$$

This is evidently a mode whose spectral mode function is the same as the classical pulse but is centered at $\omega_c + \Omega$.

Bell measurement This input is combined at a beam splitter with the classical pulse and the scattered light. At the ports of the beam splitter Stokes vector components S_y and S_z are measured by means of standard polarization measurements. Given the classical pulse in x polarization this amounts to a homodyne detection of in- and out-of-phase fields of the orthogonal polarization component. The resulting photocurrents are numerically demodulated to extract the relevant sine and cosine components at the Larmor frequency [14]. Thus one effectively measures the commuting observables

$$\begin{aligned} \tilde{x}_\mathrm{c} &= \frac{1}{\sqrt{2}}\left(x_\mathrm{c}^{\,\mathrm{out}} + y_\mathrm{c}\right), & \tilde{x}_\mathrm{s} &= \frac{1}{\sqrt{2}}\left(x_\mathrm{s}^{\,\mathrm{out}} + y_\mathrm{s}\right), \\ \tilde{q}_\mathrm{c} &= \frac{1}{\sqrt{2}}\left(p_\mathrm{c}^{\,\mathrm{out}} - q_\mathrm{c}\right), & \tilde{q}_\mathrm{s} &= \frac{1}{\sqrt{2}}\left(p_\mathrm{s}^{\,\mathrm{out}} - q_\mathrm{s}\right). \end{aligned} \tag{3.6}$$

Let the respective measurement results be given by $\tilde{X}_\mathrm{c}$, $\tilde{X}_\mathrm{s}$, $\tilde{Q}_\mathrm{c}$ and $\tilde{Q}_\mathrm{s}$.

Feedback Conditioned on these results the atomic state is then displaced by an amount $\tilde{X}_\mathrm{s} - \tilde{Q}_\mathrm{c}$ in X and $-\tilde{X}_\mathrm{c} - \tilde{Q}_\mathrm{s}$ in P. This can be achieved by means of two fast radio-frequency magnetic pulses separated by a quarter of a Larmor period. In the ensemble average the final state of atoms is simply given by

$$X^{\,\mathrm{fin}} = X^{\,\mathrm{out}} + \tilde{x}_\mathrm{s} - \tilde{q}_\mathrm{c}, \quad P^{\,\mathrm{fin}} = P^{\,\mathrm{out}} - \tilde{x}_\mathrm{c} - \tilde{q}_\mathrm{s}. \tag{3.7}$$

This description of feedback is justified rigorously in section 3.4. Relating these expressions to input operators, we find by means of equations (3.4), (3.5) and (3.6)

$$X^{\,\mathrm{fin}} = \left(1 - \frac{\kappa}{2}\right) X^{\,\mathrm{in}} - \frac{1}{\sqrt{2}}\left(1 - \frac{\kappa}{2}\right)^2 p_\mathrm{c}^{\,\mathrm{in}} + \frac{1}{\sqrt{2}} x_\mathrm{s}^{\,\mathrm{in}} - \frac{1}{\sqrt{6}}\left(\frac{\kappa}{2}\right)^2 p_{\mathrm{c},1}^{\,\mathrm{in}} + y, \tag{3.8a}$$

$$P^{\,\mathrm{fin}} = \left(1 - \frac{\kappa}{2}\right) P^{\,\mathrm{in}} - \frac{1}{\sqrt{2}}\left(1 - \frac{\kappa}{2}\right)^2 p_\mathrm{s}^{\,\mathrm{in}} - \frac{1}{\sqrt{2}} x_\mathrm{c}^{\,\mathrm{in}} - \frac{1}{\sqrt{6}}\left(\frac{\kappa}{2}\right)^2 p_{\mathrm{s},1}^{\,\mathrm{in}} + q. \tag{3.8b}$$

This is the main result of this section.

Teleportation fidelity Taking the mean of equations (3.8) with respect to the initial state all contributions due to input operators and back action modes vanish such that $\langle X^{\,\mathrm{fin}}\rangle = \langle y\rangle$ and $\langle P^{\,\mathrm{fin}}\rangle = \langle q\rangle$. Thus, the amplitude of the coherent input light pulse is mapped on atomic spin quadratures as desired. In order to prove faithful teleportation also the variances

have to be conserved. It is evident from (3.8) that the final atomic spin variances will be increased as compared to the coherent input. These additional terms describe unwanted excess noise and have to be minimized by a proper choice of the coupling κ. As a figure of merit for the teleportation protocol we use the fidelity, i.e. squared overlap, of input and final state. Given that the means are transmitted correctly the fidelity is found to be $F = 2\left[(1+2(\Delta X^{\rm fin})^2)(1+2(\Delta P^{\rm fin})^2)\right]^{-1/2}$. The variances of the final spin quadratures are readily calculated taking into account that all modes involved are independent and have initially a normalized variance of 1/2. In this way a theoretical limit on the achievable fidelity can be derived depending solely on the coupling strength κ. In figure 3.2 we take advantage of the fact that the amount of entanglement between light and atoms is a monotonously increasing function of κ such that we can plot the fidelity versus the entanglement. This has the advantage that we can compare the performance of our teleportation protocol with the canonical one [50, 51] which uses a two-mode squeezed state of the same entanglement as a resource and therefore maximizes the teleportation fidelity for the given amount of entanglement. No physical state can achieve a higher fidelity with the same entanglement. This follows from the results of [56] where it was shown that two-mode squeezed states minimize the EPR variance (and therefore maximize the teleportation fidelity) for given entanglement. The theoretical fidelity achievable in our protocol is maximized for $\kappa \simeq 1.64$ corresponding to $F \simeq .77$. But also for experimentally more feasible values of $\kappa \simeq 1$ can the fidelity well exceed the value, which can be attained by classical means, that is, without entanglement. In the next chapter we will show that this limit is of 1/2. Moreover, comparison with the values achievable with a two-mode squeezed state shows that our protocol is close to optimal.

Noise effects and Gaussian distributed input

Under realistic conditions the teleportation fidelity will be degraded by noise effects like decoherence of the atomic spin state, light absorption and reflection losses and also because the coupling constant κ is experimentally limited to values $\kappa \simeq 1$. On the other hand the classical fidelity bound to be beaten will be somewhat higher than 1/2 since the coherent input states will necessarily be drawn according to a distribution with a finite width in the mean photon number $\bar{n}$. In this section we analyze the efficiency of the teleportation protocol under these conditions and show that it is still possible to surpass any classical strategy for the transmission and storage of coherent states of light [57, 16].

During the interaction atomic polarization decays due to spontaneous

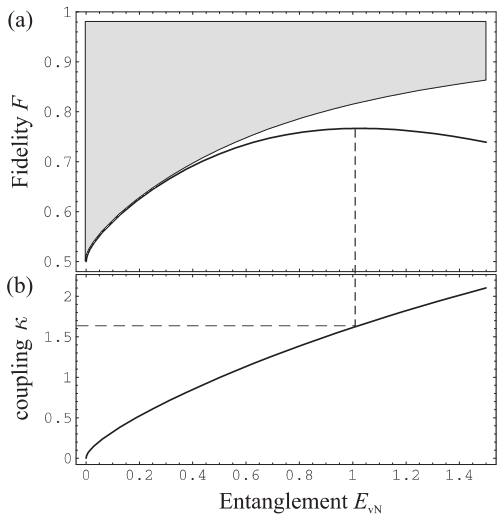

Figure 3.2: (a) Theoretical limit on the achievable fidelity F versus entanglement between atoms and light measured by the von Neumann entropy $E_{\rm vN}$ of the reduced state of atoms. The grey area is unphysical. For moderate amounts of entanglement our protocol is close to optimal. (b) Coupling strength κ versus entanglement. The dashed lines indicate the maximal fidelity of $F = .77$ which is achieved for $\kappa = 1.64$.

emission and collisional relaxation. Including a transverse decay the final state of atoms is given by

$$X^{\rm out} = \sqrt{1-\beta}(X^{\rm in} + \frac{\kappa}{\sqrt{2}} p_{\rm c}^{\rm in}) + \sqrt{\beta} f_X, \tag{3.9a}$$

$$P^{\rm out} = \sqrt{1-\beta}(P^{\rm in} + \frac{\kappa}{\sqrt{2}} p_{\rm s}^{\rm in}) + \sqrt{\beta} f_P. \tag{3.9b}$$

In these equations β is an overall atomic decay parameter including dephasing due to spontaneous decay and other mechanisms like collisions, and f_X, f_P are Langevin noise operators with zero mean. Their variance is $\langle f_X^2 \rangle = \langle f_P^2 \rangle = 1/2$.

Light absorption and reflection losses can be taken into account in the same way as finite detection efficiency. For example the statistics of measurement outcome $\tilde{X}_{\rm s}$ will not stem from the signal mode $\tilde{x}_{\rm s}$ alone but rather from the noisy mode $\sqrt{1-\epsilon}\,\tilde{x}_{\rm s} + \sqrt{\epsilon} f_{x,{\rm s}}$ where ϵ is the photon loss parameter and $f_{x,{\rm s}}$ is a Langevin noise operator of zero mean and variance $\langle f_{x,{\rm s}}^2 \rangle = 1/2$. Analogous expressions have to be used for the measurements of $\tilde{x}_{\rm c}$, $\tilde{q}_{\rm s}$ and $\tilde{q}_{\rm c}$ which will be adulterated by Langevin terms $f_{x,{\rm c}}$, $f_{q,{\rm s}}$ and $f_{q,{\rm c}}$ respectively. In principle each of the measurement outcomes can be fed back with an inde-

pendently chosen gain but for symmetry reasons it is enough to distinguish gain coefficients g_x, g_q for the measurement outcomes of sine and cosine components of x and q respectively. Including photon loss, finite gain and atomic decay, as given in (3.9), equations (3.7), describing the final state of atoms after the feed back operation, generalize to

$$X^{\,\mathrm{fin}} = \sqrt{1-\beta}X^{\,\mathrm{out}} + \sqrt{\beta}f_X + g_x\left(\sqrt{1-\epsilon}\,\tilde{x}_{\mathrm{s}} + \sqrt{\epsilon}f_{x,\mathrm{s}}\right) - g_q\left(\sqrt{1-\epsilon}\,\tilde{q}_{\mathrm{c}} + \sqrt{\epsilon}f_{q,\mathrm{c}}\right), \tag{3.10a}$$

$$P^{\,\mathrm{fin}} = \sqrt{1-\beta}P^{\,\mathrm{out}} + \sqrt{\beta}f_P - g_x\left(\sqrt{1-\epsilon}\,\tilde{x}_{\mathrm{c}} + \sqrt{\epsilon}f_{x,\mathrm{c}}\right) - g_q\left(\sqrt{1-\epsilon}\,\tilde{q}_{\mathrm{s}} + \sqrt{\epsilon}f_{q,\mathrm{s}}\right). \tag{3.10b}$$

For non unit gains a given coherent amplitude $(\langle y\rangle, \langle q\rangle)$ will not be perfectly teleported onto atoms and the corresponding fidelity will be degraded by this mismatch according to

$$F(\langle y\rangle, \langle q\rangle) = \frac{2}{\sqrt{[1+2(\Delta X^{\,\mathrm{fin}})^2][1+2(\Delta P^{\,\mathrm{fin}})^2]}} \cdot \exp\left[-\frac{(\langle y\rangle - \langle X^{\,\mathrm{fin}}\rangle)^2}{1+2(\Delta X^{\,\mathrm{fin}})^2} - \frac{(\langle q\rangle - \langle P^{\,\mathrm{fin}}\rangle)^2}{1+2(\Delta P^{\,\mathrm{fin}})^2}\right].$$

If the input amplitudes are drawn according to a Gaussian distribution $p(\langle y\rangle, \langle q\rangle) = \exp[-(\langle y\rangle^2 + \langle q\rangle^2)/2\bar{n}]/2\pi\bar{n}$ with mean photon number $\bar{n}$ the average fidelity [with respect to $(\langle y\rangle, \langle q\rangle)$] is readily calculated. The exact expression in terms of initial operators can then be derived by means of equations (3.4), (3.5), (3.6) and (3.10) but is not particularly enlightening. In figure 3.3 we plot the average fidelity, optimized with respect to gains g_x, g_q, in its dependence on the atomic decay β for various values of photon loss ϵ. We assume a realistic value $\kappa = 0.96$ for the coupling constant and a mean number of photons $\bar{n} = 4$ for the distribution of the coherent input. For feasible values of β, $\epsilon \precsim 0.2$ the average fidelity is still well above the classical bound on the fidelity [57, 16]. This proves that the proposed protocol is robust against the dominating noise effects in this system.

The experimental feasibility of the proposal is illustrated with the following example. Consider a sample of $N_{at} = 10^{11}$ Cesium atoms in a glass cell placed in a constant magnetic field along the x-direction causing a Zeeman splitting of $\Omega = 350\,\mathrm{kHz}$ in the $F = 4$ ground state multiplet. The atoms are pumped into $m_F = 4$ and probed on the D_2 $(F = 4 \to F' = 3, 4, 5)$ transition. The classical pulse contains an overall number of $N_{ph} = 2.5\,10^{13}$ photons, is detuned to the blue by $\Delta = 1\,\mathrm{GHz}$, has a duration $T = 1\,\mathrm{ms}$ and can have an effective cross section of $A \simeq 6\mathrm{cm}^2$ due to thermal motion of atoms. Under

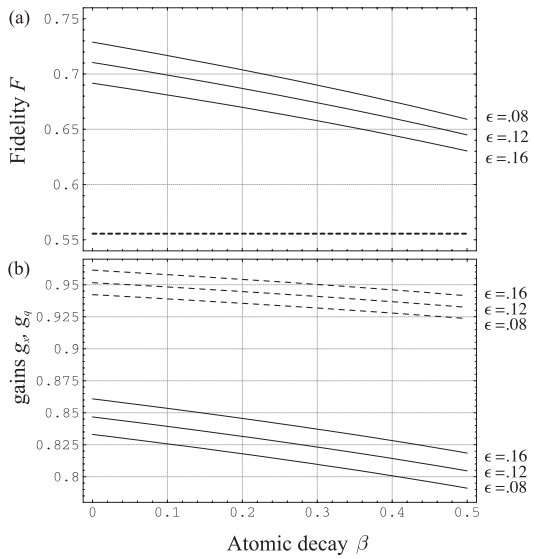

Figure 3.3: (a) Average fidelity achievable in the presence of atomic decay β, reflection and light absorption losses $\epsilon = 8\%$, .12%, .16%, coupling $\kappa = .96$ and Gaussian distributed input states with mean photon number $\bar{n} = 4$. The fidelity benchmark is in this case 5/9 (dashed line). (b) Respective optimal values for gains g_x (solid lines) and g_q (dashed lines).

these conditions the tensor polarizability can be neglected ($\Delta/\omega_{\rm hfs} \simeq 10^{-1}$). Also $n_0 = \Omega T = 350$ justifies the use of independent scattering modes. The coupling $\kappa \simeq 1$ and the depumping of ground state population $\eta \simeq 10^{-2}$ as desired.

3.3 Spin squeezing and state read-out

In this section we present a scheme for reading out either of the atomic spin components X, P by means of a probe pulse interacting with the atoms in the one way as described in section 3.1. The proposed scheme allows one, on the one hand, to verify successful receipt of the coherent input subsequent to the teleportation protocol of section 3.2 and, on the other hand, enables to generate spin squeezing if it is performed on a coherent spin state.

As discussed in section 2.7, the pure interaction V, as given in equation (3.1), can be used to perform a QND measurement of either of the transverse spin components. At first sight this seems not to be an option in the scenario under consideration since the local term H_{at}, accounting for Larmor precession, commutes with neither of the spin quadratures such that the total

Hamiltonian does not satisfy the QND criteria [48, 49]. As we have shown in section 3.1 Larmor precession has two effects: Scattered light is correlated with both transverse components and suffers from back action mediated by the atoms. Thus, in order to read out a single spin component one has to overcome both disturbing effects.

Our claim is that this can be achieved by a simultaneous measurement of $x_{\mathrm{c}}^{\mathrm{out}}$, $p_{\mathrm{s}}^{\mathrm{out}}$, $p_{\mathrm{s},1}^{\mathrm{out}}$ or $x_{\mathrm{s}}^{\mathrm{out}}$, $p_{\mathrm{c}}^{\mathrm{out}}$, $p_{\mathrm{c},1}^{\mathrm{out}}$ if, respectively, X or P is to be measured. In the following we consider in particular the former case but everything will hold with appropriate replacements also for a measurement of P.

The set of observables $x_{\mathrm{c}}^{\mathrm{out}}$, $p_{\mathrm{s}}^{\mathrm{out}}$, $p_{\mathrm{s},1}^{\mathrm{out}}$ can be measured simultaneously by a measurement of Stokes component S_y after a $\pi/2$ rotation is performed selectively on the sine component of the scattered light. The cosine component of the corresponding photocurrent will give an estimate of $x_{\mathrm{c}}^{\mathrm{out}}$ and the sine component of $p_{\mathrm{s}}^{\mathrm{out}}$. Multiplying the photocurrent's sine component by the linear function defining the back action mode, equation (3.4c), will give in addition an estimate of $p_{\mathrm{s},1}^{\mathrm{out}}$. Note that the field out of phase is conserved in the interaction such that

$$p_{\mathrm{s},1}^{\mathrm{out}} = p_{\mathrm{s},1}^{\mathrm{in}}, \quad p_{\mathrm{c},1}^{\mathrm{out}} = p_{\mathrm{c},1}^{\mathrm{in}}, \tag{3.11}$$

i.e. the results will have shot noise limited variance. It is then evident from equation (3.4d) that the respective photocurrents together with an a priori knowledge of κ are sufficient to estimate the mean $\langle X \rangle$.

The conditional variances after the indicated measurements are

$$\Delta X^2|_{\{x_{\mathrm{c}}^{\mathrm{out}}, p_{\mathrm{s}}^{\mathrm{out}}, p_{\mathrm{s},1}^{\mathrm{out}}\}} = (\Delta X^{\mathrm{in}})^2 \frac{2}{2+\kappa^2}, \tag{3.12a}$$

$$\Delta P^2|_{\{x_{\mathrm{c}}^{\mathrm{out}}, p_{\mathrm{s}}^{\mathrm{out}}, p_{\mathrm{s},1}^{\mathrm{out}}\}} = (\Delta P^{\mathrm{in}})^2 \frac{2+\kappa^2}{2}, \tag{3.12b}$$

corresponding to a pure state. Obviously the variance in X is squeezed by a factor $(1+\kappa^2/2)^{-1}$. Note that the squeezing achieved in a QND measurement without magnetic field but otherwise identical parameters is given by $(1+\kappa^2)^{-1}$. From this we conclude that the quality of the estimate for $\langle X \rangle$, as measured f.e. by input-output coefficients known from the theory of QND measurements [48, 49], can be the same as in the case without Larmor precession albeit only for a higher coupling κ.

In order to derive equations (3.12) we need to know also the input-output relations for $x_{\mathrm{c},1}$ and $x_{\mathrm{s},1}$. They can be calculated in a similar way input-output relations for the back action modes itself were derived in section 3.1.

One finds

$$x_{\mathrm{c},1}^{\mathrm{out}} = x_{\mathrm{c},1}^{\mathrm{in}} \quad - \quad \frac{1}{\sqrt{3}}\left(\frac{\kappa}{2}\right)^2 p_{\mathrm{s}}^{\mathrm{in}} + \frac{1}{\sqrt{15}}\left(\frac{\kappa}{2}\right)^2 p_{\mathrm{s},2}^{\mathrm{in}}, \tag{3.13a}$$

$$x_{\mathrm{s},1}^{\mathrm{out}} = x_{\mathrm{s},1}^{\mathrm{in}} \quad - \quad \frac{1}{\sqrt{3}}\left(\frac{\kappa}{2}\right)^2 p_{\mathrm{c}}^{\mathrm{in}} + \frac{1}{\sqrt{15}}\left(\frac{\kappa}{2}\right)^2 p_{\mathrm{c},2}^{\mathrm{in}}. \tag{3.13b}$$

In both equations the third terms on the right hand side describe contributions of second order back action modes defined by

$$p_{\mathrm{s},2}^{\mathrm{in}} = 6\left(\frac{10}{T^5}\right)^{1/2}\int_0^T \mathrm{d}\tau\left(\frac{T^2}{6} - T\tau + \tau^2\right)\sin(\Omega\tau)\bar{p}(c\tau, 0)$$

and similarly for $x_{\mathrm{s},2}^{\mathrm{in}}$ and the cosine component. These modes are again canonical and independent. As a sidemark we note that, formally, it is possible to define scattering modes of arbitrary order whose mode functions are given in general by products of Legendre polynomials and $\cos(\Omega t)$ $[\sin(\Omega t)]$ resulting in a hierarchy of input-output relations similar to (3.13). Now, for the operator valued vector $\vec{R} = (X, P, x_{\mathrm{c}}, p_{\mathrm{c}}, x_{\mathrm{s}}, p_{\mathrm{s}}, x_{\mathrm{c},1}, p_{\mathrm{c},1}, x_{\mathrm{s},1}, p_{\mathrm{s},1})$ equations (3.4), (3.11) and (3.13) define via $\vec{R}^{\mathrm{out}} = S(\kappa)\vec{R}^{\mathrm{in}}$ a symplectic linear transformation $S(\kappa)$. The contributions of $p_{\mathrm{c},2}^{\mathrm{in}}$ and $p_{\mathrm{s},2}^{\mathrm{in}}$ to $x_{\mathrm{s},1}^{\mathrm{out}}$ and $x_{\mathrm{c},1}^{\mathrm{out}}$ as given in (3.13) are treated as noise and do not contribute to the symplectic transformation S but enter the input-output relation for the correlation matrix as an additional noise term as follows. The correlation matrix is as usually defined by $\gamma_{i,j} = \mathrm{tr}\{\rho(R_iR_j + R_jR_i)\}$. The initial state is then an 10×10 identity matrix and the final state is $\gamma^{\mathrm{out}} = S(\kappa)S(\kappa)^T + \gamma_{\mathrm{noise}}$ where the diagonal matrix $\gamma_{\mathrm{noise}} = \mathrm{diag}[0,0,0,0,0,0,1,0,1,0](\kappa/2)^4/15$ accounts for noise contributions due correlations to second order back action modes c.f. equations (3.13). In order to evaluate the atomic variances after a measurement of $x_{\mathrm{c}}^{\mathrm{out}}$, $p_{\mathrm{s}}^{\mathrm{out}}$, $p_{\mathrm{s},1}^{\mathrm{out}}$ the correlation matrix γ_{out} is split up into blocks,

$$\gamma_{\mathrm{out}} = \begin{pmatrix} A & C \\ C^T & B \end{pmatrix}$$

where A is the 2×2 subblock describing atomic variances. Now, the state A' after the measurement can be found by evaluating [58]

$$A' = A - \lim_{x,n\to\infty} C\frac{1}{\Gamma + B}C^T$$

where $\Gamma = \mathrm{diag}[1/x, x, x, 1/x, n, n, x, 1/x]$ corresponds to the measured state. Note that the limit $n \to \infty$, i.e. the projection of the unobserved mode $x_{\mathrm{c},2}$, $p_{\mathrm{c},2}$ onto the identity, does not need to be taken explicitly since, remarkably, the atomic state after the measurement decouples form this mode.

The conditional variances in equation (3.12) are then just (half the) diagonal entries of A'.

3.4 Feedback in systems of continuous variables

The feedback in continuous variable quantum teleportation is sometimes described by equations equivalent to (3.7) but with a classical random variable describing the measurement outcome in place of the operators corresponding to the chosen displacement, which - though giving the right result - is mathematically questionable. We point out that relations (3.7) hold *stricto sensu* as operator identities. This is true for mixed and even for non-gaussian states, as we will show below.

Consider a bipartite system of $N+1$ modes and denote the first mode as system A and the remaining N modes as system B. Let the state of the compound system be given by ρ_{AB}. Our aim here is to describe protocols which consist of the following steps:

Measurement On system B a set of commuting observables $\{\hat{r}_1, \ldots, \hat{r}_N\}$ is measured where each of the operators $\hat{r}_i$ is either x_i or p_i, one of the quadratures of mode i in B. Let the corresponding measurement outcomes r_i be arranged in a vector $\vec{R}^B = (r_1, \ldots, r_N)$. With the eigenvalue equation $\hat{r}_i|r_i\rangle_B = r_i|r_i\rangle_B$, where $|r_i\rangle_B$ is the generalized eigenstate of $\hat{r}_i$, the normalized state of system A conditioned on the measurement outcomes is

$$\rho_A^{(1)}(\vec{R}) = {}_B\langle r_1, \ldots, r_N|\rho_{AB}|r_1, \ldots, r_N\rangle_B / p(\vec{R}).$$

$p(\vec{R})$ is the probability to get the measurement outcomes $\vec{R}$ and is normalized as $\int \mathrm{d}^N r p(\vec{R}) = 1$.

Feedback Depending on the measurement outcomes system A is then displaced in x_A and p_A by an amount $\vec{R}\vec{g}_x^T$ and $\vec{R}\vec{g}_p^T$ respectively where $\vec{g}_{x(p)}$ are any real N dimensional (row) vectors determining the strength with which each outcome is fed back into system A. In teleportation protocols these coefficients are usually referred to as gains. The state of system A after the feedback operation is then

$$\rho_A^{(2)}(\vec{R}) = D_A^\dagger \rho_A^{(1)}(\vec{R}) D_A.$$

$D_A = D_A(\vec{R}\vec{g}_x^T, \vec{R}\vec{g}_p^T) \doteq \exp(i\vec{R}\vec{g}_x^T p_A)\exp(-i\vec{R}\vec{g}_p^T x_A)$ is the unitary displacement operator effecting the desired transformations $D_A x_A D_A^\dagger = x_A + \vec{R}\vec{g}_x^T$ and $D_A p_A D_A^\dagger = p_A + \vec{R}\vec{g}_p^T$.

Ensemble average On average over all measurement outcomes, weighted with their respective probabilities, the state of system A is

$$\bar{\rho}_A = \int \mathrm{d}^N r p(\vec{R}) \rho_A^{(2)}(\vec{R}).$$

Combining this with the expressions for $\rho_A^{(2)}$ and $\rho_A^{(1)}$ above one can express

$$\begin{aligned} \bar{\rho}_A &= \int \mathrm{d}^N r D_{AB}^\dagger \langle r_1, \ldots, r_N | \rho_{AB} | r_1, \ldots, r_N \rangle_B D_A \\ &= \int \mathrm{d}^N r_B \langle r_1, \ldots, r_N | D_{AB}^\dagger \rho_{AB} D_{AB} | r_1, \ldots, r_N \rangle_B \\ &= \mathrm{tr}_B \{ D_{AB}^\dagger \rho_{AB} D_{AB} \} \end{aligned} \tag{3.14}$$

where the trace in the last line is now taken with respect to both system A and B. In going from the first line to the second line we made use of the identity

$$|r_1, \ldots, r_N\rangle_B D_A = D_{AB} |r_1, \ldots, r_N\rangle_B \tag{3.15}$$

with the unitary operator D_{AB} defined as

$$D_{AB} = D_{AB}(\hat{\vec{R}}\vec{g}_x^T, \hat{\vec{R}}\vec{g}_p^T) \doteq \exp(i\hat{\vec{R}}\vec{g}_x^T p_A)\exp(-i\hat{\vec{R}}\vec{g}_p^T p_A)$$

where $\hat{\vec{R}} = (\hat{r}_1, \ldots, \hat{r}_N)$ is now the vector of *operators* $\hat{r}_i^B$ and D_{AB} acts on *both* systems A and B. Note that identity (3.15) is valid only for commuting observables $\hat{r}_i^B$. The resulting equation (3.14) is the key point in this consideration.

Observables in the ensemble average Consider finally the mean of, for example, x_A after the measurement and feedback procedure, i.e. with respect to the ensemble averaged state $\bar{\rho}_A$. It is given by

$$\begin{aligned} \langle x_A \rangle &= \mathrm{tr}_A \{ x_A \bar{\rho}_A \} = \mathrm{tr}_{AB} \{ D_{AB} x_A D_{AB}^\dagger \rho_{AB} \} \\ &= \mathrm{tr}_{AB} \{ (x_A + \hat{\vec{R}}\vec{g}_x^T) \rho_{AB} \}. \end{aligned}$$

From this identity and the corresponding expression for $\langle p_A \rangle$, which both are true for all initial states ρ_{AB}, we can deduce the operator identities

$$x_A^{\mathrm{fin}} = x_A + \hat{\vec{R}}\vec{g}_x^T, \quad p_A^{\mathrm{fin}} = p_A + \hat{\vec{R}}\vec{g}_p^T$$

where $x_A^{\text{fin}}, p_A^{\text{fin}}$ describe the final state of system A in the Heisenberg picture and means have to be taken with respect to the unchanged initial state of both systems A and B. If ρ_{AB} is a pure Gaussian state the last two equations fully determine the final state $\bar{\rho}_A$. This was used in equation (3.7). Note that these considerations are easily extended to situations in which system A consists of more than one mode.

In conclusion we have presented a simple and realistic protocol for teleportation of a coherent state, carried by a propagating pulse of light, onto the collective spin of an atomic ensemble, a suitable stationary carrier of quantum information of continuous variables. The scheme can be implemented with state of the art technique and allows one to surpass any classical strategy for the transmission and storage of coherent states under realistic experimental conditions. Straight forward extensions of it to other quantum information primitives like entanglement swapping opens up the way to large distance entanglement distribution. The basic resource in the protocol is a multimode entangled state as it results form the interaction of light with atoms in the presence of an external magnetic field. Though the interaction is not of QND type it is still possible to perform a state readout on the atomic spin as well as to create significant spin squeezing. We expect that a proper tailoring of the Larmor rotation with time dependent magnetic fields would open up interesting possibilities to further enhance the creation of entanglement and to deliberately shape scattering modes.

Chapter 4

Quantum benchmark for transmission and storage of states

Coherent distribution, storage and manipulation of quantum states is a technical challenge which received extensive theoretical and experimental interest in the last years stimulated by the promises of quantum information science [1]. A wide class of schemes can be very generally understood as an attempt to establish a channel for the reliable transmission of quantum states. This applies in particular to quantum teleportation [33, 34, 35, 36, 37, 38, 39, 40, 41, 42, 43, 44, 45, 46, 50, 51, 59], where states are sent through an entanglement assisted classical channel, but just as well to the concept of a quantum memory [11, 60, 61, 62, 63, 64, 65, 66, 8], where the channel acts in time rather than in space and the accent is on the state transfer between light and atoms. Concerning the reliable transmission and storage of quantum states it is clear that in the ideal case a quantum channel will always surpass a classical channel, i.e. any strategy where the quantum state is measured, the corresponding classical data stored or transmitted and then used to reconstruct the initial state as good as possible. This is a direct consequence of the no-cloning theorem for quantum states [67, 68, 69]. However, under realistic conditions a quantum channel suffers inevitably from imperfections such that it might become possible to achieve the same effect by means of a classical channel. Therefore there is need for a criterion which allows one to distinguish an imperfect quantum channel from a perfect classical channel and justifies proclamation of success in the experimental demonstration of quantum teleportation and quantum memories.

Such a criterion has been derived some time ago for channels acting on finite dimensional systems [70, 71, 72, 73] and found applications in seminal

experiments on quantum teleportation with single photons [33, 34, 35, 36, 37, 38, 39] and ions [45, 46]. For channels acting on infinite dimensional systems a corresponding criterion was *conjectured* some time ago in [40, 57]. Though a proof for this criterion was yet to be found the claim for successful teleportation was based exclusively on this ground in several, likewise seminal teleportation experiments using EPR-squeezed light [40, 41, 42, 43, 44]. The same criterion was applied very recently to a quantum memory experiment [11] where coherent states of light were stored in the collective spin of atoms. It applies in particular also to the protocols presented in chapters 3 and 5.

In this chapter we solve this longstanding problem and provide a rigorous proof for the criterion conjectured in [40, 57]. This puts the central claims of experiments [40, 41, 42, 43, 44] - to have demonstrated a quantum gain in the transmission or storage of coherent states - on logically firm grounds. We emphasize that only now the success of these key experiments is rigorously validated. Moreover, the present result gives a solution to the state estimation problem for coherent states and leads to a closed expression for the accessible fidelity introduced in [74].

The chapter is organized as follows: We first characterize a general classical channel mathematically and state the optimization problem to be solved here. Then we present this solution and give an elementary and rigorous proof. We close by relating the result to other work.

4.1 Quantum benchmark for transmission and storage

The figure of merit in terms of which the quality of a channel is quantified is usually taken to be the average fidelity achieved when the channel acts on a predefined set of input states. Let $\{|\psi_x\rangle\}$ be this set and let an input $|\psi_x\rangle$ occur with a probability $p(x)$. If the channels's output is $E(|\psi_x\rangle)$ then the average fidelity is defined as

$$\bar{F} = \sum_x p(x)\langle\psi_x|E(|\psi_x\rangle)|\psi_x\rangle.$$

This number is equal to one only for the ideal channel transmitting or storing every state perfectly. Now the task is to find the maximal value of $\bar{F}$ achievable with a classical channel, i.e. to identify the optimal measure-and-prepare strategy. Any channel yielding a higher average fidelity is then necessarily quantum in the sense that it outperforms every strategy which is based on the mere storage or transmission of classical information. Any classical channel can be described by a POVM [1] measurement $\{M_y\}$, $M_y = M_y^\dagger$, where

y denotes the outcome occurring with a probability $\langle\psi_x|M_y|\psi_x\rangle$ and a reconstruction rule $y \to \rho_y$ determining which state ρ_y is prepared when y was the measurement outcome. The channel then acts as

$$E(|\psi_x\rangle) = \sum_y \langle\psi_x|M_y|\psi_x\rangle\rho_y.$$

The fidelity bound for classical channels relative to the set of input states $\{|\psi_x\rangle\}$ is then

$$F_{\max} = \sup_{\{M_y\}} \sup_{\{\rho_y\}} \sum_x \sum_y p(x)\langle\psi_x|M_y|\psi_x\rangle\langle\psi_x|\rho_y|\psi_x\rangle. \tag{4.1}$$

This optimization problem is known under the title state estimation in the theory of quantum detection and has in fact a long history [75, 76, 77, 78]. From the plethora of results known in this field the one concerning channels acting on $\mathbb{C}^2$ and an input set consisting of all pure states with a uniform distribution over the Bloch sphere received particular practical relevance in the last years. In [71] it was shown that for this case $F_{\max} = 2/3$. This value was the appropriate benchmark in several teleportation experiments using single photons [33, 34, 35, 36, 37, 38, 39] and recently also trapped ions [45, 46] and was beaten by measured fidelities ranging from .70 to .89 in [33, 34, 35, 36, 37, 38, 39] and from .75 to .78 in [45, 46] proving the presence and necessity of entanglement in these experiments.

Less is known for channels acting on an infinite dimensional Hilbert space. Despite the increasing importance of coherent states $\{|\alpha\rangle\}$ for quantum communication and in particular quantum cryptography by now no classical-quantum bound has been proven for channels acting on these states. In [57] it was shown that if the coherent states are distributed in phase space according to a Gaussian distribution $p(\alpha) = \lambda/\pi \exp(-\lambda|\alpha|^2)$ an average fidelity $\bar{F} = (1+\lambda)/(2+\lambda)$ can be achieved by means of a heterodyne measurement, described by a POVM $\{|\alpha\rangle\langle\alpha|/\pi\}$, and the preparation of appropriate coherent states. It was conjectured there that this might be optimal but since then this question remained open. In fact, in the state estimation problem with minimum mean square error the heterodyne measurement turned out to be optimal [77]. However, this problem is different from the present one with respect to the figure of merit and due to the fact that in [77] the reconstruction of the state, which is crucial in our context, is not considered. Nevertheless, the value of $1/2$ attained for the flat distribution ($\lambda \to 0$) was used as a criterion to verify teleportation in experiments [40, 41, 42, 43, 44] using EPR-squeezed light where measured average fidelities range from .58 to .64.

In the following we will settle this question by proving that for any classical strategy

$$F_{\max} \leq \frac{1+\lambda}{2+\lambda} \tag{4.2}$$

holds necessarily. Moreover, this bound is tight since it can be achieved by means of the strategy derived in [57], and thus equality holds in (4.2). This is the main result of this section.

4.2 Proof of quantum benchmark for coherent states

The proof we are going to present now is elementary and we start by simplifying and conveniently reformulating the problem. The first simplification relies on the fact that without loss of generality we can restrict the optimization in equation (4.1) to POVMs consisting of projectors $M_y = |\phi_y\rangle\langle\phi_y|$ ($|\phi_y\rangle$ not necessarily normalized) and also to pure states $\rho_y = |\chi_y\rangle\langle\chi_y|$. This is easily seen by noting that we can always decompose the POVM elements $M_y = \sum_v |m_{v,y}\rangle\langle m_{v,y}|$ and similarly the states $\rho_y = \sum_w q_{w,y}|r_{w,y}\rangle\langle r_{w,y}|$ such that we can write the average fidelity as

$$\bar{F} = \sum_x \sum_{y,v,w} p(x)|\langle\psi_x|\sqrt{q_{w,y}}|m_{v,y}\rangle|^2|\langle\psi_x|r_{w,y}\rangle|^2.$$

Absorbing the redundant parameters v, w into y and identifying $\sqrt{q_{w,y}}|m_{v,y}\rangle$ and $|r_{w,y}\rangle$ with $|\phi_y\rangle$ and $|\chi_y\rangle$ respectively we see that for any POVM there exists always another one which has the desired properties and yields the same average fidelity.

We therefore have for coherent input states $\{|\alpha\rangle\}$ with a Gaussian distribution $p(\alpha) = \lambda/\pi \exp(-\lambda|\alpha|^2)$

$$\bar{F} = \sum_y \int d\alpha p(\alpha)|\langle\alpha|\phi_y\rangle|^2|\langle\alpha|\chi_y\rangle|^2.$$

Note that the sum over y stands symbolically for sums or integrations over a suitable measurable set. Using this expression for $\bar{F}$ and defining

$$A_{\phi_y} = \int \mathrm{d}\alpha p(\alpha)|\langle\alpha|\phi_y\rangle|^2|\alpha\rangle\langle\alpha|.$$

equation (4.1) can be reformulated more compactly as

$$F_{\max} = \sup_{\{|\phi_y\rangle\}} \sup_{\{|\chi_y\rangle\}} \sum_y \langle\chi_y|A_{\phi_y}|\chi_y\rangle = \sup_{\{|\phi_y\rangle\}} \sum_y ||A_{\phi_y}||_\infty. \tag{4.3}$$

The optimization with respect to the reconstructed states $|\chi_y\rangle$ is trivial and implicitly performed in the last identity by noting that it is clearly best to prepare the state corresponding to the largest eigenvalue of A_{ϕ_y} for a given measurement outcome y [1].

We proceed by proving a statement which is even stronger than (4.2) namely that

$$||A_\phi||_p \leq \frac{1+\lambda}{[(2+\lambda)^p - 1]^{1/p}} ||A_\phi||_1 \tag{4.4}$$

holds for all states $|\phi\rangle$ and all p-norms $||A||_p = [\mathrm{tr}\{|A|^p\}]^{1/p}$. The main statement, equation (4.2), is deduced from equations (4.3) and (4.4) by taking the limiting case $p \to \infty$ of equation (4.4) in combination with the POVM property $\sum_y |\phi_y\rangle\langle\phi_y| = \mathbf{1}$, which in turn implies $\sum_y ||A_{\phi_y}||_1 = 1$.

In order to prove inequalities (4.4) we exploit a trick which was already utilized in the context of additivity of output purities of bosonic channels in [79]. The properties of the trace allow us to write

$$\begin{aligned} ||A_\phi||_p^p = \mathrm{tr}\left\{A_\phi^p\right\} = &\iint \mathrm{d}\alpha_1 \cdots \mathrm{d}\alpha_p p(\alpha_1)\cdots p(\alpha_p)\, |\langle\phi|\alpha_1\rangle|^2 \cdots |\langle\phi|\alpha_p\rangle|^2 \\ &\times \mathrm{tr}\left\{|\alpha_1\rangle\langle\alpha_1|\alpha_2\rangle \cdots \langle\alpha_{p-1}|\alpha_p\rangle\langle\alpha_p|\right\} \\ =&\mathrm{tr}\left\{|\phi\rangle\langle\phi|^{\otimes p} B\right\}, \\ ||A_\phi||_1^p = \mathrm{tr}\left\{A_\phi\right\}^p =&\mathrm{tr}\left\{|\phi\rangle\langle\phi|^{\otimes p} C\right\} \end{aligned}$$

where we defined

$$\begin{aligned} B &= \iint \mathrm{d}\alpha_1 \cdots \mathrm{d}\alpha_p p(\alpha_1)\cdots p(\alpha_p) \langle\alpha_1|\alpha_2\rangle \cdots \langle\alpha_p|\alpha_1\rangle \\ &\quad \times |\alpha_1\rangle\langle\alpha_1| \otimes \cdots \otimes |\alpha_p\rangle\langle\alpha_p|, \\ C &= \bigotimes_{i=1}^{p} \int \mathrm{d}\alpha_i p(\alpha_i)\, |\alpha_i\rangle\langle\alpha_i|. \end{aligned}$$

These two operators can be diagonalized in the same basis. To do so it is convenient to represent these operators in terms of their characteristic function, which is defined by

$$\chi_O(\alpha, \alpha^*) = \mathrm{tr}\left\{O e^{\alpha^* a - \alpha a^\dagger}\right\}$$

[1] The norm used in equations (4.3) and (4.4) is a special case of a p-norm defined by $||A||_p = \mathrm{tr}\{|A|^p\}^{1/p}$. $||A||_\infty$ is just the largest eigenvalue of A and $||A||_1 = \mathrm{tr}\{A\}$. For all $p' \geq p$ it holds that $||A||_{p'} \leq ||A||_p$.

for an operator O for a single mode and generalizes straight forward for many modes. By means of relations

$$\begin{aligned}\chi_{|\alpha_i\rangle\langle\alpha_i|}(\gamma_i) &= e^{\gamma_i\alpha_i^* - \gamma_i^*\alpha_i} e^{-|\gamma_i|^2/2},\\ \langle\alpha_i|\alpha_{i+1}\rangle &= e^{-(|\alpha_i|^2+|\alpha_{i+1}|^2)/2+\alpha_i^*\alpha_{i+1}},\end{aligned}$$

where $\alpha_{p+1}=\alpha_1$, the corresponding characteristic functions are

$$\begin{aligned}\chi_B(\vec{\gamma}) &= \left(\frac{\lambda}{\pi}\right)^p \iint \mathrm{d}\alpha_1 \cdots \mathrm{d}\alpha_p e^{-(1+\lambda)\vec{\alpha}\vec{\alpha}^\dagger + \vec{\alpha}G\vec{\alpha}^\dagger} e^{\vec{\gamma}\vec{\alpha}^\dagger - \vec{\alpha}\vec{\gamma}^\dagger} e^{-\vec{\gamma}\vec{\gamma}^\dagger/2},\\ \chi_C(\vec{\gamma}) &= \left(\frac{\lambda}{\pi}\right)^p \iint \mathrm{d}\alpha_1 \cdots \mathrm{d}\alpha_p e^{-\lambda\vec{\alpha}\vec{\alpha}^\dagger} e^{\vec{\gamma}\vec{\alpha}^\dagger - \vec{\alpha}\vec{\gamma}^\dagger} e^{-\vec{\gamma}\vec{\gamma}^\dagger/2},\end{aligned}$$

where we defined

$$\begin{aligned}\vec{\alpha} &= (\alpha_1,\ldots,\alpha_p),\\ \vec{\gamma} &= (\gamma_1,\ldots,\gamma_p),\\ G &= \begin{pmatrix} 0 & 0 & 0 & \cdots & 0 & 1\\ 1 & 0 & 0 & & 0 & 0\\ 0 & 1 & 0 & & 0 & 0\\ \vdots & & & \ddots & & \vdots\\ 0 & 0 & 0 & & 0 & 0\\ 0 & 0 & 0 & \cdots & 1 & 0 \end{pmatrix}.\end{aligned}$$

G is a circulant shift matrix [80] and can be diagonalized by a Fourier transform, *i.e.* a unitary matrix Y such that $G = YDY^\dagger$ and $D=\mathrm{diag}(d_1,\ldots,d_p)$ with $|d_i|=1$. Defining $\vec{\beta}=\vec{\alpha}Y$, $\vec{\eta}=\vec{\gamma}Y$ we have

$$\begin{aligned}\chi_B(\vec{\eta}) &= \left(\frac{\lambda}{\pi}\right)^p \iint \mathrm{d}\beta_1 \cdots \mathrm{d}\beta_p e^{-\vec{\beta}[(1+\lambda)\mathbf{1}-D]\vec{\beta}^\dagger} e^{\vec{\eta}\vec{\beta}^\dagger - \vec{\beta}\vec{\eta}^\dagger} e^{-\vec{\eta}\vec{\eta}^\dagger/2}\\ &= \frac{\lambda^p}{|(1+\lambda)\mathbf{1}-G|} e^{-\vec{\eta}\{[(1+\lambda)\mathbf{1}-D]^{-1}+\mathbf{1}/2\}\vec{\eta}^\dagger},\\ \chi_C(\vec{\eta}) &= \left(\frac{\lambda}{\pi}\right)^p \iint \mathrm{d}\beta_1 \cdots \mathrm{d}\beta_p e^{-\lambda\vec{\beta}\vec{\beta}^\dagger} e^{\vec{\eta}\vec{\beta}^\dagger - \vec{\beta}\vec{\eta}^\dagger} e^{-\vec{\eta}\vec{\eta}^\dagger/2}\\ &= e^{-[\lambda^{-1}+1/2]\vec{\eta}\vec{\eta}^\dagger}.\end{aligned}$$

For the second identity we used $\prod_{i=1}^p(1+\lambda-d_i) = |(1+\lambda)\mathbf{1}-G|$. Operators B and C are diagonal in a Fock basis representation since for an operator $O=z^{a^\dagger a}$ the characteristic function is given by

$$\chi_O(\eta) = \frac{1}{1-z} e^{-(\frac{z}{1-z}+\frac{1}{2})|\eta|^2}.$$

Applying this to the expressions for the characteristic functions for B and C above yields directly

$$B = \frac{\lambda^p}{(2+\lambda)^p - 1} \bigotimes_{i=1}^{p} \sum_{n_i=0}^{\infty} \left(\frac{1}{2+\lambda-d_i} \right)^{n_i} |n_i\rangle\langle n_i|, \tag{4.5a}$$

$$C = \left(\frac{\lambda}{1+\lambda} \right)^p \bigotimes_{i=1}^{p} \sum_{n_i=0}^{\infty} \left(\frac{1}{1+\lambda} \right)^{n_i} |n_i\rangle\langle n_i|. \tag{4.5b}$$

Finally, let a product state $|\phi\rangle^{\otimes p}$ have an expansion in terms of Fock states given by $|\phi\rangle^{\otimes p} = \sum_{n_1,\ldots,n_p} c_{n_1,\ldots,n_p} |n_1,\ldots,n_p\rangle$. By construction we know that $0 \leq \mathrm{tr}\left\{|\phi\rangle\langle\phi|^{\otimes p} B\right\}$ and therefore

$$\begin{aligned}
\mathrm{tr}\left\{|\phi\rangle\langle\phi|^{\otimes p} B\right\} &= \frac{\lambda^p}{(2+\lambda)^p - 1} \left| \sum_{n_1,\ldots,n_p=0}^{\infty} \prod_{i=1}^{p} \left(\frac{1}{2+\lambda-d_i} \right)^{n_i} |c_{n_1,\ldots,n_p}|^2 \right| \\
&\leq \frac{\lambda^p}{(2+\lambda)^p - 1} \sum_{n_1,\ldots,n_p=0}^{\infty} \prod_{i=1}^{p} \left| \frac{1}{2+\lambda-d_i} \right|^{n_i} |c_{n_1,\ldots,n_p}|^2 \\
&\leq \frac{\lambda^p}{(2+\lambda)^p - 1} \sum_{n_1,\ldots,n_p=0}^{\infty} \prod_{i=1}^{p} \left(\frac{1}{1+\lambda} \right)^{n_i} |c_{n_1,\ldots,n_p}|^2 \\
&= \frac{(1+\lambda)^p}{(2+\lambda)^p - 1} \mathrm{tr}\left\{|\phi\rangle\langle\phi|^{\otimes p} C\right\}.
\end{aligned}$$

Taking the p^{th} root of this sequence yields directly relation (4.4) and completes the proof.

The result assures that (in the case of a flat distribution) the fidelity limit of 1/2 is in fact appropriate in comparing quantum channels for coherent states of continuous variables with an optimal classical channel, justifying its application as a benchmark in continuous variable teleportation [40, 41, 42, 43, 44] ex post and in future experiments testing the performance of continuous variable quantum memories [60, 61, 11, 66]. In a recent experimental demonstration of the quantum state transfer from light onto atoms [11] the bound (4.2) has been used to demonstrate that the quantum memory has indeed exceeded the classical limit of the measure-and-prepare strategy. The present proof provides firm grounds for such a statement. In particular, the teleportation protocol of chapter 3 and the quantum memory protocol of chapter 5 allow to surpass the bound derived here.

We note that a measure-and-prepare scheme can be considered as a 1-to-∞ cloning machine, when we just duplicate the preparation device. In

fact, in this context for the special case of a flat distribution ($\lambda \to 0$) an independent proof based on the covariance of the problem is given in [81].

The criterion derived here allows one to test wether a given channel yields a higher quality of storage or transmission (measured in terms of the average fidelity) than what is possible by classical means. We would like to point out that there exist other criteria in the literature [81, 82, 83, 84] allowing to test different requirements. In particular if a channel has to be secure (in the sense that its action excludes the existence of a clone of the input state holding a higher fidelity than the channel's output) it has to outperform the best 1-to-2 cloning machine, which is more demanding than what was considered here [83]. For channels acting on the set of coherent states with a flat distribution this was analyzed in [81, 82, 83]. As shown in [82, 83] the best Gaussian 1-to-2 cloning machine yields a fidelity benchmark of 2/3 while the optimal non-Gaussian strategy yields a value of ≈ 0.6826 as was derived in [81].

Finally, we would like to point out that an experimental demonstration of a fidelity larger than 1/2 does not disprove the existence of a classical model in the sense of a local hidden variable theory able to describe the physical process [84, 85]. When we claim that it does prove the non-classicality or quantumness of the respective channel then this has to be understood in the sense that no classical measure-and-prepare strategy can give the same result within the framework of quantum mechanics.

In conclusion, we presented and proved a tight upper bound on the average fidelity achievable by a classical channel for coherent states of continuous variables subject to a Gaussian distribution over the phase space. This limit has to be surpassed by a quantum channel in order to outperform any competing classical strategy and is thus of direct experimental relevance in quantum teleportation of and quantum memories for continuous variables. The presented result in particular validate the outstanding experimental achievements in storing and teleporting continuous variable quantum states. The techniques, which led to the proof of the bound, in principle apply also to other sets of states in both continuous variable and finite dimensional systems. Depending on the considered sets and distributions they might thus yield similar quantum benchmarks in other contexts.

Chapter 5

Quantum memory and entanglement of light with atoms

Recent years have seen significant progress towards an efficient quantum interface between light pulses carrying quantum information and atomic ensembles suitable for storing and processing this information. Two approaches based on probabilistic photon detection [86, 87, 88] or on deterministic homodyne measurements [11, 47] have been developed. Of particular importance in the context of quantum information are means to swap the state of light and atoms - enabling a quantum memory for light - and to create Einstein-Podolsky-Rosen (EPR) type of entanglement of light and atoms - the basic resource for quantum teleportation.

Concerning the quest for a quantum memory, an important experimental advance was the recent demonstration of the storage of weak coherent light pulses in atoms [11], based on a Quantum Non Demolition (QND) interaction, measurement of light and feedback on atoms. However, reliable retrieval of the stored state by means of the same protocol would require the use of short pulses of squeezed light which are difficult to couple to atomic ensembles in an efficient way. The design of less demanding protocols for storage and retrieval of states of light remained a challenge, also from a theoretical perspective. Several protocols have been put forward, all relying on multiple passes of light through the atomic ensemble [89, 18, 19, 90, 91, 92]. The most efficient of these schemes, complying with the experimental requirement to use Larmor precessing atomic spins, require eight passes of a single pulse [91] or two pulses each crossing twice an atomic cell [92]. In this chapter we present a protocol, which consists of only *two* passes of a *single* pulse and achieves a state exchange of light and atoms scaling *exponentially*

in the coupling strength κ, defined operationally as the signal to noise ratio of the underlying QND interaction. This scheme allows one to perform the complete transfer of a quantum state of light onto atoms and back under modest experimental conditions, as we show for both, coherent states as well as arbitrary superpositions of vacuum and a single photon Fock state.

Moreover, the same double pass setup serves with a slightly changed geometry as a deterministic source of EPR entanglement between light and atoms. The entanglement scales thereby again exponentially in κ. Together, these two protocols add to the growing toolbox for quantum information processing with room temperature atomic vapors, which has already provided the possibility to entangle two atomic ensembles via a Bell-measurement on two Larmor precessing spins [10]. In combination these tools undoubtedly pave the way towards numerous relevant applications, of which the demonstration of a complete quantum memory and quantum teleportation are just the most immediate.

To be more specific, the setup of both protocols consists of an ensemble placed in an external magnetic field with large spin polarization along the axis of this field, such that the transverse spin components precess at frequency Ω. A coherent pulse is directed through the atomic sample such, that it crosses it twice under an angle of 90 degrees in the plane orthogonal to the axis of the magnetic field. The length d of the loop in the optical path is small, such that Larmor precession is frozen on a time scale $d/c \ll \Omega^{-1}$, but the pulse length is large as compared to the Larmor period, $T \gg \Omega^{-1}$. Under these conditions and the assumption that $\Omega T \gg \kappa^2$, which is well fulfilled in current experiments, we carefully solve the Maxwell-Bloch equations describing the dynamics of this scattering process. We identify the relevant light modes, which can be stored and retrieved or get entangled with atoms and characterize their temporal profile. The central frequency of these modes lies at the upper or lower sideband of the carrier frequency, which is to be expected given the splitting of ground state levels of Ω, and their slowly varying amplitude is exponential of the form $\exp(\pm\kappa^2 t/2T)$. The modes can thus be easily accessed. Note that this setup is, apart from the magnetic field, similar to the one treated in [91]. It is precisely the presence of the magnetic field what enables us to achieve our results with the simple setup described above.

The chapter is organized as follows. In section 5.1 we introduce the basic idea of our protocol and summarize the central results. In section 5.2 and 5.3 we provide the detailed derivation for the quantum memory and the EPR source respectively. Finally, section 5.4 deals with sources of noise under realistic conditions.

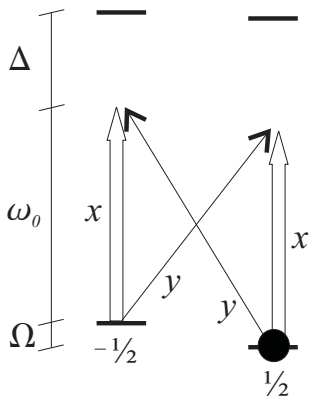

Figure 5.1: Relevant internal levels with quantization along $\hat{x}$. Thick arrows represent the strong coherent field in $\hat{x}$ polarization, thin arrows indicate the quantum field in $\hat{y}$ polarization.

5.1 Basic idea and central results

It will be helpful to have again a look at the configuration of the light-matter interaction of chapter 2 with an external magnetic field applied, as in chapter 3. The pulse of light is propagating along $\hat{z}$ and the atomic sample is assumed to be spin polarized along $\hat{x}$, while the magnetic field is orientated along the opposite direction. The pulse of light consists of a strong coherent $\hat{x}$-polarized component of central frequency ω_0, which is detuned by Δ from the atomic transition, and a copropagating quantum field in $\hat{y}$ polarization. Atoms have a relevant internal structure as shown in figure 5.1. With $\hat{x}$ being the quantization axis, the classical light field drives the $m = \pm 1/2 \rightarrow m' = \pm 1/2$ transitions, while the copropagating quantum field couples to the $m = \mp 1/2 \rightarrow m' = \pm 1/2$. In the case of a dominant ground state population of $m = 1/2$ levels, creation and annihilation operators of collective atomic excitations can be defined by $b^\dagger = \Sigma_i |-1/2\rangle\langle 1/2|/\sqrt{N_{\mathrm{at}}}$ and b, respectively, where N_{at} is the total number of atoms in the ensemble. Creation of an atomic excitation will then be accompanied by the absorption (emission) of a photon at frequency $\omega_0 + \Omega$, $(\omega_0 - \Omega)$, that is, at the upper (lower) sideband, where Ω is the Larmor frequency. Note that only the polarization, and not the energy of the sideband photons are relevant, so the notion of upper/lower sideband is rather arbitrary. Although we will finally deal with light interacting with atoms in free space, it is instructive to consider first the case, where atoms are placed inside a cavity supporting both sideband modes. Related setups employing cavities are considered in [93, 94]. We assume in the following that the cavity life time is much smaller than the Larmor period

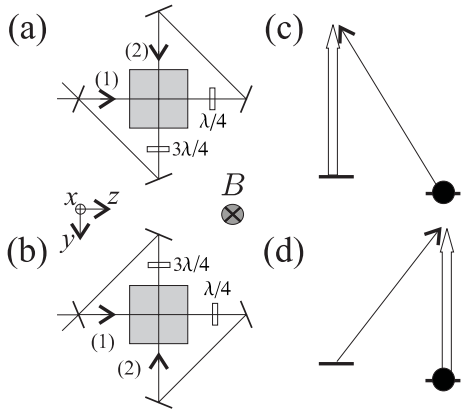

Figure 5.2: Setups for having (a) a beam splitter or (b) a two mode squeezing like dynamics. (c) and (d) show the effective transitions.

.

Ω^{-1} and let the creation operators for the upper and lower sideband be given by $a^\dagger_{us}$ and $a^\dagger_{ls}$ respectively. In the dispersive limit, the effective Hamiltonian describing the interaction is given by $H \propto (b\, a^\dagger_{us} - b^\dagger a^\dagger_{ls} + \text{h.c.})$, where the signs follow from Clebsch-Gordan coefficients. Note that if ground state levels were degenerate, such that $a_{us} = a_{ls} \equiv a$, the Hamiltonian would be $H \propto (b - b^\dagger)(a - a^\dagger)$, which is just the result obtained already in chapter 2. Including Zeeman splitting, the interaction consists of a passive and an active part, $H = H_{pas} - H_{act}$, where the passive part is a beam splitter Hamiltonian $H_{pas} \propto b\, a^\dagger_{us} + \text{h.c.}$ and acts only on the upper sideband, while the active part $H_{act} \propto b^\dagger a^\dagger_{ls} + h.c.$ can be identified with a two-mode-squeezing interaction, which involves exclusively the lower sideband. Now, either of these two interactions can be selected in one of the setups shown in figure 5.2a or 5.2b. The interaction in every second pass will again be given by H but with phase changes $a_{ls(us)} \rightarrow i a_{ls(us)}$, due to the $\lambda/4$ wave plate, and $b \rightarrow \pm ib$, due to the change of the direction of light propagation, where the upper sign holds for setup in figure 5.2a and the lower for 5.2b. The resulting Hamiltonian is $H'_\pm \propto \pm(b\, a^\dagger_{us} + b^\dagger a^\dagger_{ls} + \text{h.c.})$. Together, we get for setup 5.2a an interaction $H + H'_+ = H_{pas}$ and for 5.2b $H + H'_- = -H_{act}$. In either setup one of the two Λ-type transitions in figure 5.1 is canceled by interference, and one is left with the transitions shown in figures 5.2c and 5.2d. Note that these configurations remind of the Raman scattering processes put forward in [6] for the realization of a quantum repeater. Without a cavity, in setups as shown in figure 5.3, the effects still persists, as we will show by solving the corresponding Maxwell-Bloch equations. In contrast to the dynamics inside

a cavity, where Larmor precession of the atomic spin is not crucial, it is well so for propagation in free space. This can be understood by noting that both setups shown in figure 5.3, possess a certain asymmetry in how the two transverse spin components in $\hat{y}$ and $\hat{z}$ direction are affected by light. This was calculated in great detail in [91], where amongst others the setup of figure 5.3 was examined without magnetic field. We emphasize that Larmor precession helps to remove this asymmetry.

In the rest of this section we collect the results for both, the quantum memory and the two mode squeezing protocol. This will be done in the language of canonical operators $X = (b + b^\dagger)/\sqrt{2}$ and $P = -i(b - b^\dagger)/\sqrt{2}$ and likewise for light, since solutions to Maxwell Bloch equations are more conveniently derived in this formalism.

Quantum memory Within the memory scheme, figure 5.3a, the transfer of a quantum state of light onto atoms or vice versa approaches perfect mapping exponentially in the coupling strength. We have

$$\begin{pmatrix} X^{\text{out}} \\ P^{\text{out}} \end{pmatrix} = e^{-\frac{\kappa^2}{2}} \begin{pmatrix} X^{\text{in}} \\ P^{\text{in}} \end{pmatrix} + \sqrt{1 - e^{-\kappa^2}} \begin{pmatrix} x_+^{\text{in}} \\ p_+^{\text{in}} \end{pmatrix},$$

for the write-in procedure, where $X^{\text{in/out}}$ and $P^{\text{in/out}}$ are the atomic input/output quadratures of the scheme and $x_+^{\text{in/out}}$ and $p_+^{\text{in/out}}$ refer to the write-in light mode. It lies at the upper sideband (according to the configuration considered above) and is modulated by a slowly varying envelope with an exponential profile $\exp(+\kappa^2 t/T)$, which is a propagation effect. For the retrieval the inverse accented light mode, with an envelope $\exp(-\kappa^2 t/T)$, is used. We denote the corresponding operators by $x_-^{\text{in/out}}$ and $p_-^{\text{in/out}}$ and the input-output relations are

$$\begin{pmatrix} x_-^{\text{out}} \\ p_-^{\text{out}} \end{pmatrix} = -\sqrt{1 - e^{-\kappa^2}} \begin{pmatrix} X^{\text{in}} \\ P^{\text{in}} \end{pmatrix} + e^{-\frac{\kappa^2}{2}} \begin{pmatrix} x_+^{\text{in}} \\ p_+^{\text{in}} \end{pmatrix}.$$

Note that for large κ the state exchange is perfect. It is remarkable that both pairs of input-output relations have a form which reminds of a decoherence process, with the important difference that we have modes in place of Langevin noise operators, which can be controlled at will. The Fidelity for the complete state transfer - write in and subsequent retrieval of a state of light- is given in figure 5.4(a) and (b) for coherent input states and light qubits respectively.

EPR source The active version of the protocol, figure 5.3b, generates correlations between atoms and light, which grow exponentially in the coupling.

The input-output relations for the relevant modes are

$$\begin{pmatrix} X^{\rm out} \\ P^{\rm out} \end{pmatrix} = e^{\frac{\kappa^2}{2}} \begin{pmatrix} X^{\rm in} \\ P^{\rm in} \end{pmatrix} + \sqrt{e^{\kappa^2}-1} \begin{pmatrix} p_-^{\rm in} \\ x_-^{\rm in} \end{pmatrix}.$$
$$\begin{pmatrix} p_+^{\rm out} \\ x_+^{\rm out} \end{pmatrix} = \sqrt{e^{\kappa^2}-1} \begin{pmatrix} X^{\rm in} \\ P^{\rm in} \end{pmatrix} + e^{\frac{\kappa^2}{2}} \begin{pmatrix} p_-^{\rm in} \\ x_-^{\rm in} \end{pmatrix}.$$

One can define interspecies EPR modes

$$x_1 = \frac{1}{\sqrt{2}}(X - p_+), \qquad p_1 = \frac{1}{\sqrt{2}}(P + x_+),$$
$$x_2 = \frac{1}{\sqrt{2}}(X + p_+), \qquad p_2 = \frac{1}{\sqrt{2}}(P - x_+).$$

The input-output relations imply that x_1 and p_2 are squeezed, while x_2 and p_1 are antisqueezed,

$$\begin{aligned} (\Delta x_1)^2 &= (\Delta p_2)^2 = e^{-2z}, \\ (\Delta p_1)^2 &= (\Delta x_2)^2 = e^{2z}, \end{aligned}$$

where $z = \cosh^{-1}(e^{\frac{\kappa^2}{2}})$. The EPR variance of the generated state is depicted in figure 5.5.
The results presented above will be derived in the following sections. We remark that each protocol can be realized involving either the upper or the lower sideband. The sideband mode involved can be changed by either inverting the ground state polarization or changing the orientation of the magnetic field. Losses will be considered in section 5.4 and it will be shown that the proposed protocols are robust against the dominant sources of noise.

5.2 Quantum memory

Write-in

As follows from the results of chapter 2, the double-pass interaction in setup 5.3a can be described by

$$H = H_{\rm at} + H_{\rm li} + V_1 + V_2 \ .$$

$H_{\rm at} = \frac{\hbar\Omega}{2}(X^2 + P^2)$ refers to Zeeman-splitting of the atomic ground state causing Larmor precession of the transverse spin components represented by X and P. The interaction terms V_1 and V_2 account for the off-resonant

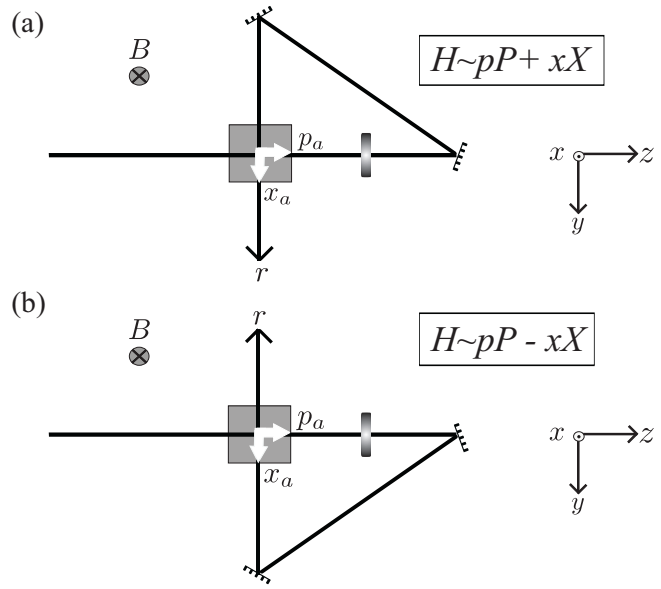

Figure 5.3: Schemes for realization of a quantum memory (a) and a source of EPR entanglement (b). **(a)** In the first pass a pP-interaction occurs. Subsequently the pulse is sent through a $\frac{\lambda}{4}$ - plate, which interchanges x and p. The pulse is reflected back onto the sample. This happens at a timescale much shorter than the Larmor precession of the atoms. Therefore the transverse components of the collective spin can be assumed to remain in their place to a very good approximation. Finally the pulse passes the atoms along $\hat{y}$. Due to the changed geometry the atomic quadratures are also interchanged. $P \to X$ and $X \to -P$, which means, that the light field couples to X in it's second passage, hence leading to a xX -interaction. In **(b)** the changed geometry introduces a different sign in the exchange of atomic quadratures, which leads to a $-xX$ interaction in the second pass.

scattering interaction in the first and second passage of the pulse respectively. They are given by

$$V_1 = \frac{\hbar\kappa}{\sqrt{T}} P p(0) \quad \text{and} \quad V_2 = \frac{\hbar\kappa}{\sqrt{T}} X x(d) \ ,$$

where T is the duration of the pulse. V_1 was already introduced. V_2 describes basically the same kind of interaction, but due to the changed geometry in the second pass atomic quadratures are interchanged $P \to X$. Since the beam is sent through a quarter wave plate between it's passes through the atomic sample, light quadratures are interchanged as well $p \to x$. The arguments of the light-operators in V_1 and V_2 indicate that the first scattering interaction

occurs at $r = 0$, while the second interaction happens after the light has traveled some distance d in the small loop between the mirrors. The length of the laser pulse is hereby supposed to be large compared with the distance within the loop. In typical experiments pulses of a length of several hundred km are used, therefore the pulse encounters itself in the sample. $H_{\rm li}$ represents free propagation of light.

Evaluating the Heisenberg equations gives

$$\begin{aligned}
\frac{\partial}{\partial t}X(t) &= \Omega P(t) + \frac{\kappa}{\sqrt{T}}p(0,t)\ , \\
\frac{\partial}{\partial t}P(t) &= -\Omega X(t) - \frac{\kappa}{\sqrt{T}}x(d,t)\ , \\
\left(\frac{\partial}{\partial t} + c\frac{\partial}{\partial r}\right)x(r,t) &= \frac{\kappa c}{\sqrt{T}}P(t)\delta(r)\ , \\
\left(\frac{\partial}{\partial t} + c\frac{\partial}{\partial r}\right)p(r,t) &= -\frac{\kappa c}{\sqrt{T}}X(t)\delta(r-d)\ .
\end{aligned}$$

By performing the variable transformation $\xi = ct - r$ we obtain the Maxwell-Bloch equations

$$\frac{\partial}{\partial t}X(t) = \Omega P(t) + \frac{\kappa}{\sqrt{T}}\bar{p}(ct,t), \tag{5.1}$$

$$\frac{\partial}{\partial t}P(t) = -\Omega X(t) - \frac{\kappa}{\sqrt{T}}\bar{x}(ct-d,t), \tag{5.2}$$

$$\frac{\partial}{\partial t}\bar{x}(\xi,t) = \frac{\kappa c}{\sqrt{T}}P(t)\delta(ct-\xi), \tag{5.3}$$

$$\frac{\partial}{\partial t}\bar{p}(\xi,t) = -\frac{\kappa c}{\sqrt{T}}X(t)\delta(ct-\xi-d). \tag{5.4}$$

As before, light modes depending on the new variables are denoted by a bar $\bar{x}(\xi,t) = x(ct-\xi,t)$. This set of coupled differential equations has now to be solved. As a first step we treat the equations for light. In the first pass a pP -interaction occurs and x picks up some P contribution. The delta function in (5.3) reflects the fact that a certain piece ξ of the pulse gets a contribution from the atomic state at $t = \xi/c$ (which is the instant of time the piece in consideration passes by). In the second pass a xX -interaction occurs, and the atomic x -quadrature is written onto p. A piece ξ of the pulse, which interacted with p at time ξ/c gets a contribution from x after it has traveled a distance d in the loop. Therefore the atomic x quadrature is picked up at $t = \xi/c + d/c$ which is indicated by the delta-function in equation (5.4). By integrating equations (5.3) and (5.4) formally, these delta functions turn into

Heaviside functions,

$$\begin{aligned}
\bar{x}(\xi,t) &= \bar{x}(\xi,0)+\frac{\kappa c}{\sqrt{T}}\int_0^t d\tau P(\tau)\delta(c\tau-\xi)\\
&= \bar{x}(\xi,0)+\frac{\kappa}{\sqrt{T}}P(\xi/c)\Theta(t-\xi/c),\\
\bar{p}(\xi,t) &= \bar{p}(\xi,0)-\frac{\kappa c}{\sqrt{T}}\int_0^t d\tau X(\tau)\delta(c\tau-\xi-d)\\
&= \bar{p}(\xi,0)-\frac{\kappa}{\sqrt{T}}X(\xi/c+d/c)\Theta(t-\xi/c-d/c).
\end{aligned}$$

Now $\bar{p}(ct,t)$ and $\bar{x}(ct-d,t)$ are calculated, since these expressions have to be plugged into the atomic differential equations (5.1) and (5.2). The fact that the arguments are different for x and p can be understood by considering the processes going on in the course of the double pass scheme. During the pP-interaction in the first passage X picks up some p contribution. If we consider this process at a certain instant of time t, the relevant piece of the pulse is the one, which is at $r=0$, which means for which $\xi=ct-r=ct$. P is acted upon by x in the second pass by the piece of the pulse which passes $r=d$ at time t. So it gets a contribution from $\bar{p}(ct-d,t)$. One finds

$$\begin{aligned}
\bar{x}(ct-d,t) &= \bar{x}(ct-d,0)+\frac{\kappa}{\sqrt{T}}P(t-d/c)\Theta(d/c)\\
&= \bar{x}(ct-d,0)+\frac{\kappa}{\sqrt{T}}P(t-d/c),\\
\bar{p}(ct,t) &= \bar{p}(ct,0)-\frac{\kappa}{\sqrt{T}}X(t+d/c)\Theta(-d/c)\\
&= \bar{p}(ct,0).
\end{aligned}$$

Note that $\bar{p}(ct,t)$ is conserved. This feature is due to the time-delay in the loop and will turn out to be crucial for the characteristic exponential behavior of the whole scheme. After inserting these results into (5.1) and (5.2) the atomic differential equations read

$$\begin{aligned}
\frac{\partial}{\partial t}X(t) &= \Omega P(t)+\frac{\kappa}{\sqrt{T}}\bar{p}(ct,0),\\
\frac{\partial}{\partial t}P(t) &= -\Omega X(t)-\frac{\kappa}{\sqrt{T}}\bar{x}(ct-d,0)-\frac{\kappa^2}{T}P(t-d/c).
\end{aligned}$$

Now we assume $d/c \ll \Omega^{-1}$, such that the elapsed time during the run in the loop is definitely much shorter than any other relevant process. d/c can be

assumed to be of the order of ns while atoms rotate slowly with a Larmor period of the order of μs. With this approximation

$$\frac{\partial}{\partial t}\begin{pmatrix} X(t) \\ P(t) \end{pmatrix} = \left\{ \Omega \begin{pmatrix} 0 & 1 \\ -1 & 0 \end{pmatrix} - \frac{\kappa^2}{T} \begin{pmatrix} 0 & 0 \\ 0 & 1 \end{pmatrix} \right\} \begin{pmatrix} X(t) \\ P(t) \end{pmatrix} + \frac{\kappa}{\sqrt{T}} \begin{pmatrix} \bar{p}(ct,0) \\ -\bar{x}(ct,0) \end{pmatrix}. \tag{5.5}$$

This differential equation consists of a homogeneous part and a driving term. The first term of the homogeneous part - being proportional to the Larmor frequency - reflects the fact that atoms turn with Ω in the external magnet field. The second term in the homogeneous part represents damping of P. Although only one quadrature is damped, the effect is distributed among both quadratures by Larmor precession. This leads to a symmetry between x and p, which is a characteristic feature of our proposal. The solution to the differential equation is

$$\begin{pmatrix} X(t) \\ P(t) \end{pmatrix} = \quad A(t) \begin{pmatrix} X(0) \\ P(0) \end{pmatrix} + A(t) \frac{\kappa}{\sqrt{T}} \int_0^t d\tau \; A^{-1}(\tau) \begin{pmatrix} \bar{p}(c\tau,0) \\ -\bar{x}(c\tau,0) \end{pmatrix},$$

where $A(t) = e^{Gt}$, $G = \Omega \begin{pmatrix} 0 & 1 \\ -1 & 0 \end{pmatrix} - \frac{\kappa^2}{T} \begin{pmatrix} 0 & 0 \\ 0 & 1 \end{pmatrix}$. We suppose $\Omega T \gg \kappa^2$, which matches experimental conditions, since typically $\Omega T \approx 300$ while κ^2 is of order unity. With this assumption

$$A(t) = e^{-\frac{\kappa^2 t}{2T}} R^{-1}(t) \; ,$$

where $R^{-1}(t)$ is an orthogonal matrix,

$$R^{-1}(t) = \begin{pmatrix} \cos(\Omega t) & \sin(\Omega t) \\ -\sin(\Omega t) & \cos(\Omega t) \end{pmatrix}.$$

The inverse is taken for later convenience. Therefore the atomic time evolution is given by

$$\begin{pmatrix} X(t) \\ P(t) \end{pmatrix} = e^{-\frac{\kappa^2 t}{2T}} R^{-1}(t) \begin{pmatrix} X^{\text{in}} \\ P^{\text{in}} \end{pmatrix} + e^{-\frac{\kappa^2 t}{2T}} R^{-1}(t) \frac{\kappa}{\sqrt{T}} \int_0^t d\tau e^{\frac{\kappa^2 \tau}{2T}} R(\tau) \begin{pmatrix} \bar{p}(c\tau,0) \\ -\bar{x}(c\tau,0) \end{pmatrix}. \tag{5.6}$$

Now the atomic output quadratures $X^{\text{out}} = X(T)$ and $P^{\text{out}} = P(T)$ can be directly written down. With the assumption $\Omega T = 2\pi n$ for some natural number n,

$$\begin{pmatrix} X^{\text{out}} \\ P^{\text{out}} \end{pmatrix} = e^{-\frac{\kappa^2}{2}} \begin{pmatrix} X^{\text{in}} \\ P^{\text{in}} \end{pmatrix} + e^{-\frac{\kappa^2}{2}} \frac{\kappa}{\sqrt{T}} \int_0^T dt \; e^{\frac{\kappa^2 t}{2T}} R(t) \begin{pmatrix} \bar{p}(ct,0) \\ -\bar{x}(ct,0) \end{pmatrix}.$$

The atomic output-quadratures consist of some atomic input contribution which is damped exponentially with κ^2 and an additional light contribution which they pick up during the scattering interaction. The definition of the appropriate light-mode can be taken from this result right away,

$$\begin{pmatrix} x_+^{\text{in}} \\ p_+^{\text{in}} \end{pmatrix} = \frac{\kappa}{\sqrt{T}\sqrt{e^{\kappa^2}-1}} \int_0^T dt\; e^{\frac{\kappa^2 t}{2T}} R(t) \begin{pmatrix} \bar{p}(ct,0) \\ -\bar{x}(ct,0) \end{pmatrix}, \tag{5.7}$$

where the prefactor assures normalization such that $[x_+^{\text{in}}, p_+^{\text{in}}] = i$. This new defined light mode is essentially the upper sideband mode x_{us}, p_{us}, which is given by

$$\begin{pmatrix} x_{us}^{\text{in}} \\ p_{us}^{\text{in}} \end{pmatrix} = \frac{1}{\sqrt{T}} \int_0^T dt\; R(t) \begin{pmatrix} \bar{p}(ct,0) \\ -\bar{x}(ct,0) \end{pmatrix}. \tag{5.8}$$

The only difference is given by the fact that the stored mode $x_+^{\text{in}}, p_+^{\text{in}}$ is defined with a slowly varying envelope of the form $\exp(+\kappa^2 t/2T)$. The index " $+$ " refers to the sign of the argument in this exponential function (later on we will also have to deal with corresponding " $-$ " modes). With use of (5.7) the atomic input-output relations can be written in a compact form

$$\begin{pmatrix} X^{\text{out}} \\ P^{\text{out}} \end{pmatrix} = e^{-\frac{\kappa^2}{2}} \begin{pmatrix} X^{\text{in}} \\ P^{\text{in}} \end{pmatrix} + \sqrt{1-e^{-\kappa^2}} \begin{pmatrix} x_+^{\text{in}} \\ p_+^{\text{in}} \end{pmatrix}. \tag{5.9}$$

These equations describe the write-in process for a signal, which is encoded at the mode described above. Remarkably, mapping of such a quantum state of light onto atoms approaches perfect read-in exponentially in the coupling strength. This arises from the fact, that in the course of the double pass scattering interaction x picks up some contribution from the atomic p -quadrature, while p in contrast is conserved. Therefore we do not get a rotating term in the basic differential equation (5.5), which would lead to sines and cosines in the solution, as we would expect for a beam splitter like interaction, but an exponential effect, which is characteristic for the setup.

Read-out

In order to perform the read-out, a pulse of light has to be sent through the double-pass setup, just like for the write-in procedure, but since we are now looking at the reverse process, the appropriate light mode for this task has to be accented in an inverse fashion. While in the write-in process the rear part of the pulse was emphasized, now the front part of the pulse has to be weighted in order to pick up atomic information best. As the exponent in the

mode definition is negative this read-out mode will be denoted by a minus sign. Since we now deal with a new beam of light which is independent from the write-in pulse, read-out beam variables carry an accent,

$$\begin{pmatrix} \acute{x}_-^{\rm in} \\ \acute{p}_-^{\rm in} \end{pmatrix} = \frac{\kappa}{\sqrt{T}\sqrt{1-e^{-\kappa^2}}} \int_0^T dt\, e^{-\frac{\kappa^2 t}{2T}} R(t) \begin{pmatrix} \acute{\hat{p}}(ct,0) \\ -\acute{\hat{x}}(ct,0) \end{pmatrix},$$

with a new normalization constant $\kappa/(\sqrt{T}\sqrt{1-e^{-\kappa^2}})$. The input-output relations for this mode can be derived by changing the time argument of light operators from 0 to T, reflecting the fact that we now look at the light quadratures after the whole pulse run trough the atomic sample

$$\begin{pmatrix} \acute{x}_-^{\rm out} \\ \acute{p}_-^{\rm out} \end{pmatrix} = \frac{\kappa}{\sqrt{T}\sqrt{1-e^{-\kappa^2}}} \int_0^T dt e^{-\frac{\kappa^2 t}{2T}} R(t) \begin{pmatrix} \acute{\hat{p}}(ct,T) \\ -\acute{\hat{x}}(ct,T) \end{pmatrix}.$$

To evaluate this expression in terms of input-operators the integrated versions of equations (5.3) and (5.4)

$$\begin{aligned} \acute{\hat{x}}(\xi,t) &= \acute{\hat{x}}(\xi,0) + \frac{\kappa}{\sqrt{T}} P(\xi/c)\Theta(t-\xi/c), \\ \acute{\hat{p}}(\xi,t) &= \acute{\hat{p}}(\xi,0) - \frac{\kappa}{\sqrt{T}} X(\xi/c)\Theta(t-\xi/c). \end{aligned}$$

are used. Therefore

$$\begin{aligned} \begin{pmatrix} \acute{x}_-^{\rm out} \\ \acute{p}_-^{\rm out} \end{pmatrix} &= \frac{\kappa}{\sqrt{T}\sqrt{1-e^{-\kappa^2}}} \int_0^T dt\; e^{-\frac{\kappa^2 t}{2T}} R(t) \\ &\quad \times \left[\begin{pmatrix} \acute{\hat{p}}(ct,0) \\ -\acute{\hat{x}}(ct,0) \end{pmatrix} - \frac{\kappa}{\sqrt{T}} \begin{pmatrix} X(t) \\ P(t) \end{pmatrix} \Theta(T-t) \right], \\ &= \begin{pmatrix} \acute{x}_-^{\rm in} \\ \acute{p}_-^{\rm in} \end{pmatrix} - \frac{\kappa^2}{T\sqrt{1-e^{-\kappa^2}}} \int_0^T dt e^{-\frac{\kappa^2 t}{2T}} R(t) \begin{pmatrix} X(t) \\ P(t) \end{pmatrix}. \end{aligned}$$

Now the atomic time evolution (5.6) has to be inserted. The resulting expression can be simplified by interchanging the order of the double-integral $\int_0^T dt \int_0^t d\tau \to \int_0^T d\tau \int_\tau^T dt$. With help of equation (5.7) the readout output can then be written as a sum of an atomic contribution and some contribution from the plus-mode.

$$\begin{pmatrix} \acute{x}_-^{\rm out} \\ \acute{p}_-^{\rm out} \end{pmatrix} = -\sqrt{1-e^{-\kappa^2}} \begin{pmatrix} X^{\rm in} \\ P^{\rm in} \end{pmatrix} + e^{-\frac{\kappa^2}{2}} \begin{pmatrix} \acute{x}_+^{\rm in} \\ \acute{p}_+^{\rm in} \end{pmatrix} \qquad (5.10)$$

Note that this expression resembles the formula for the write-in procedure with the roles of light- and atomic modes interchanged.

Fidelity for the complete state transfer

The fidelity for the complete state transfer is given by the overlap of the initial input state and the final output state after storage and subsequent retrieval. By inserting the output of the write-in procedure (5.9) into the read-out equation (5.10) one obtains

$$\begin{aligned} x_-^{\text{fin}} &= -\left(1-e^{-\kappa^2}\right) x_+^{\text{in}} - e^{-\frac{\kappa^2}{2}}\sqrt{1-e^{-\kappa^2}}X^{\text{in}} + e^{-\frac{\kappa^2}{2}}\acute{x}_-^{\text{in}}, \\ p_-^{\text{fin}} &= -\left(1-e^{-\kappa^2}\right) p_+^{\text{in}} - e^{-\frac{\kappa^2}{2}}\sqrt{1-e^{-\kappa^2}}P^{\text{in}} + e^{-\frac{\kappa^2}{2}}\acute{p}_-^{\text{in}}. \end{aligned} \tag{5.11}$$

For infinite coupling κ^2 the original input-signal is retrieved within the final quadratures of the read-out pulse $x_-^{\text{fin}} = -x_+^{\text{in}}$ and $p_-^{\text{fin}} = -p_+^{\text{in}}$, while the noise terms (atomic and read-out beam input contributions) vanish.
The quantum state to be stored is supposed to be unknown. It is assumed to be taken from a certain set of possible input-states. In the following two subsections we will consider coherent input states and light qubits respectively. We will first calculate the fidelity for a single state transfer and take the average over the complete set of possible input states in the next step in each case. The results will be compared to the corresponding classical limits, i.e. the maximum average fidelity, that can be achieved by classical means c.f. chapter 4.

Fidelity for coherent input states

We first consider storage of a coherent state of light. The overlap between an initial state with quadratures x_+^{in}, p_+^{in} and the final state with $\acute{x}_-^{\text{fin}}$, $\acute{p}_-^{\text{fin}}$ is given by

$$\begin{aligned} F_{coh} = &\frac{2}{\sqrt{[1+2(\Delta\acute{x}_-^{\text{fin}})^2][1+2(\Delta\acute{p}_-^{\text{fin}})^2]}} \\ &\times \exp\left\{-\frac{(\langle x_+^{\text{in}}\rangle + \langle\acute{x}_-^{\text{fin}}\rangle)^2}{1+2(\Delta\acute{x}_-^{\text{fin}})^2} - \frac{(\langle p_+^{\text{in}}\rangle + \langle\acute{p}_-^{\text{fin}}\rangle)^2}{1+2(\Delta\acute{p}_-^{\text{fin}})^2}\right\}. \end{aligned} \tag{5.12}$$

The expectation values and variances of the final light state follow directly from (5.11). Since the atoms and the read-out plus mode are initially in a vacuum state we have $\langle x_-^{\text{fin}}\rangle = -(1-e^{-\kappa^2})\langle x_+^{\text{in}}\rangle$ and $\langle p_-^{\text{fin}}\rangle = -(1-e^{-\kappa^2})\langle p_+^{\text{in}}\rangle$, while the variances are given by $(\Delta x_-^{\text{fin}})^2 = (\Delta p_-^{\text{fin}})^2 = \frac{1}{2}$, as one expects for a passive transformation. Therefore

$$F_{coh} = e^{-\frac{1}{2}(\langle x_+^{\text{in}}\rangle^2 + \langle p_+^{\text{in}}\rangle^2)e^{-2\kappa^2}} .$$

Now the average fidelity is computed by averaging over the complete set of all possible coherent input states. For this purpose the amplitudes x_+^{in} and p_+^{in} are assumed to be taken according to a Gaussian distribution centered at zero with a certain width n.

$$\begin{aligned}\bar{F}_{coh}(n,\kappa) &= \frac{1}{2\pi n}\int\int d\langle x_+^{\text{in}}\rangle d\langle p_+^{\text{in}}\rangle\; e^{-\frac{\langle x_+^{\text{in}}\rangle^2+\langle p_+^{\text{in}}\rangle^2}{2n}} F_{coh}(\langle x_+^{\text{in}}\rangle,\langle p_+^{\text{in}}\rangle,\kappa)\\ &= \frac{1}{(2-e^{-\kappa^2}-2\sqrt{1-e^{-\kappa^2}}+\frac{1}{n})n}.\end{aligned}$$

Figure 5.4a shows the average fidelity for different widths corresponding to mean photon numbers of the distribution. The corresponding classical limit $\bar{F}_{coh}^{cl}=\frac{2n+1}{4n+1}$.

Fidelity for light qubits

Now the fidelity for light-qubits is calculated. The light-qubit input state is represented by

$$|\Psi^{\text{in}}\rangle = (\alpha+\beta a_+^{\text{in}\dagger})|vac\rangle,$$

where $a_+^{\text{in}\dagger}=\frac{1}{\sqrt{2}}(x_+^{\text{in}}-ip_+^{\text{in}})$ is the creation operator for a photon in the write-in mode. The write-in and read-out procedure is given by a passive transformation U

$$\begin{aligned}|\Psi^{\text{fin}}\rangle = U|\Psi^{\text{in}}\rangle &= (\alpha+\beta U a_+^{\text{in}\dagger})|vac\rangle\\ &= (\alpha+\beta U a_+^{\text{in}\dagger}U^\dagger)|vac\rangle\\ &= (\alpha+\beta a_-^{\text{fin}\dagger})|vac\rangle\ ,\end{aligned}\tag{5.13}$$

where $U|vac\rangle=|vac\rangle$ was used. Here $a_-^{\text{fin}\dagger}=\frac{1}{\sqrt{2}}(x_-^{\text{fin}}-ip_-^{\text{fin}})$ is the creation operator after mapping and subsequent retrieval. It can be directly calculated, since the complete input-output relations for the light-quadratures are known. With use of equations (5.11)

$$a_-^{\text{fin}\dagger}=-(1-e^{-\kappa^2})a_+^{\text{in}\dagger}-e^{-\frac{\kappa^2}{2}}\sqrt{1-e^{-\kappa^2}}a_A^{\text{in}\dagger}+e^{-\frac{\kappa^2}{2}}\acute{a}_-^{\text{in}\dagger},\tag{5.14}$$

where $a_+^{\text{in}\dagger}$, $a_A^{\text{in}\dagger}$ and $\acute{a}_-^{\text{in}\dagger}$ refer to the light state to be stored, the atoms and the read-out mode respectively. The Fidelity is given by the state overlap between $|\Psi^{\text{fin}}\rangle$ and the optimal final state $|\Psi_{opt}^{\text{fin}}\rangle=(\alpha-\beta a_+^{\text{in}\dagger})|vac\rangle$. By inserting (5.14) into expression (5.13) F_{qubit} can easily be determined. One obtains

$$F_{qubit}=|\langle\Psi^{\text{fin}}|\Psi_{opt}^{\text{fin}}\rangle|^2=|(|\alpha|^2+\{1-e^{-\kappa^2}\}|\beta|^2)|^2.$$

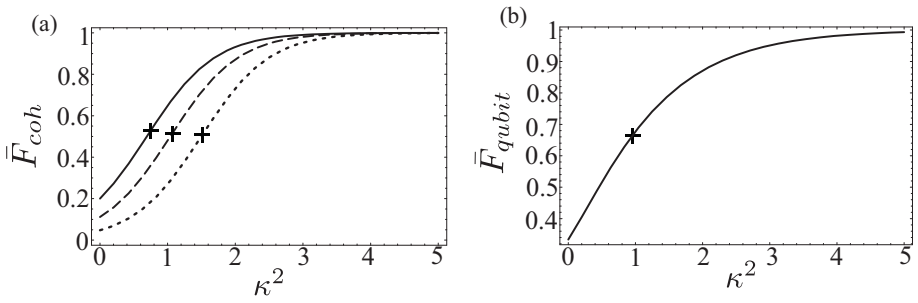

Figure 5.4: Average fidelity for write-in and subsequent read-out of a light state versus coupling κ^2. Crosses indicate the classical limit in each case. **(a)** Average fidelity for coherent light states according to distributions with different mean photon numbers (solid line: n=4, dashed line: n=8, dotted line: n=20) **(b)** Average fidelity for light qubits.

The average fidelity is calculated by setting $\alpha = \cos(\frac{\theta}{2})$ and $\beta = \sin(\frac{\theta}{2})e^{i\phi}$ and integrating over the whole Bloch-sphere,

$$\begin{aligned} \bar{F}_{qubit}(\kappa) &= \frac{1}{4\pi}\int_0^{\pi} d\theta \int_0^{2\pi} d\phi \sin(\theta) F_{qubit}(\theta,\phi) \\ &= 1 - e^{-\kappa^2} + \frac{1}{3}e^{-2\kappa^2}. \end{aligned}$$

Figure 5.4b shows this result. The maximal average fidelity that can be achieved for qubit states by a classical strategy $\bar{F}^{cl}_{qubit} = \frac{2}{3}$ [70, 71, 72] is indicated by a cross.

5.3 Two mode squeezing

The interaction which governs the squeezing scheme pictured in figure 5.3(b), is given by

$$\tilde{H} = H_{\rm at} + H_{\rm li} + V_1 - V_2 \ .$$

This Hamiltonian differs from the one used in the memory section just by a sign in the interaction term referring to the second passage. The pulse runs along $-\hat{y}$ in the second pass of the squeezing scheme (instead of $\hat{y}$ in the previous case) and sees therefore $-X$. Hence we have the minus sign in front of V_2 for the new setup.

Input-output relations

The atomic input-output relations can now be derived in complete analogy to section 5.2. By evaluating the Heisenberg equations as above we get

$$\frac{\partial}{\partial t}\begin{pmatrix} X(t) \\ P(t) \end{pmatrix} = \left\{\Omega\begin{pmatrix} 0 & 1 \\ -1 & 0 \end{pmatrix} + \frac{\kappa^2}{T}\begin{pmatrix} 0 & 0 \\ 0 & 1 \end{pmatrix}\right\}\begin{pmatrix} X(t) \\ P(t) \end{pmatrix} + \frac{\kappa}{\sqrt{T}}\begin{pmatrix} \bar{p}(ct,0) \\ \bar{x}(ct,0) \end{pmatrix}.$$

With the usual approximation $\kappa^2 \ll 2\Omega T$ we obtain

$$\begin{pmatrix} X(t) \\ P(t) \end{pmatrix} = e^{\frac{\kappa^2 t}{2T}} R^{-1}(t)\begin{pmatrix} X^{\text{in}} \\ P^{\text{in}} \end{pmatrix} + e^{\frac{\kappa^2 t}{2T}} R^{-1}(t)\frac{\kappa}{\sqrt{T}}\int_0^t d\tau e^{-\frac{\kappa^2 \tau}{2T}} R(\tau)\begin{pmatrix} \bar{p}(c\tau,0) \\ \bar{x}(c\tau,0) \end{pmatrix}.$$

These equations are in a significant way different from the atomic time evolution (5.6) in the memory scheme. Note first the signs in the arguments of the exponential functions. We now have exponential enhancement of the atomic input instead of exponential damping. Furthermore light is involved in form of a minus mode in the atomic input-output relations because of the minus sign in the exponent within the integral. Note second, that the minus sign, which was present in front of $\bar{x}(ct,0)$ in the memory scheme, does not appear in this case. Therefore the lower sideband

$$\begin{pmatrix} p_{ls}^{\text{in}} \\ x_{ls}^{\text{in}} \end{pmatrix} = \frac{1}{\sqrt{T}}\int_0^T dt\ R(t)\begin{pmatrix} \bar{p}(ct,0) \\ \bar{x}(ct,0) \end{pmatrix} \tag{5.15}$$

is involved instead of the upper one (5.8). Hence the minus mode showing up in the atomic time evolution is defined slightly differently from the memory section

$$\begin{pmatrix} \tilde{p}_-^{\text{in}} \\ \tilde{x}_-^{\text{in}} \end{pmatrix} = \frac{\kappa}{\sqrt{T}\sqrt{1-e^{-\kappa^2}}}\int_0^T dt e^{-\frac{\kappa^2 t}{2T}} R(t)\begin{pmatrix} \bar{p}(ct,0) \\ \bar{x}(ct,0) \end{pmatrix}.$$

With use of this definition and the assumption $\Omega T = 2\pi n$ for some natural number n, the atomic input-output relations read

$$\begin{pmatrix} X^{\text{out}} \\ P^{\text{out}} \end{pmatrix} = e^{\frac{\kappa^2}{2}}\begin{pmatrix} X^{\text{in}} \\ P^{\text{in}} \end{pmatrix} + \sqrt{e^{\kappa^2}-1}\begin{pmatrix} \tilde{p}_-^{\text{in}} \\ \tilde{x}_-^{\text{in}} \end{pmatrix}. \tag{5.16}$$

Light input-output relations for this process can be derived in analogy to the procedure in section 5.2. The inverse accented counter-part of the light

mode used in the atomic evolution is given by

$$\begin{pmatrix} \tilde{p}_+^{\rm in} \\ \tilde{x}_+^{\rm in} \end{pmatrix} = \frac{\kappa}{\sqrt{T}\sqrt{e^{\kappa^2}-1}} \int_0^T dt\; e^{\frac{\kappa^2 t}{2T}} R(t) \begin{pmatrix} \bar{p}(ct,0) \\ \bar{x}(ct,0) \end{pmatrix}.$$

We refer now to the same pulse as in (5.16), while in the derivation of the input-output relations for atoms and light in section 5.2 two independent beams were considered. We obtain

$$\begin{pmatrix} \tilde{p}_+^{\rm out} \\ \tilde{x}_+^{\rm out} \end{pmatrix} = \sqrt{e^{\kappa^2}-1} \begin{pmatrix} X^{\rm in} \\ P^{\rm in} \end{pmatrix} + e^{\frac{\kappa^2}{2}} \begin{pmatrix} \tilde{p}_-^{\rm in} \\ \tilde{x}_-^{\rm in} \end{pmatrix}. \tag{5.17}$$

Please note that the input-output relations (5.16) and (5.17) are active versions of (5.9) and (5.10) respectively.

Creation of entanglement

As can be seen from the input-output relations for atoms and light given in equations (5.16) and (5.17) respectively, correlations between atoms and light are created which grow exponentially in the coupling strength. We define new modes appropriate to the type of correlations produced in the system by setting

$$\begin{aligned} x_1 &= \frac{1}{\sqrt{2}}(X - \tilde{p}_+), \qquad p_1 = \frac{1}{\sqrt{2}}(P + \tilde{x}_+), \\ x_2 &= \frac{1}{\sqrt{2}}(X + \tilde{p}_+), \qquad p_2 = \frac{1}{\sqrt{2}}(P - \tilde{x}_+). \end{aligned}$$

The corresponding variances can be calculated easily from (5.16) and (5.17). We get

$$\begin{aligned} (\Delta x_1)^2 &= (\Delta p_2)^2 = \left(\sqrt{e^{\kappa^2}-1} - e^{\frac{\kappa^2}{2}}\right)^2 = e^{-2z}, \\ (\Delta p_1)^2 &= (\Delta x_2)^2 = \left(\sqrt{e^{\kappa^2}-1} + e^{\frac{\kappa^2}{2}}\right)^2 = e^{2z}, \end{aligned}$$

with $z = \cosh^{-1}(e^{\frac{\kappa^2}{2}})$. We get a two mode squeezed state where x_1 and p_2 are squeezed, while p_1 and x_2 are antisqueezed. In the limit of infinite coupling the state becomes an EPR state in which X, $\tilde{p}_+$ and P, $\tilde{x}_+$ are perfectly correlated. For the state under consideration, the EPR-variance $\Delta_{EPR} = \frac{1}{2}(\Delta x_1^2 + \Delta p_2^2) = e^{-2z}$ is an entanglement measure [56]. For separable states $\Delta_{EPR} = 1$. For inseparable states Δ_{EPR} decreases with increasing entanglement. The amount of entanglement created in the scheme is shown in figure 5.5.

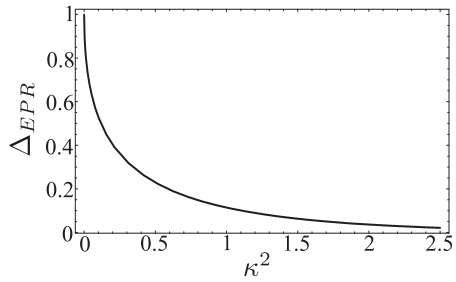

Figure 5.5: Entanglement produced in the two mode squeezing scheme versus coupling κ^2. The entanglement is hereby measured by the EPR variance Δ_{EPR}.

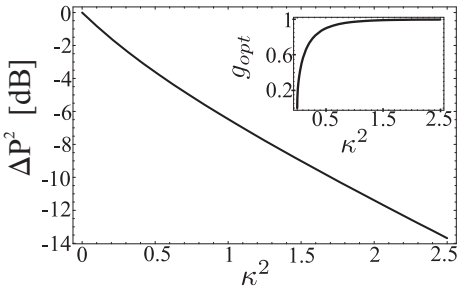

Figure 5.6: Atomic squeezing $(\Delta P)^2$ in db versus coupling κ^2 for optimal gainfactor g_{opt}. The inset shows how the optimal gainfactor depends on the coupling.

Spin squeezing

The correlations created in the proposed scheme can be used to produce atomic squeezing. This can be achieved by performing a measurement on the plus light mode and subsequent feedback onto the atomic spin based on the measurement outcome. The squeezing protocol is symmetric with respect to interchange of $\{X,\ \tilde{p}_L\}$ and $\{P,\ \tilde{x}_L\}$. Here squeezing of $(\Delta P)^2$ is illustrated. In order to acquire information about P, $\tilde{x}_+$ has to be measured. The outcome of this measurement is governed by the operator equation

$$\tilde{x}_+^{\text{out}} = \sqrt{e^{\kappa^2} - 1}\ P^{\text{in}} + e^{\frac{\kappa^2}{2}}\tilde{x}_-^{\text{in}}.$$

If the measurement outcome q_+ is obtained P^{out} is displaced by an amount $g\ q_+$, where $g \in \mathbb{R}$ is some gain factor. For this feedback procedure the operator identity

$$p_A^{\text{fb}} = P^{\text{out}} - g\ \tilde{x}_+^{\text{out}}$$

holds in the ensemble average, as is shown in section 3.4. With help of the atomic input-output relations (5.16) and the expression for the measurement outcome above

$$p_A^{\mathrm{fb}} = \left(e^{\frac{\kappa^2}{2}} - g\sqrt{e^{\kappa^2}-1} \right) P^{\mathrm{in}} + \left(\sqrt{e^{\kappa^2}-1} - g e^{\frac{\kappa^2}{2}} \right) \tilde{x}_-^{\mathrm{in}} \ .$$

Thus the variance of this quadrature is given by

$$(\Delta p_A^{\mathrm{fb}})^2 = \left(e^{\frac{\kappa^2}{2}} - g\sqrt{e^{\kappa^2}-1} \right)^2 \frac{1}{2} + \left(\sqrt{e^{\kappa^2}-1} - g e^{\frac{\kappa^2}{2}} \right)^2 \frac{1}{2}.$$

$(\Delta p_A^{\mathrm{fb}})^2$ is now optimized with respect to the gainfactor g. We obtain

$$\begin{aligned} g_{opt} &= \frac{e^{\frac{\kappa^2}{2}}\sqrt{e^{\kappa^2}-1} + e^{\kappa^2}\sqrt{1-e^{-\kappa^2}}}{2e^{\kappa^2}-1} \ , \\ (\Delta p_{A\ opt}^{\mathrm{fb}})^2 &= \frac{1}{2}\ \frac{1}{2e^{\kappa^2}-1} \ . \end{aligned}$$

Note that the atoms are left in a minimum uncertainty state, since

$$(\Delta X)^2 = \frac{1}{2}(2e^{\kappa^2}-1) = \frac{1}{4}\ \frac{1}{(\Delta p_A^{\mathrm{fb}})^2} \ .$$

The amount of squeezing depending on the coupling κ^2 is shown in figure 5.6.

5.4 Consideration of noise

We consider losses for both components of the protocol - atoms and light - and treat them perturbatively within the Gaussian formalism. Concerning the atomic sample we take transverse decoherence of the atomic spin state at a rate of $\frac{\eta}{T}$ into account. As in experiments atomic vapor is usually contained within a glass cell, the dominant source of noise concerning light are reflection losses. These affect quantum variables and classical field as well and will be characterized by the reflection coefficient r.

Quantum memory with noise

In this section we derive results for write-in and read-out in the presence of losses. We will first give a brief account of the resulting imperfections and then present a detailed description of the generalized quantum memory

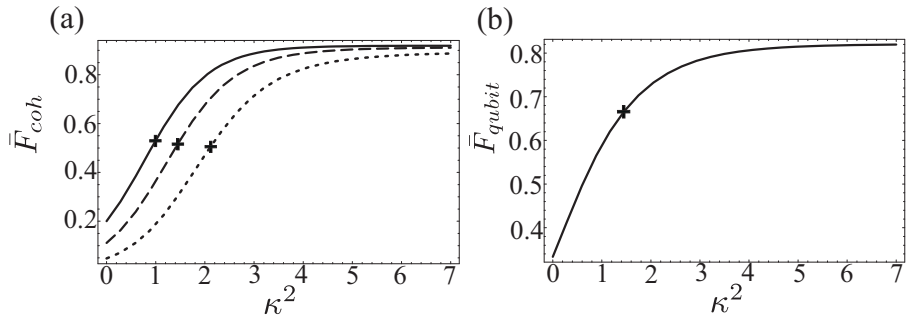

Figure 5.7: Average fidelity with losses versus coupling. The atomic decay rate η and the reflection coefficient r both have a value of 7.5%. Crosses mark the corresponding classical limits. (a) Fidelity for coherent input states according to distributions with different mean photon numbers. (solid line: $n = 4$, dashed line: $n = 8$, dotted line: $n = 20$) (b) Fidelity for light qubits.

scheme including noise. Consideration of losses leads to a modification of the original write-in mode. The generalized write-in quadratures preferred by the system are given by

$$\begin{pmatrix} x^{\text{in}} \\ p^{\text{in}} \end{pmatrix} \propto \int_0^T dt e^{\frac{wt}{2}} R(t) \Big[(1-r) \begin{pmatrix} \bar{p}(ct,0) \\ -\bar{x}(ct,0) \end{pmatrix} + 2r \begin{pmatrix} \bar{p}(ct,0) \\ \bar{x}(ct,0) \end{pmatrix} \Big],$$

where $w = \eta/T + \kappa^2(1-2r)/T$. Both sources of noise - reflection losses and spontaneous decay as well - give rise to a generalized exponent in the exponential modulation function. In addition to the changed envelope the light mode appearing in the atomic input-output relation is further disturbed: it lies no longer exactly at the upper sideband, but contains a small contribution from the lower one, as can be seen by comparing the expression above to (5.8) and (5.15). Since it is experimentally advantageous to encode the input signal at sideband modes, we define a generalized write-in mode (denoted by capital letters)

$$\begin{pmatrix} X^{\text{in}}_{\text{us+}} \\ P^{\text{in}}_{\text{us+}} \end{pmatrix} = \sqrt{\frac{w}{e^{wT}-1}} \int_0^T dt\, e^{\frac{wt}{2}} R(t) \begin{pmatrix} \bar{p}(ct,0) \\ -\bar{x}(ct,0) \end{pmatrix},$$

which takes full account of noise concerning the exponential modulation, but lies precisely at the upper sideband. (i.e. the small orthogonal contribution from the lower one is treated as noise.) To perform the read-out, the inverse accented counter part of this mode is measured. Figure 5.7 shows the average fidelity for write-in and subsequent retrieval versus coupling for

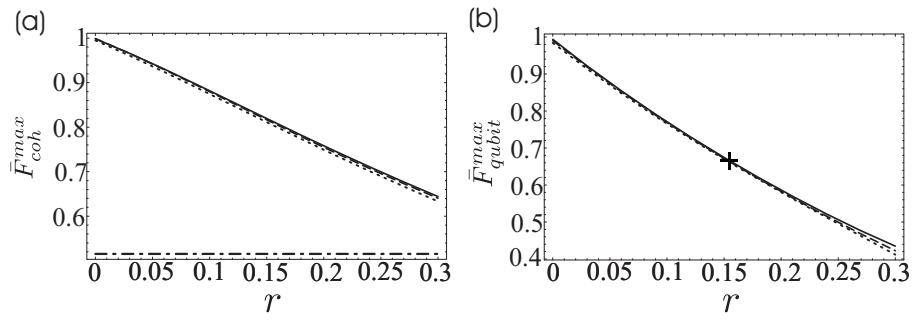

Figure 5.8: Maximal attainable average fidelity for coherent input states according to a distribution with mean photon number $n = 8$ (a) and light qubits (b) versus reflection coefficient r for different atomic decay parameters η. (solid lines: $\eta = 5\%$, dashed lines: $\eta = 10\%$, dotted lines: $\eta = 25\%$) The dash-dotted line and the cross indicate the classical limits.

$r = \eta = 7.5\%$. Plots (a) and (b) refer to coherent input states and light qubits respectively. The corresponding classical limits are marked by crosses. As illustrated by these graphs losses decrease not only the quality of the state transfer for a given coupling strength, but limit also the attainable fidelity. The crucial limiting factor in this scheme are reflection losses. Figure 5.8 shows the maximum average fidelity versus r for different values of the atomic decay parameter η. Plot (a) shows results for coherent inputs, while plot (b) depicts the maximal attainable fidelity for qubits. The dash-dotted line and the cross indicate the classical limits in each case. Within moderate couplings fidelities well above the classical limit can be achieved, showing that the protocol is robust against the dominant sources of noise. In the next sections we will give a detailed derivation of these results.

Write-in and read-out including noise

Atomic noise can be incorporated into the framework of section 5.2 by including decay terms in Bloch equations (5.1) and (5.2)

$$\begin{aligned}\frac{\partial}{\partial t}X(t) &= \Omega P(t) + \frac{\kappa}{\sqrt{T}}\bar{p}(ct,t) - \frac{\eta}{2T}X(t) + \sqrt{\frac{\eta}{T}}f_X(t),\\ \frac{\partial}{\partial t}P(t) &= -\Omega X(t) - \frac{\kappa}{\sqrt{T}}\bar{x}(ct-d,t) - \frac{\eta}{2T}P(t) + \sqrt{\frac{\eta}{T}}f_P(t),\end{aligned} \quad (5.18)$$

as explained in section 2.6.

Each time light crosses one of the cell walls, reflection losses occur. This happens four times. We neglect losses due to the very first crossing, since these can be compensated by using a more intense input signal. Losses due to the second and third transit of a cell wall affect only the second scattering interaction. We take this into account by modifying the undisturbed equations for the light field quadratures to be inserted into (5.18)

$$\begin{aligned} \bar{x}(ct-d,t) &= \bar{x}(ct-d,0)+\frac{\kappa}{\sqrt{T}}P(t-d/c), \\ \bar{p}(ct,t) &= \bar{p}(ct,0), \end{aligned}$$

by introducing light quadrature damping with a factor $2r$ (the factor 2 reflects the fact that crossing of a cell wall happens twice) and corresponding light-Langevin operators f_x and f_p, and obtain

$$\begin{aligned} \bar{x}(ct-d,t) &= \sqrt{1-2r}\Big(\bar{x}(ct-d,0)+\frac{\kappa}{\sqrt{T}}P(t-d/c)\Big)+\sqrt{2r}f_x(t), \\ \bar{p}(ct,t) &= \bar{p}(ct,0). \end{aligned}$$

$\bar{p}(ct,t)$ remains unchanged, since this quadrature affects the atoms only in the first passage (during the pP -interaction), which means that each part of the pulse contributes before it is subjected to reflection losses. Therefore p is conserved as in the undisturbed case. The classical light field is impaired by reflection losses as well. Since the coupling strength of the scattering interaction is proportional to the amplitude of the classical field we have a reduced coupling $\tilde{\kappa}=\sqrt{1-2r}\,\kappa$ for the second (xX -) interaction due to the light crossing two cell walls before it's second passage. By considering this and inserting the expressions above into equations (5.18) we obtain

$$\begin{aligned} \frac{\partial}{\partial t}X(t) &= \Omega P(t)+\frac{\kappa}{\sqrt{T}}\bar{p}(ct,0)-\frac{\eta}{2T}X(t)+\sqrt{\frac{\eta}{T}}f_X(t), \\ \frac{\partial}{\partial t}P(t) &= -\Omega X(t)-\frac{\tilde{\kappa}}{\sqrt{T}}\Big[\sqrt{1-2r}\Big(\bar{x}(\xi,0)+\frac{\kappa}{\sqrt{T}}P(t)\Big) \\ &\qquad +\sqrt{2r}f_x(t)\Big]-\frac{\eta}{2T}P(t)+\sqrt{\frac{\eta}{T}}f_P(t). \end{aligned}$$

We can ignore reflection losses arising in the very last transit through a cell wall, since the light field of the write-in beam is of no relevance after the second scattering interaction. By neglecting the time delay d/c as in section

5.2, the atomic differential equations generalize to

$$\begin{aligned}\frac{\partial}{\partial t}\begin{pmatrix}X(t)\\P(t)\end{pmatrix} = &\left\{\Omega\begin{pmatrix}0&1\\-1&0\end{pmatrix}-\frac{\eta}{2T}\begin{pmatrix}1&0\\0&1\end{pmatrix}-\frac{\kappa^2(1-2r)}{T}\begin{pmatrix}0&0\\0&1\end{pmatrix}\right\}\begin{pmatrix}X(t)\\P(t)\end{pmatrix}\\&+\frac{\kappa}{\sqrt{T}}\begin{pmatrix}\bar{p}(ct,0)\\-(1-2r)\bar{x}(ct,0)\end{pmatrix}\\&+\sqrt{\frac{\eta}{T}}\begin{pmatrix}f_X(t)\\f_P(t)\end{pmatrix}+\frac{\kappa\sqrt{2r}}{\sqrt{T}}\begin{pmatrix}0\\-\sqrt{1-2r}f_x(t)\end{pmatrix}.\end{aligned}$$

We introduce the abbreviation $w = \eta/T + \kappa^2(1-2r)/T$, which is the generalization of the exponent κ^2/T of the previous sections and change the previous assumption $2\Omega T \gg \kappa^2$ into $2\Omega T \gg wT = \eta + \kappa^2(1-2r)$. Therefore we get the homogeneous solution $A(t) = e^{\frac{wt}{2}}R^{-1}(t)$, (where $R(t)$ is the rotation matrix from section 5.2) and thus

$$\begin{aligned}\begin{pmatrix}X^{\text{out}}\\P^{\text{out}}\end{pmatrix} = &\; e^{\frac{-wT}{2}}\begin{pmatrix}X^{\text{in}}\\P^{\text{in}}\end{pmatrix}\\&+e^{\frac{-wT}{2}}\frac{\kappa}{\sqrt{T}}\int_0^T dt e^{\frac{wt}{2}}R(t)\begin{pmatrix}\bar{p}(ct,0)\\-(1-2r)\bar{x}(ct,0)\end{pmatrix}\\&+e^{\frac{-wT}{2}}\sqrt{\frac{\eta}{T}}\int_0^T dt e^{\frac{wt}{2}}R(t)\begin{pmatrix}f_X(t)\\f_P(t)\end{pmatrix}\\&+e^{\frac{-wT}{2}}\frac{\kappa\sqrt{2r}}{\sqrt{T}}\int_0^T dt e^{\frac{wt}{2}}R(t)\begin{pmatrix}0\\-\sqrt{1-2r}f_x(t)\end{pmatrix},\end{aligned} \tag{5.19}$$

where $R(T) = \mathbb{1}$ was used. The first two lines represent atomic- and light contributions, while the third and fourth term account for atomic noise and light noise respectively. The light mode, which is naturally mapped onto the atomic sample, is no longer a modulation of the upper sideband, as can be seen from the factor $(1-2r)$ attached to $\bar{x}(ct,0)$ in the second line. Since it is advantageous to encode the signal at sideband modes, the term involving the new disturbed light mode is decomposed into a generalization of the familiar plus mode connected to the upper sideband

$$\begin{pmatrix}X^{\text{in}}_{\text{us+}}\\P^{\text{in}}_{\text{us+}}\end{pmatrix} = \sqrt{\frac{w}{e^{wT}-1}}\int_0^T dt\; e^{\frac{wt}{2}}R(t)\begin{pmatrix}\bar{p}(ct,0)\\-\bar{x}(ct,0)\end{pmatrix} \tag{5.20}$$

and a small contribution from an orthogonal plus mode lying at the lower sideband

$$\begin{pmatrix}P^{\text{in}}_{\text{ls+}}\\X^{\text{in}}_{\text{ls+}}\end{pmatrix} = \sqrt{\frac{w}{e^{wT}-1}}\int_0^T dt\; e^{\frac{wt}{2}}R(t)\begin{pmatrix}\bar{p}(ct,0)\\\bar{x}(ct,0)\end{pmatrix}.$$

Generalized light modes are denoted by capital letters. With this decomposition the atomic input-output relations with noise read

$$\begin{aligned}\begin{pmatrix} X^{\text{out}} \\ P^{\text{out}} \end{pmatrix} &= e^{\frac{-wT}{2}} \begin{pmatrix} X^{\text{in}} \\ P^{\text{in}} \end{pmatrix} \\ &+\sqrt{1-e^{-wT}}\ \frac{\kappa(1-r)}{\sqrt{wT}} \begin{pmatrix} X^{\text{in}}_{\text{us}+} \\ P^{\text{in}}_{\text{us}+} \end{pmatrix} \\ &+\sqrt{1-e^{-wT}}\frac{\kappa r}{\sqrt{wT}} \begin{pmatrix} P^{\text{in}}_{\text{ls}+} \\ X^{\text{in}}_{\text{ls}+} \end{pmatrix} \\ &+e^{\frac{-wT}{2}}\ \sqrt{\frac{\eta}{T}} \int_0^T dt e^{\frac{wt}{2}} R(t) \begin{pmatrix} f_X(t) \\ f_P(t) \end{pmatrix} \\ &+e^{\frac{-wT}{2}} \frac{\kappa\sqrt{2r}}{\sqrt{T}} \int_0^T dt e^{\frac{wt}{2}} R(t) \begin{pmatrix} 0 \\ -\sqrt{1-2r} f_x(t) \end{pmatrix}. \end{aligned} \tag{5.21}$$

In order to perform the read-out, a second pulse of light is sent through the double pass scheme. Subsequently the light mode, which is the inverse accented counter-part of the mode appearing in the atomic time evolution (5.19) should be measured. Instead we choose the generalized minus mode analogous to the write-in quadratures (5.20). The corresponding output quadratures are given by

$$\begin{pmatrix} \acute{X}^{\text{out}}_{\text{us}-} \\ \acute{P}^{\text{out}}_{\text{us}-} \end{pmatrix} = \sqrt{\frac{w}{1-e^{-wT}}} \int_0^T dt\ e^{-\frac{wt}{2}} R(t) \begin{pmatrix} \acute{p}(ct,T) \\ -\acute{x}(ct,T) \end{pmatrix}.$$

This can be evaluated by inserting the generalized expressions for $\acute{p}(ct,T)$ and $\acute{x}(ct,T)$. For $\acute{p}(ct,T)$ we have

$$\acute{p}(ct,T) = \sqrt{1-2r}\ \acute{p}\ (ct,0) + \sqrt{2r}\acute{f}_p(t) - \frac{\tilde{\kappa}}{\sqrt{T}} X(t).$$

$\acute{p}$ is damped after the first (p-conserving) interaction and picks up some noise in return. Subsequently it gets some X -contribution during the second (xX-) interaction. The reduced coupling strength $\tilde{\kappa} = \sqrt{1-2r}\ \kappa$ accounts for the damped classical field in the second passage. $\acute{x}(ct,T)$ on the other hand is given by

$$\acute{x}(ct,T) = \sqrt{1-2r}\left(\acute{x}(ct,0) + \frac{\kappa}{\sqrt{T}} P(t)\right) + \sqrt{2r}\acute{f}_x(t).$$

$\acute{x}$ gets some P contribution during the first scattering interaction i.e. before the relevant transits through cell walls occur. Subsequently this is damped and appropriate noise is added. All together both quadratures are damped,

since both carry the argument (ct, T). This means each piece of the pulse contributes after it ran trough the sample twice and has therefore already experienced the two relevant transits trough cell walls. The rest of the calculation is straight forward. In the end reflection losses due to the fourth crossing of a cell wall have to be considered by damping the calculated result by a factor $\sqrt{1-r}$ and adding appropriate noise terms. The resulting input-output relations for the read-out mode are

$$\begin{aligned}\begin{pmatrix} \acute{X}^{\text{out}}_{\text{us}-} \\ \acute{P}^{\text{out}}_{\text{us}-} \end{pmatrix} &= c_1 \begin{pmatrix} X^{\text{in}} \\ P^{\text{in}} \end{pmatrix} + c_2 \begin{pmatrix} \acute{X}^{\text{in}}_{\text{us}+} \\ \acute{P}^{\text{in}}_{\text{us}+} \end{pmatrix} \\ &+c_3 \begin{pmatrix} \acute{P}^{\text{in}}_{\text{ls}+} \\ \acute{X}^{\text{in}}_{\text{ls}+} \end{pmatrix} + c_4 \begin{pmatrix} \acute{X}^{\text{in}}_{\text{us}-} \\ \acute{P}^{\text{in}}_{\text{us}-} \end{pmatrix} + c_5 \begin{pmatrix} \acute{P}^{\text{in}}_{ls-} \\ \acute{X}^{\text{in}}_{ls-} \end{pmatrix} \\ &+c_6 \begin{pmatrix} F_X \\ F_P \end{pmatrix} + c_7 \begin{pmatrix} \breve{F}_x \\ \breve{F}_p \end{pmatrix} + c_8 \begin{pmatrix} \acute{F}_x \\ \acute{F}_p \end{pmatrix} \\ &+c_9 \int_0^T dt R(t) [e^{-wT} e^{\frac{wt}{2}} - e^{-\frac{wt}{2}}] \begin{pmatrix} 0 \\ -\acute{f}_x(t) \end{pmatrix}. \end{aligned} \tag{5.22}$$

The coefficients c_1 to c_9 can easily be calculated. Since we want to focus on the structure of the equation, we don't insert these prefactors in order to avoid complicated expressions. The new read-out equations differ from (5.10) by the appearance of noise terms (third and fourth line) and extra light modes (second line). These contributions are small and can be treated as perturbations. $(F_X,\, F_P)$ is an atomic noise mode, while $(\breve{F}_x,\, \breve{F}_p)$, refers to the light mode which is due to the very last reflection. It is independent from the light mode $(\acute{F}_p,\, \acute{F}_x)$ which accounts for the reflections happening between the scattering interactions. These intermediate reflections give also rise to terms in which only noise associated to x contributes. They are summarized in the expression preceded by c_8. The appearance of light modes other than $(\acute{X}_{\text{us}+}\, \acute{P}_{\text{us}+})$ is due to a asymmetry between the pP -interaction and the xX present in a realistic setup in contrast to the ideal case. The light field has to cross two glass walls between the first and the second pass (thus affecting only the xX -interaction). Thus contributions from the lower sideband appear and contributions from the minus mode do not cancel as in the ideal case.

Fidelity for coherent input states

In order to compute the fidelity for coherent input states, means and variances of the final quadratures have to be calculated. $\langle \acute{X}^{\text{fin}}_{-} \rangle$, $\langle \acute{P}^{\text{fin}}_{-} \rangle$ and $(\Delta \acute{P}^{\text{fin}}_{-})^2$, $(\Delta \acute{X}^{\text{fin}}_{-})^2$ can be derived from the expression describing the complete state

transfer by using the assumption $2\Omega T \gg wT = \eta + \kappa^2(1-2r)$ (which is a direct generalization from the approximation $2\Omega T \gg \kappa^2$ made in the ideal case) and help of the noise operator properties $\langle f_x \rangle = \langle f_p \rangle = \langle f_x f_p + f_p f_x \rangle = 0$ and $\langle f(t) f(t') \rangle = \delta(t-t')\frac{1}{2}$. The obtained expressions have to be inserted into equation (5.12), which gives the state overlap between the input-state to be stored and the final state received. By considering a gaussian distribution of width n for coherent amplitudes the average fidelity can be directly calculated as in section 5.2.

Fidelity for light qubit input states including noise

The initial qubit state $|\Psi_{\text{in}}\rangle = (\alpha + \beta a_{\text{in}}^\dagger)|vac\rangle$ is subjected to the write-in and read-out procedure which is represented by the unitary transformation U_N. We obtain

$$\begin{aligned} |\Psi_{\text{fin}}\rangle &= U_N|\Psi_{\text{in}}\rangle = (\alpha + \beta U_N a_{\text{in}}^\dagger U_N^\dagger) U_N|vac\rangle \\ &= (\alpha + \beta a_{\text{fin}}^\dagger) U_N|vac\rangle. \end{aligned}$$

In contrast to the ideal case, where $U|vac\rangle = |vac\rangle$ could be used, U_N is a general Bogoliubov transformation. We remark that for $r = 0$ the state transfer can still described by a passive transformation. The active contribution is entirely due to reflection losses. This can be understood, by noting that reflection losses occurring between the first and the second scattering interaction impair only the scattering in the second pass. Therefore the active part of the second interaction cannot compensate the active part in the first pass as in the ideal case. This leads to a term in the generalized atomic input-output relations (5.21) which contains only one light quadrature and can therefore not be expressed as a mode-contribution. It plays an isolated role in the commutator relations, but adds some extra noise to the variances. Losses due to atomic decay on the other hand are included into the dynamics of the scheme in a symmetric way.
The fidelity for the complete state transfer is given by the overlap between the target state $|\Psi_{\text{fin}}^{opt}\rangle = (\alpha - \beta a_{\text{in}}^\dagger)|vac\rangle$ and the light state $|\Psi_{\text{fin}}\rangle$ which is effectively retrieved

$$F_{qubit} = |\langle \Psi_{\text{fin}}^{opt}|\Psi_{\text{fin}}\rangle|^2 = \langle vac|(\alpha^* - \beta^* a_{\text{in}})(\alpha + \beta a_{\text{fin}}^\dagger) U_N|vac\rangle|^2. \tag{5.23}$$

$a_{\text{fin}}^\dagger$ is known, since the input-output relations for the complete state transfer are known. They can be written in terms of creation and annihilation operators such that all occurring modes are independent. The transformation is

of general Bogoliubov type

$$U_N a_{\text{in}}^\dagger U_N^\dagger = \sum_{i=1}^{n} k_i a_i^\dagger + \sum_{j=1}^{m} k_j c_j, \tag{5.24}$$

where the coefficients k_i, k_j are complex numbers. $a_1^\dagger = a_{\text{in}}^\dagger$ refers to the state to be stored, while $a_2^\dagger$ to $a_n^\dagger$ represent all creation operators which appear in the equation, namely contributions from the atomic input, atomic noise, light-input from the read-out beam and light noise. Since we also have noise terms, which cannot be expressed as a noise mode (compare equation (5.21) last term) and contributions from the lower sideband (compare equation (5.22)) in which the x- and p quadratures are interchanged, we also have annihilation operators in this equation which are represented by c_1 to c_j. Since theses contributions are small, they are treated as perturbations to the system.
The transformation given in (5.24) can be understood as an orthogonal transformation $P = P_a \otimes P_c$, where P_a acts on the creation operators and P_c acts on the annihilation operators, followed by an active transformation S. With normalization constants $N_a = \sqrt{\sum_{i=1}^{n} |k_i|^2}$ and $N_c = \sqrt{\sum_{j=1}^{m} |k_j|^2}$, where $N_a^2 - N_c^2 = 1$ and $N_c \ll 1$, (5.24) can be written as

$$\begin{aligned} a_{\text{fin}}^\dagger &= N_a\Big(\sum_{i=1}^{n} \frac{k_i}{N_a} a_i^\dagger\Big) + N_c\Big(\sum_{j=1}^{m} \frac{k_j}{N_c} c_j\Big) && (5.25)\\ &= N_a P_a a_1^\dagger P_a^\dagger + N_c P_c c_1 P_c^\dagger = N_a a_P^\dagger + N_c c_P \\ &= \sqrt{1+N_c^2}\, a_P^\dagger + N_c c_P = S a_P^\dagger S^\dagger && (5.26) \end{aligned}$$

and we have $U_N = S(P_a \otimes P_c)$. In order to compute F_{qubit} from equation (5.23) the expression $U_N|vac\rangle$ has to be determined. $U_N|vac\rangle = S(P_a \otimes P_c)|vac\rangle = S|vac\rangle$, since P is a passive transformation. S on the other hand refers to a two mode squeezing operation. As mentioned above active contributions are treated perturbatively. The corresponding time evolution $S = e^{N_c(a_P c - a_P^\dagger c^\dagger)}$ is expanded in a series to first order and we obtain

$$U_N|vac\rangle \simeq \frac{1}{\sqrt{1+|N_c|^2}}(1 - N_c a_P^\dagger c_P^\dagger)|vac\rangle$$

By inserting this expression in equation (5.23) and inserting the right hand side of (5.24) for $a_{\text{fin}}^\dagger$ the fidelity can be directly calculated. We find

$$F_{qubit} = \frac{1}{1+|N_c|^2}\left(|\alpha|^2 - |\beta|^2 k_1\left(1 - \frac{|N_c|^2}{\sqrt{1+|N_c|^2}}\right)\right)^2.$$

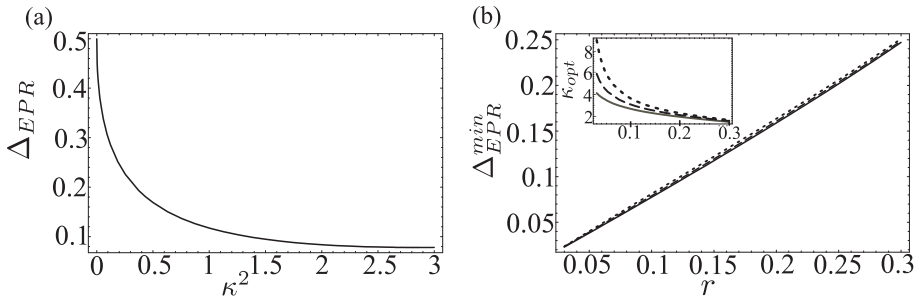

Figure 5.9: (a) EPR variance Δ_{EPR} versus coupling κ^2 in the presence of losses. The reflection coefficient r and the atomic decay rate are both chosen to have a value of 10%. (b) Optimized EPR variance versus coupling for different atomic decay parameters. (solid line: $\eta = 5\%$, dashed line: $\eta = 10\%$, dotted line: $\eta = 25\%$) The inset shows how the optimal coupling k_{opt} varies with r.

In order to obtain the average fidelity we set $\alpha = \cos(\frac{\theta}{2})$ and $\beta = \sin(\frac{\theta}{2})e^{i\phi}$ and integrate over the whole Bloch sphere $\bar{F}_{qubit} = \frac{1}{4\pi}\int_0^{\pi}\int_0^{2\pi} F_{qubit}(\theta,\phi)\sin(\theta)d\theta d\phi$. The results are shown in figures 5.7 and 5.8.

Two mode squeezing with noise

Consideration of noise within the two mode squeezing protocol is done along the same lines outlined in the section above. The entanglement created by the scheme in the presence of losses is depicted in figure 5.9(a) for $r = \eta = 0.1$. The EPR variance increases for higher values of κ^2. An optimal value κ^2_{opt} exists for which the proposed protocol works best and a maximal amount of entanglement is generated. Figure 5.9(b) shows the κ-optimized EPR variance versus r,while the dependence of κ_{opt} on the reflection coefficient is given within the inset. As can be seen from these plots atomic decay plays a minor role.
Spin squeezing can be performed with a lower and limited quality in the presence of losses. In contrast to the ideal case the optimal gainfactor does not approach unity with increasing coupling but converges towards an higher value witch depends on the amount of losses impairing the system. Figure 5.10(a) shows the squeezed atomic variance in *db* and the dependence of g_{opt} on the coupling for $r = \eta = 0.1$. The maximal attainable squeezing versus r is given in figure 5.10(b) for different atomic decay parameters.

In conclusion we presented two protocols based on a double-pass scheme for a single atomic ensemble in a magnetic field. The first protocol provides

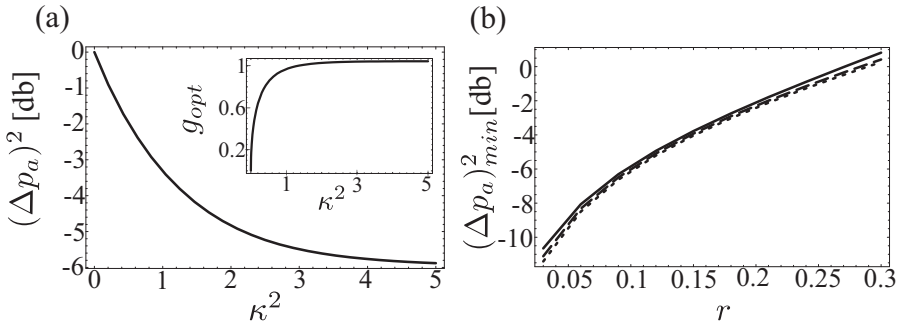

Figure 5.10: (a) Spin squeezing in *db* versus coupling κ^2 in the presence of losses. The reflection coefficient r and the atomic decay rate both have a value of 10%. The inset shows how the optimal gainfactor g_{opt} depends on the coupling. (b) Maximal spin squeezing versus reflection coefficient r for different atomic decay parameters. (solid line: $\eta = 5\%$, dashed line: $\eta = 10\%$, dotted line: $\eta = 25\%$).

an exponential scaling interspecies beam-splitter interaction. Therefore it is suitable for high fidelity storage and retrieval of an unknown quantum state under modest experimental conditions, as was shown for coherent input states and light qubits as well. The second protocol generates deterministically EPR entanglement between atoms and light. The proposed protocols provide therefore the ingredients to realize a variety of interesting quantum communication protocols. They are also shown to remain experimentally feasible under realistic conditions.

Chapter 6

Simulation of interactions and creation entanglement

After the first experiments [40] on quantum teleportation using two–mode squeezed states of light [50, 51], as well as those [95, 10, 52] dealing with entanglement in atomic ensembles [96, 13], a significant amount of work has been devoted to develop a quantum information theory of continuous variable systems [47]. So far, most of the theoretical work has focused on the entanglement properties of the quantum states involved in all these experiments, the so–called *Gaussian states*. Some examples of the achievements in this field are the following. The problem of qualifying entanglement has been solved in the general bipartite setting [97, 98, 99, 55] and in the three mode case [100]. The distillation problem has also been answered in the general case [32], as well as in the case in which the class of allowed operations is restricted to those that conserve the Gaussian form [58, 101, 102]. In contrast to all this theoretical work on (the static) entanglement properties of Gaussian states, very few general results have been obtained on the dynamics of entanglement on these systems, i.e., on how to use the interactions provided by the physical setups in order to entangle the systems in the most efficient way, see however [103, 104, 105, 106]. In this chapter we provide a rather complete theory of the dynamics of entanglement in these experimental settings.

The dynamics of entanglement has been recently analyzed in systems of two or more qubits [107, 108, 109, 110, 111, 112]. In that case one distinguishes between two scenarios. In the first one [107, 109], the interaction between the qubits is described by a Hamiltonian H. The goal is to determine the sequence of local gates for which the increase of entanglement after some small (infinitesimal) time is maximal for a given initial state. In the second one [108, 110, 112], the interaction is given in terms of a non–local gate, which can be applied only once. Apart from its fundamental inter-

est, these studies give some practical ways of creating entanglement in the most efficient way and may become relevant in several experimental situations. Another interesting and related problem is the one of Hamiltonian and gate simulation [113, 114, 115, 116, 117, 118]. Here, one assumes that the two qubits interact via some given Hamiltonian H and the goal is to determine a sequence of local instantaneous gates in order to obtain in minimal time either a complete time-evolution generated by some other Hamiltonian [Hamiltonian simulation] or some desired unitary gate (gate engineering).

In this chapter we analyze all these problems for two–mode pure Gaussian states and interaction Hamiltonians which preserve the Gaussian character. We also study the generation of squeezing, since although it has no counterpart in the qubit case, it is a valuable resource in present experiments [119]. Given the fact that we touch on several different topics and therefore develop different mathematical tools, we have decided to write a section which explains in detail the different problems we consider and the corresponding results. In the following sections we give detailed derivations of these results.

We stress the fact that the problems studied here are all motivated by the experimental situation in which light gets entangled with an atomic ensemble via the Kerr–like interaction [28, 120, 121, 13] treated in chapter 2. In chapter 7 we address the question of implementations of the proposed protocols under realistic conditions.

The chapter is organized as follows: The Sec. 6.1 should be considered as a survey of the results presented in the chapter. In Sec. 6.2 we show which Hamiltonians can be simulated using a given interaction and how to do so optimally. We also show that, in fact, any general Gaussian operation can be generated in the considered set–up. In Sec. 6.3 we determine the optimal rate of entanglement generation as well as of squeezing generation for arbitrary input states. Finally, in Sec. 6.3 we give an optimal entanglement generation scheme for finite times, starting out from a product (unsqueezed) state.

6.1 Overview

This section gives an overview of the content of this chapter and it is composed of three subsections. In the first one, we explain the physical set-up that we are going to analyze. In the second one we collect the main definitions used thereafter. In the third section we give the main results of the chapter without proving them. For the detailed derivations we refer the reader to the following sections.

Setup

We consider a continuous variable system composed of two one–mode systems coupled via some interaction Hamiltonian. The goal is to analyze which kind of evolutions we can achieve with such an interaction if certain instantaneous local operations can be applied at will. In particular, we study optimal methods of creating or increasing the entanglement shared by the two modes.

The interaction Hamiltonian has the general form

$$H = aX_1X_2 + bP_1P_2 + cP_1X_2 + dX_1P_2 \tag{6.1}$$

where a, b, c and d are real parameters, and $X_{1,2}$ and $P_{1,2}$ are canonical operators for the first and second mode, respectively. We use dimensionless units throughout the chapter. We assume that local operations, generated by the Hamiltonians

$$H_{\mathrm{loc},i} = g(X_i^2 + P_i^2), \tag{6.2}$$

can be applied instantaneously, where g is a real number that can be tuned at will. These operations can neither change the entanglement nor the squeezing present in the state. Lastly, we assume that the initial state is pure and Gaussian.

Our choice of the Hamiltonian interaction as well as the instantaneous local operations is motivated by current experiments with atomic ensembles [61, 10, 52, 95]. As explained in chapter 2, the Hamiltonian describing the interaction between the atomic ensemble and the light can be written as

$$H_0 = aX_1X_2, \tag{6.3}$$

which is a particular case of Eq. (6.1); in the following we will put the coupling constant $a = 1$ when referring to H_0. In the same scenario, simple and fast local operations can be performed on the atoms and the electromagnetic field. For example, a magnetic field or a polarizer gives rise to the local Hamiltonians Eq. (6.2). Since the interaction between atoms and light is typically weak, with moderate magnetic fields the operations generated locally can be regarded as instantaneous. On the other hand, if the atoms and the light are completely polarized, the corresponding state in terms of our continuous variable description is the tensor product of two vacuum states, in particular it is a pure Gaussian state. We emphasize that even though we have motivated our choices with some particular physical set-up, our description is applicable to other physical situations and our results apply to the general interaction Hamiltonian Eq. (6.1).

Now we consider the following general *strategy* for state or gate engineering which can be realized using the tools described above. Starting with a

pure initial state, described by the density operator $\rho(0)$, we perform fast local operations $V_0 \otimes W_0$ on the state and we then let H act on it for a time t_1. Then we perform again local rotations, $V_1 \otimes W_1$ followed by the non–local interaction generated by H for a time t_2 and so on until $\sum_k t_k = t$. This yields to the total time-evolution operator

$$\mathcal{U}(t) = [V_n \otimes W_n]U(t_n)\cdots U(t_2)[V_1 \otimes W_1]U(t_1)[V_0 \otimes W_0], \tag{6.4}$$

so that $\rho(t) = \mathcal{U}(t)\rho(0)\mathcal{U}(t)^\dagger$. Here $U(t) = e^{-iHt}$.

First, we want to analyze which $\mathcal{U}$ are achievable with this strategy. Second, for a given $\rho(0)$ we look for the best choice of n, $\{t_1, \ldots, t_n\}$, and the local operations $\{V_1 \otimes W_1, \ldots, V_n \otimes W_n\}$ in order to maximize the created entanglement/squeezing. We consider two different regimes. First, we choose $\sum_k t_k = \delta t \ll \tau(H)$ (the characteristic time of the interaction) so that we can expand all the U as well as $\mathcal{U}(t)$ in lowest order in t_k. Second, we choose t_k finite. In the following we refer to those two regimes as infinitesimal and finite respectively.

Some definitions

Since all the Hamiltonians we are considering are at most quadratic in X and P, an initial Gaussian state will be Gaussian at all times. This means that we can fully describe it by the first and second moments of R_k, with $\vec{R} = (X_1, P_1, X_2, P_2)^T$, i.e. the expectation values $d_k = \mathrm{tr}(\rho R_k)$, (also called displacements) and $\mathrm{tr}[\rho(R_k - d_k)(R_l - d_l)]$. The latter are collected in the *correlation matrix* (CM) of the state ρ, the real, symmetric, positive matrix γ defined by

$$\gamma_{kl} = 2\Re\{\mathrm{tr}[\rho(R_k - d_k)(R_l - d_l)]\}. \tag{6.5}$$

In our description, the displacements are of no importance: they have no influence on the entanglement and squeezing properties of the states and can be brought to zero by local displacement operations, which can be easily implemented in our physical set-up. Therefore we take $d_k = 0$ in this chapter.

We often write the correlation matrix in the block form

$$\gamma = \begin{pmatrix} A & C \\ C^T & B \end{pmatrix}. \tag{6.6}$$

with 2×2 matrices A, B, C, where A refers to the first system and B to second system. The matrix C describes the correlations between both systems and vanishes for product states.

All the states and operations we consider here are pure. Therefore, and since we look at two-mode states only, we can always write their CM in the

form [122]

$$\gamma = (S_1 \oplus S_2) \begin{pmatrix} \cosh(r)\mathbb{1} & \sinh(r)\sigma_z \\ \sinh(r)\sigma_z & \cosh(r)\mathbb{1} \end{pmatrix} (S_1^T \oplus S_2^T), \tag{6.7}$$

which we refer to as the *pure state standard form* of γ. Here, $S_{1,2}$ are local symplectic matrices, $r \geq 0$, and σ_z is the Pauli matrix $\mathrm{diag}(1,-1)$. The parameter r contains all information about the entanglement of the state, whereas S_1 and S_2 contain information about local squeezing. Given a CM γ, one can find its pure state standard form as follows: We have $S_k = O_k D_k O_k'$, where O, O' are rotations and $D_k = \mathrm{diag}(e^{r_k}, e^{-r_k})$. The six matrices are determined as follows: $O_{1(2)}$ diagonalize $A(B)$. The rotations O_k' realize the singular value decomposition of $D_1^{-1} O_1^T C O_2 D_2^{-1}$. The two-mode squeezing parameter r is given by $\cosh r = \sqrt{\det(A)}$, while the squeezing parameters r_1, r_2 of S_k can be calculated by the trace of A and B, resp.: $\cosh 2r_1 = (\mathrm{tr}A)/(2\cosh r), \cosh 2r_2 = (\mathrm{tr}B)/(2\cosh r)$.

Concerning the bilinear interaction Hamiltonians, it is convenient to rewrite the Hamiltonian of Eq. (6.1) as follows

$$H = (X_1, P_1) K \begin{pmatrix} X_2 \\ P_2 \end{pmatrix} \quad \text{where} \quad K = \begin{pmatrix} a & d \\ c & b \end{pmatrix}. \tag{6.8}$$

We denote by $s_1 = \sigma_1$, $s_2 = \mathrm{sign}[\det(K)]\sigma_2$. where the sign function is defined as $\mathrm{sign}(x) = \pm 1$ if $x \gtrless 0$ and $\mathrm{sign}(x) = 0$ if $x = 0$. with $\sigma_1 \geq \sigma_2 \geq 0$ the singular values of K. We refer to the s_k as the *restricted singular values* of K. Note that, local rotations can always bring any H to the diagonal form $s_1 X_1 X_2 + s_2 P_1 P_2$.

Results

We state here the main results of this chapter. To give a clear picture of them we do not use more mathematically tools and definitions than necessary.

First we characterize the interactions which we are able to generate within the setting described by Eq. (6.4). In the infinitesimal regime the problem is usually called Hamiltonian simulation, whereas for t finite it is usually called gate simulation. Then we use these results to find the optimal strategy to generate entanglement/squeezing both in the infinitesimal and finite regime.

Hamiltonian Simulation

Given two Hamiltonians H and H' of the form (6.1) we want to see the conditions under which H can simulate H'. That is, for a given sufficiently

small t' we want to find out if it is possible to have

$$e^{-iH't'} = [V_n \otimes W_n]e^{-iHt_n} \cdots e^{-iHt_2}[V_1 \otimes W_1]e^{-iHt_1}[V_0 \otimes W_0]. \tag{6.9}$$

with t_k small as well. If it is possible to choose $t \equiv \sum_k t_k = t'$ we say that H can simulate H' *efficiently*.

Defining the matrices K and K' as in Eq. (6.8), as well as their respective restricted singular values $s_{1,2}$ and $s'_{1,2}$, we find the following results: (i) The Hamiltonian H can efficiently simulate H' if and only if

$$s_1 + s_2 \geq s'_1 + s'_2 \quad \text{and} \quad s_1 - s_2 \geq s'_1 - s'_2, \tag{6.10}$$

(ii) If it is not possible to simulate H' efficiently with H, then the minimal time needed to simulate the evolution corresponding to H' for the time t' is $t_{\min} := \min_t\{t : (s_1 + s_2)t \geq (s'_1 + s'_2)t', (s_1 - s_2)t \geq (s'_1 - s'_2)t'\}$.
Thus except for the cases $s_1 = \pm s_2$ every Hamiltonian of the form (6.1) can simulate all other Hamiltonians of that form (including the $s'_1 = \pm s'_2$ case). In particular, with the Hamiltonian H_0 describing the atom-light interaction one can simulate every bilinear Hamiltonian (6.1) and can do so efficiently as long as $|s'_1| + |s'_2| \leq 1$. In this case, the interaction existing in the physical setup can be considered universal.

Gate simulation and state generation

We show that starting from the Hamiltonians H and $H_{\text{loc},i}$ of Eqs. (6.1,6.2) it is possible to generate any desired unitary evolution of the form $\mathcal{U} = e^{-i\tilde{H}}$, where $\tilde{H}$ is an arbitrary self–adjoint operator quadratic in $\{X_1, P_1, X_2, P_2\}$, if and only if $|s_1| \neq |s_2|$. In particular, the Hamiltonian H_0, together with the local operations given in Eq. (6.2) and local displacements, allows one to generate all unitary linear operations, and therefore to generate arbitrary Gaussian states out of any pure Gaussian state. This shows that $H, H_{\text{loc},i}$ generate a set of universal linear gates for continuous variables smaller than the one given in Ref. [123].

Let us analyze some important applications of these results in the case of atomic ensembles interacting with light. They imply that with current experiments with atomic ensembles one can generate all unitary linear operations, as well as arbitrary Gaussian states. In particular, one can generate local squeezing operators for which $\tilde{H} = X_1^2 - P_1^2$ [which are not included among the Hamiltonians of the form (6.1) and therefore cannot be simulated infinitesimally by any of them] and therefore one can generate squeezing in the atomic system, light system or both independently (without performing

measurements). On the other hand, one can use H_0 to generate the swap operator, which (in the Heisenberg picture) transforms

$$X_1 \leftrightarrow X_2, \quad P_1 \leftrightarrow P_2. \tag{6.11}$$

This operation can be generated in a finite time. Thus, one can use the interaction H_0 to realize a perfect interface between light and atoms, which allows one to use the atomic ensemble as a quantum memory for light, as opposed to the case in Ref. [61] where this result is obtained in the limit of very strong interaction.

Optimal entanglement generation: infinitesimal case

The problem that we consider now can be stated as follows. Let us assume that we have some initial pure Gaussian state and we have some interaction described by the general Hamiltonian (6.1) at our disposal for a short time δt. The initial state at time t_0 is described by some correlation matrix of the form $\gamma(t_0)$ and possesses an entanglement $E(t_0)$, where E is some measure of entanglement. We would like to increase the entanglement as much as possible. In order to simplify our notation we choose, without loss of generality, $t_0 = 0$. We omit the argument for all quantities referring to the initial state, e.g $\gamma = \gamma(0)$.

Since for the case of two modes in a pure state there is a single parameter that describes the entanglement [cf. Eq. (6.38)], all entanglement measures are monotonically dependent on each other. One particular measure is the parameter r appearing in Eq. (6.7), $E_0(\gamma) = r$. In fact, E_0 is the log-negativity [124] of the Gaussian state. Thus, every entanglement measure E can be expressed in terms of r. We use the obvious notation $E(t) \equiv E[\gamma(t)]$ when considering the time-evolution of E. Mathematically, our goal is to maximize the *entanglement rate* [107]

$$\left.\frac{dE}{dt}\right|_{t_0} = \lim_{\delta t \to 0} \frac{E(t_0 + \delta t) - E(t_0)}{\delta t} \tag{6.12}$$

by using the fast local operations. We find the following result:

$$\left.\frac{dE}{dt}\right|_{t_0,\mathrm{opt}} = \left.\frac{dE}{dr}\right|_{r(t_0)} \Gamma_{E,\mathrm{opt}}(\gamma, H). \tag{6.13}$$

The function Γ_E, which genuinely contains the optimal entanglement increase, is given by

$$\Gamma_{E,\mathrm{opt}}(\gamma, H) = s_1 e^{l} - s_2 e^{-l}, \tag{6.14}$$

where s_1, s_2 characterize the given interaction Hamiltonian, while l is a parameter that only depends on the local squeezing of our state and can be determined through the following relation [using the notation of Eqs. (6.6,6.7)]

$$\begin{aligned} \cosh(2l) &= \frac{\det(A)}{-2\det(C)}\mathrm{tr}(A^{-2}CC^T) \\ &= \frac{1}{2}\mathrm{tr}[(S_1^T S_1)^{-1}\sigma_z S_2^T S_2 \sigma_z]. \end{aligned} \tag{6.15}$$

Note that there is no divergence as $\det C \to 0$ as is seen by the second expression in Eq. (6.15) and the fact the S_k's in Eq. (6.7) are uniquely defined only if γ is not a product state (i.e., iff $C \neq 0$). Given a product state with CM $\tilde{S}_1\tilde{S}_1^T \oplus \tilde{S}_2\tilde{S}_2^T$, the S_k are defined only up to local rotations $S_k = \tilde{S}_k O_k$. These O_k can be chosen such that $O_1(S_1^T S_1)O_1^T = \mathrm{diag}(\sigma_{1-}, \sigma_{1+})$ and $O_2(S_2^T S_2)O_2^T = \mathrm{diag}(\sigma_{2+}, \sigma_{2-})$, where $\sigma_{k+} = e^{r_k} \geq \sigma_{k-} = e^{-r_k}, r_k > 0$ are the singular values of $S_k^T S_k$. This local operation achieves the maximum $\cosh(r_1 + r_2)$ for the RHS in Eq. (6.15) as given by von Neumann's trace theorem [125].

Thus we see that the entanglement rate depends on the local symplectic matrices S_1, S_2, i.e. on both the amount of (local) squeezing in the two modes and the angle between the squeezed quadratures (which, e.g., is zero, if both X_1 and X_2 are squeezed). However, it does not depend on the entanglement of the state. Rewriting $\Gamma_{E,\mathrm{opt}}$ as $(s_1 - s_2)\cosh l + (s_1 + s_2)\sinh l$ we see that some Hamiltonians can produce entanglement even if there is no local squeezing present in the state (which implies that $l = 0$), while others (notably the beam splitter with $s_1 = s_2 = 1$) cannot.

Note that the rate goes to infinity as local squeezing is increased, in contrast to the case of qubits. Given a CM γ, there are typically local rotations that enhance the entanglement rate.

From these results we conclude that if the goal is to create as much entanglement as possible it is more efficient to squeeze the state locally first (if possible) before using the interaction; in particular, the use of squeezed light [96] is advantageous compared to coherent light [126].

Optimal squeezing generation: infinitesimal case

Now we consider the problem of optimal squeezing generation in the same set-up as in the previous subsection. We take as a measure of squeezing of a correlation matrix γ, $\mathcal{S} = \mathcal{S}(Q)$, any monotonically increasing function of Q, where Q is minus the logarithm of the smallest eigenvalue of γ. We find

$$\left.\frac{d\mathcal{S}}{dt}\right|_{t_0,\mathrm{opt}} = \left.\frac{d\mathcal{S}}{dQ}\right|_{Q(t_0)} g_S[\gamma] C_S(H). \tag{6.16}$$

$C_S(H)$ is the *squeezing capability* of the Hamiltonian and it is given by $s_1 - s_2$, where the s_i's are the restricted singular values of K, given in (6.8) and

$$g_S(\gamma) = 2\|\vec{x}_1\|\|\vec{x}_2\| \leq 1, \tag{6.17}$$

quantifies how "squeezable" the state γ is by interactions of the type (6.1). Here $\hat{x}^T = (\vec{x}_1, \vec{x}_2)$, with $\vec{x}_1, \vec{x}_2 \in \mathbb{R}^2$ is the normalized eigenvector corresponding to the minimal eigenvalue of γ.

Optimal squeezing and entanglement: finite case

Finally we consider the situation in which we start with both modes in the vacuum state and we have a Hamiltonian H for a finite time (as well as instantaneous local operations). We show that the optimal way to create entanglement is to apply local instantaneous operations flipping the X and P variables of both systems periodically after small times Δt. After a finite time t (and for $\Delta t \to 0$) this produces (up to local rotations) a two-mode squeezed state, which is both optimally squeezed and entangled. In particular, $Q(t) = (s_1 - s_2)t$ and $E_0(t) = (s_1 - s_2)t$.

We also show that it is not possible to increase the entanglement using Gaussian measurements during the evolution. We consider a system with CM γ and ancilla systems in vacuum state. We allow for linear passive interactions (described by a symplectic and orthogonal matrix O) between one system and the ancillas and show that a Gaussian measurement does neither increase the squeezing nor the entanglement. This result implies that our method is optimal even if we allow for feedback, something which has been recently considered in the context of spin squeezing generation [103, 106].

For the case of atomic ensembles our result implies that there is a method to improve the entanglement generation in present experiments [95].

6.2 Simulation of interactions

In this section we characterize all the unitary evolutions which we can generate within the given setup. That is we define the set of unitary operators which can be written as (6.4). The first part of this section is devoted to the infinitesimal regime, where we will in general derive the necessary and sufficient conditions for Hamiltonian simulation. In the second part we are concerned with the finite time regime. There we show that with (almost) any Hamiltonian H as in Eq. (6.1) and the local operations corresponding to the Hamiltonians given in (6.2) it is possible to generate any unitary gate.

Method of Hamiltonian simulation

A central result in the theory of Hamiltonian simulation [116] states that an alternating sequence of manipulations and interactions as given in (6.9) is equivalent to a fictitious free evolution due to a certain effective Hamiltonian H_{eff}, i.e. produces a unitary transformation

$$\mathcal{U} = e^{-iH_{\text{eff}}t'}$$

and

$$\kappa H_{\text{eff}} = \sum_{k=1}^{n} p_k \left(\widetilde{V}_k^\dagger \otimes \widetilde{W}_k^\dagger\right) H \left(\widetilde{V}_k \otimes \widetilde{W}_k\right) \tag{6.18}$$

where $\kappa := t'/t$, $t := \sum_{i=1}^{n} t_i$, the $p_k := t_k/t$ form a probability distribution and the $\widetilde{V}_i \otimes \widetilde{W}_i$ follow uniquely from the interspersed control operations $V_j \otimes W_j$ (and vice versa). Obviously one can in this way *simulate* an evolution due to a Hamiltonian H_{eff} by means of a given Hamiltonian H.

Eq. (6.18) has a clear interpretation: A protocol proceeding in infinitesimal time steps yields a mean Hamiltonian which is a weighted sum of locally transformed variants of the original Hamiltonian H. The so-called *simulation factor* κ is the ratio of simulated time t' and time of simulation t and, therefore, is a measure for the efficiency of the simulation. The case $\kappa \geq 1$ corresponds to the *efficient simulation*.

Necessary and sufficient condition

We associate to the general non–local interaction Hamiltonian (6.1) the real 2×2 matrix K as in (6.8). The action of a local rotation $V(\varphi) = \exp[-i(X^2 + P^2)\varphi/2]$ on the canonical operators X and P can be expressed by

$$V \begin{pmatrix} X \\ P \end{pmatrix} V^\dagger = \bar{R} \begin{pmatrix} X \\ P \end{pmatrix} \quad \text{where}$$
$$\bar{R} = R(\varphi) = \begin{pmatrix} \cos\varphi & -\sin\varphi \\ \sin\varphi & \cos\varphi \end{pmatrix} \in SO(2,\mathbb{R}). \tag{6.19}$$

Thus we can associate to all local rotations V_i, W_i (6.2) real orthogonal 2×2 matrices $\bar{R}, \bar{S} \ldots$ with determinant $+1$. Consequently we have

$$(V \otimes W)\, H \left(V^\dagger \otimes W^\dagger\right) = (X_1, P_1)\bar{R}^T K \bar{S} \begin{pmatrix} X_2 \\ P_2 \end{pmatrix}. \tag{6.20}$$

Furthermore we use that for any matrix K as given in (6.8) there exists a singular value decomposition $K = OD\tilde{O}$ where $O, \tilde{O} \in O(2,\mathbb{R})$, $D =$

$\mathrm{diag}(\sigma_1, \sigma_2)$ and the singular values $\sigma_1 \geq \sigma_2 \geq 0$ of K are unique. If we restrict ourselves on *special* orthogonal matrices we can still find matrices $R, S \in SO(2, \mathbb{R})$ such that

$$K = R \begin{pmatrix} s_1 & 0 \\ 0 & s_2 \end{pmatrix} S \tag{6.21}$$

and $s_1 = \sigma_1$, $s_2 = \mathrm{sign}[\det(K)]\sigma_2$. Without loss of generality we may always assume that

$$s_1 \geq |s_2| \,. \tag{6.22}$$

Then these two values are uniquely defined and shall be called *restricted singular values* of K.

Assume now we want to simulate, in the above sense, some Hamiltonian H' by means of some other Hamiltonian H, both of the form (6.8). Let s_1, s_2 and s_1', s_2' denote their respective restricted singular values. Then we have the following result:

H can efficiently simulate H' iff

$$\begin{array}{rcl} s_1 + s_2 & \geq & s_1' + s_2' \\ s_1 - s_2 & \geq & s_1' - s_2'. \end{array} \tag{6.23}$$

First we prove necessity. If H can simulate H' efficiently (6.18) has to hold for $\kappa = 1$ and $H_{\mathrm{eff}} = H'$. Therefore and because of (6.8) and (6.20) there must exist a probability distribution $\{p_i\}_{i=1}^n$ and special orthogonal matrices $\{R_i, S_i\}_{i=1}^n$ such that

$$\begin{pmatrix} s_1' & 0 \\ 0 & s_2' \end{pmatrix} = \sum_{i=1}^{n} p_i R_i \begin{pmatrix} s_1 & 0 \\ 0 & s_2 \end{pmatrix} S_i. \tag{6.24}$$

Rotation matrices which should in principle appear on the left hand side can be removed by left and right multiplication with corresponding transposed matrices. In (6.24) we assume these ones to be already included in the R_i, S_i on the right hand side.

By using the fact that the vector of the diagonal elements of a product $R\ \mathrm{diag}(s_1, s_2)\ S$ can be written as $(R \circ S^T)(s_1, s_2)^T$ where $R \circ S^T$ denotes the component-wise (so-called Hadamard) product of matrices we can express the last equation in compact form as

$$\begin{pmatrix} s_1' \\ s_2' \end{pmatrix} = \sum_{i=1}^{n} p_i \left(R_i \circ S_i^T\right) \begin{pmatrix} s_1 \\ s_2 \end{pmatrix} =: N \begin{pmatrix} s_1 \\ s_2 \end{pmatrix}. \tag{6.25}$$

The definition of the matrix N in (6.25) is obvious. Using that all matrices R_i, S_i are elements of $SO(2,\mathbb{R})$ it can be seen easily that

$$N_{11} = N_{22}, \quad N_{12} = N_{21} \quad \text{and}$$
$$|N_{11} \pm N_{21}| \leq 1.$$

Conditions (6.23) follow now directly from (6.25) and these properties of N:

$$s_1' + s_2' = (N_{11} + N_{21})(s_1 + s_2) \leq s_1 + s_2$$

The same holds identically for all plus signs replaced by minus signs proving necessity.

To demonstrate sufficiency we show that conditions (6.23) guarantee the existence of a matrix N as in (6.25) which in turn admits to connect the primed and unprimed restricted singular values as in (6.24). This provides an efficient simulation protocol of the form (6.9).

Given s_1, s_2 and s_1', s_2' fulfilling (6.23) we can for the time being assume that $s_1 \neq |s_2|$ and define

$$N := \begin{pmatrix} e & f \\ f & e \end{pmatrix}, \text{ where}$$
$$e = \frac{s_1 s_1' - s_2 s_2'}{s_1^2 - s_2^2}, \quad f = \frac{s_1 s_2' - s_2 s_1'}{s_1^2 - s_2^2}.$$

With this definition we have $(s_1', s_2')^T = N(s_1, s_2)^T$. Next we have to show that N can be written as a convex sum of Hadamard products of rotation matrices which is in fact exactly what inequalities (6.23) ensure.

It is again easy to check that if $|e| + |f| \leq 1$ we can find probabilities $\{p_i : p_i \geq 0, \sum_{i=1}^4 p_i\}_{i=1}^4$ such that $e = p_1 - p_2$ and $f = p_3 - p_4$ and therefore

$$\begin{aligned} N = p_1 \begin{pmatrix} 1 & 0 \\ 0 & 1 \end{pmatrix} \circ \begin{pmatrix} 1 & 0 \\ 0 & 1 \end{pmatrix} + p_2 \begin{pmatrix} 1 & 0 \\ 0 & 1 \end{pmatrix} \circ \begin{pmatrix} -1 & 0 \\ 0 & -1 \end{pmatrix} \\ + p_3 \begin{pmatrix} 0 & 1 \\ -1 & 0 \end{pmatrix} \circ \begin{pmatrix} 0 & 1 \\ -1 & 0 \end{pmatrix} + p_4 \begin{pmatrix} 0 & 1 \\ -1 & 0 \end{pmatrix} \circ \begin{pmatrix} 0 & -1 \\ 1 & 0 \end{pmatrix}. \end{aligned} \tag{6.26}$$

This decomposition of N allows one to pass from (6.25) to (6.24) conserving the diagonal structure as can be checked easily. Thus it suffices to show how (6.23) implies $|e| + |f| \leq 1$. Multiplying the first [second] line of (6.23) by $(s_1 - s_2)$ $[(s_1 + s_2)]$ yields respectively

$$s_1^2 - s_2^2 \geq (s_1 s_1' - s_2 s_2') + (s_1 s_2' - s_2 s_1'),$$
$$s_1^2 - s_2^2 \geq (s_1 s_1' - s_2 s_2') - (s_1 s_2' - s_2 s_1').$$

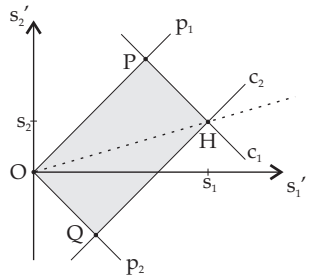

Figure 6.1: Illustration of the accessible region in the (s_1', s_2')-plane for the case $s_2 > 0$. Coordinates of relevant points: $H = (s_1, s_2)$, $P = \frac{s_1+s_2}{2}(1,1)$, $Q = \frac{s_1-s_2}{2}(1,-1)$. See text for explanation.

The first term on the right hand sides is nonnegative due to premise (6.22) such that these inequalities are equivalent to

$$s_1^2 - s_2^2 \geq |s_1 s_1' - s_2 s_2'| + |s_1 s_2' - s_2 s_1'|$$

which is, regarding the definition of e and f, exactly what we had to show and proves sufficiency for the case $s_1 \neq |s_2|$.

The complementary cases $s_1 = |s_2|$ turn out to be trivial, since conditions (6.23) then require $s_1' = s_2' = s_1$ or $s_1' = -s_2' = s_1$ respectively and this means that we can exclusively simulate Hamiltonians where $H' = (U \otimes V)\, H \left(U^\dagger \otimes V^\dagger\right)$ for some local rotations $U \otimes V$, i.e. H' has to be - in this sense - locally equivalent to H. Hence, nothing has to be shown in this case. □

We point out that this proof provides the possibility to construct simulation protocols explicitly. Given H and H' one has to calculate the decomposition in 6.26. Then the probabilities and rotations appearing there will fix the time steps t_i and control operations $U_i \otimes V_i$ in (6.9). As can be seen such a protocol will contain at most three intervals of interaction and control operations being rotations about $\pm\pi/2$ and π.

Discussion

Since the number of relevant parameters characterizing an interaction Hamiltonian is two, one can nicely illustrate the above result: The Fig. 6.1 illustrates the following geometrical relations: Point $H = (s_1, s_2)$ denotes the original general Hamiltonian. Lines p_1 and p_2 indicate the boundaries where $s_1' = \pm s_2'$ respectively and are due to premise $s_1' \geq |s_2'|$. Lines c_1 and c_2 stem respectively from the first and second inequality constituting the necessary and sufficient condition. The region of accessible Hamiltonians, i.e. points

$H' = (s_1', s_2')$ is thus contained in the rectangle $OPHQ$. One can even visualize how this set deepens with increasing time of simulation by parameterizing $H(t) = (s_1 t, s_2 t)$. Thus, H moves outward on the dashed line while P and Q move on p_1 and p_2 respectively. It is therefore just a matter of time to reach any point in the quadrant enclosed by p_1 and p_2.

It is also quite instructive to consider certain special cases: (i) For $s_2 = s_1$ ($s_2 = -s_1$) the dashed line coincides with p_1 (p_2), respectively. This is a trivial case where we are confined to simulate locally equivalent variants of the original Hamiltonian. Therefore, Hamiltonians whose restricted singular values are of equal modulus are nearly useless for the purpose of Hamiltonian simulation. (ii) For $s_2 = 0$ or, equivalently, $\det(K) = 0$ the picture gets symmetric with respect to the s_1'-axis. This symmetrization can be interpreted in terms of time efficiencies, as we shall explain in the following.

Based on the criterion above one can ask for time efficiencies and especially for *time optimal protocols*. Time optimal simulation is achieved if the simulation factor $\kappa = t'/t$ [see Eq. (6.18)] gets maximal. Without loss of generality we set $t' = 1$ such that $\kappa = 1/t$. Given now H and H' with restricted singular values s_1, s_2 and s_1', s_2' we can determine the minimal time of simulation as $t_{\min} := \min_t \{t : (s_1 + s_2)t \geq (s_1' + s_2'), (s_1 - s_2)t \geq (s_1' - s_2')\}$. We find

$$t_{\min} = \begin{cases} \frac{s_1' + s_2'}{s_1 + s_2} & \text{if} \quad \frac{s_2'}{s_1'} \geq \frac{s_2}{s_1} \\ \frac{s_1' - s_2'}{s_1 - s_2} & \text{if} \quad \frac{s_2'}{s_1'} < \frac{s_2}{s_1} \end{cases} . \tag{6.27}$$

Thus the efficiency of simulation depends strongly on whether $\mathrm{sign}(s_2') = \mathrm{sign}(s_2)$ or not, the last case being more time consuming. Only when $s_2 = 0$ [case (ii) above] it is equally expensive (in terms of costs of interaction time) to simulate either kind of Hamiltonians H' [$\mathrm{sign}(s_2') \lessgtr 0$], a fact which is reflected in the above mentioned symmetrization. Correspondingly, the optimal time of simulation or, so to say, the *minimal interaction costs* [117] are in this case uniquely determined by

$$t_{\min} = (s_1' + |s_2'|)/s_1. \tag{6.28}$$

Application to X_1X_2-interaction

Let us outline some conclusions out of this result for the interaction $H = X_1X_2$. The restricted singular values of H are obviously $s_1 = 1$ and $s_2 = 0$. Therefore we can efficiently ($\kappa = 1$, i.e. $t' = t$) implement all Hamiltonians H' whose restricted singular values fulfill

$$s_1' + |s_2'| \leq 1. \tag{6.29}$$

As an example as well as to give a basis for further results we shall consider here two kinds of well known unitary transformations: the *beam-splitter* operator

$$U_{\rm bs}(t) := e^{-iH_{\rm bs}t} \quad \text{where} \quad H_{\rm bs} = X_1P_2 - P_1X_2 \tag{6.30}$$

and the *two-mode squeezer*

$$U_{\rm tms}(t) := e^{-iH_{\rm tms}t} \quad \text{where} \quad H_{\rm tms} = X_1X_2 - P_1P_2. \tag{6.31}$$

As mentioned already, the action of $U_{\rm bs}(\pi/2)$ corresponds to swapping the states of the first and the second mode, i.e. it transforms $X_1, P_1 \to -X_2, -P_2$ and $X_2, P_2 \to X_1, P_1$. Note that the global phase thereby acquired by subsystem 1 can be corrected locally.

Application of $U_{\rm tms}(t)$ squeezes the EPR modes $(X_1 + X_2)$ and $(P_1 - P_2)$ by a factor e^{-2t} and therefore also entangles the two systems, as we shall see.

In order to perform these operations by means of the X_1X_2-interaction we have to determine the restricted singular values of $H_{\rm bs}$ and $H_{\rm tms}$. One finds for $H_{\rm bs}$ $s_1 = 1, s_2 = 1$ and for $H_{\rm tms}$ $s_1 = 1, s_2 = -1$. Since in both cases condition (6.29) is not met we cannot *efficiently* simulate these Hamiltonians. But nevertheless we can determine strategies for infinitesimal simulations being time optimal. The minimal time of simulation can be calculated using (6.28) and yields a maximal simulation factor $\kappa = 1/t_{\rm min} = 1/2$ for both, the beam-splitter and the squeezer. Thus, in order to implement $U_{\rm bs}(t')$ we need at least a time $t = 2t'$ and to create squeezing by a factor $e^{-2t'}$ it will take a time $2t'$, i.e. to implement $U_{\rm tms}(t')$ we need a time $t = 2t'$.

Simulation of unitary operators and state engineering

Until now we have focused on the regime of infinitesimal times in order to clarify which *unitary evolutions* we can simulate by means of the given interaction. We found that we can do so – more or less efficiently – for all evolutions governed by Hamiltonians of the form (6.8), but no more. This leaves open the question which *unitary operations* can in general, i.e., for finite times, be realized with a given interaction and local rotations.

As we show in the following, any interaction described by some Hamiltonian H where $s_1 \neq |s_2|$ together with local rotations is sufficient to realize *any unitary operation* of the form $\exp(iG)$, where G is a quadratic expression in the operators X_k, P_k. That is, any Gaussian unitary transformation of the two modes can be obtained. This implies, that any desired pure Gaussian state can be "engineered" starting from any given (pure Gaussian) input state.

As we show below, any $U = \exp(-iG)$ can be decomposed as

$$\begin{aligned} U &= (V_5 \otimes W_5)\, U_{\rm bs}(t_5)\, (V_4 \otimes W_4) \times \\ &\quad \times U_{\rm tms}(t_4)\, (V_3 \otimes W_3)\, U_{\rm bs}(t_3)\, (V_2 \otimes W_2)\, U_{\rm tms}(t_2) \times \\ &\quad \times (V_1 \otimes W_1)\, U_{\rm bs}(t_1)\, (V_0 \otimes W_0)\,, \end{aligned} \tag{6.32}$$

where all $(V_i \otimes W_i)$ are local rotations, $U_{\rm bs}(t_i)$ is a beam-splitter and $U_{\rm tms}(t_i)$ a two-mode squeezing operation as defined in Eqs. (6.30) and (6.31). Since all Hamiltonians with $s_1 \neq |s_2|$ can be used to simulate beam-splitters and two-mode squeezers one can reach any desired unitary U and therefore also any desired Gaussian state.

To show that any unitary $U = \exp(-iG)$ where G is quadratic expression in the operators X_k, P_k can be decomposed as given in (6.32) we will proceed in three steps:

(i) As shown in [122, 127] any such U can be decomposed into a sequence of one passive transformation, single mode squeezing and another passive transformation. That is to say the symplectic matrix S corresponding to the unitary transformation U can be decomposed as $S = OD\widetilde{O}$ where $O, \widetilde{O}$ are orthogonal, symplectic and, therefore, passive transformations and the diagonal matrix $D = \mathrm{diag}(e^{\alpha+\beta}, e^{-(\alpha+\beta)}, e^{\alpha-\beta}, e^{-(\alpha-\beta)})$ amounts to local squeezing. Note that this is basically a singular value decomposition of S.

(ii) Passive transformations contain essentially beam-splitter transformations and local rotations and it is well known from quantum optics that any such transformation on two modes can be decomposed into a sequence of a pair of local rotations, one beam-splitter operation and another pair of local rotations. Thus, a unitary U_O corresponding to a orthogonal symplectic transformation O can be decomposed as $U_O = (V \otimes W) U_{\rm bs}(t_0) (\widetilde{V} \otimes \widetilde{W})$ where $U_{\rm bs}(t)$ is defined in (6.30).

(iii) What is left to be shown, is how to attain single mode squeezing. For this we split the matrix D into two components,

$$D = \mathrm{diag}(e^{\alpha}, e^{-\alpha}, e^{\alpha}, e^{-\alpha}) \mathrm{diag}(e^{\beta}, e^{-\beta}, e^{-\beta}, e^{\beta})$$

and show how each of them can be attained by means of beam-splitters and two-mode squeezing. Let us denote by $\overline{U}_{\rm bs}(t)$ and $\overline{U}_{\rm tms}(t)$ the variants of beam splitter and two-mode squeezing operators which are attained from (6.30) and (6.31) respectively by locally rotating $X_2 \to P_2, P_2 \to -X_2$. Then it can be easily shown that the sequence $\overline{U}_{\rm bs}(-\pi/4) U_{\rm tms}(\alpha) \overline{U}_{\rm bs}(\pi/4)$ generates a symplectic transformation $\mathrm{diag}(e^{\alpha}, e^{-\alpha}, e^{\alpha}, e^{-\alpha})$ and $U_{\rm bs}(-\pi/4) \overline{U}_{\rm tms}(\beta)$ $\times U_{\rm bs}(\pi/4)$ correspondingly $\mathrm{diag}(e^{\beta}, e^{-\beta}, e^{-\beta}, e^{\beta})$.

Collecting things together and ordering all passive components as in (ii), i.e. such that it contains only one application of a beam-splitter operation, decomposition (6.32) follows immediately.

6.3 Entanglement and Squeezing

In the previous section we characterized the time-evolutions on the joint system which can be realized using a given interaction Hamiltonian of the form (6.1) and the control operations provided by Eq. (6.2). In this section we determine the optimal way to use these tools for the generation of entanglement and squeezing between the two subsystems in both, the infinitesimal and the finite regime.

Our derivations make extensive use of the formalism of Gaussian states and operations. The necessary concepts and notation are introduced in section 6.3 and then put to work in the cases of infinitesimal (6.3) and finite (6.3) times.

State Transformations and Measures of Entanglement and Squeezing

We show here how Gaussian states evolve under a general quadratic Hamiltonian and then introduce some entanglement and squeezing measures for Gaussian states.

State Transformation

A quadratic interaction Hamiltonian (6.1) characterized by a matrix K as in Eq. (6.8) generates a linear time-evolution of the X and P operators. Solving the Heisenberg equations for $\vec{R} = (X_1, P_1, X_2, P_2)^T$ we find

$$\vec{R}(t) = e^{Mt}\vec{R}(0) = S(t)\vec{R}(0), \tag{6.33}$$

where

$$M = \begin{pmatrix} 0 & L \\ \tilde{L} & 0 \end{pmatrix}, \tag{6.34}$$

with

$$L = \begin{pmatrix} c & b \\ -a & -d \end{pmatrix} = J^T K, \text{ and } \tilde{L} = -JL^T J^T = J^T K^T, \tag{6.35}$$

where

$$J = \begin{pmatrix} 0 & -1 \\ 1 & 0 \end{pmatrix}. \tag{6.36}$$

Note that for $0 \neq -\det(L) =: \alpha$ we have $\tilde{L} = \alpha L^{-1}$. Using the fact that $M^2 = \alpha \mathbb{1}$ we can easily re-express Eq. (6.33) and find

$$S(t) = \cosh(\sqrt{\alpha}t)\mathbb{1} + \sinh(\sqrt{\alpha}t)/\sqrt{\alpha}M. \tag{6.37}$$

Thus, every evolution generated by a Hamiltonian (6.1) is uniquely characterized by a symplectic transformation $S(t)$ of the form (6.37). Note that any such transformation can be written in its *standard form*

$$S(t) = \cosh(\sqrt{\alpha}t)(O_1 \oplus O_2) \begin{pmatrix} 1 & 0 & h_1 & 0 \\ 0 & 1 & 0 & -h_2 \\ h_2 & 0 & 1 & 0 \\ 0 & -h_1 & 0 & 1 \end{pmatrix} (O_1 \oplus O_2)^T, \tag{6.38}$$

where $O_1, O_2 \in SO(2, \mathbb{R})$ perform the restricted singular value decomposition of L, and $h_k = \tanh(\sqrt{\alpha}t)/\sqrt{\alpha}s_k$, where s_k are the restricted singular values of L, which clearly coincide with those of K. In particular the Hamiltonian $H_0 = X_1X_2$ of Eq. (6.3) generates an time-evolution described by the symplectic matrix

$$S_0(t) = \begin{pmatrix} 1 & 0 & 0 & 0 \\ 0 & 1 & -t & 0 \\ 0 & 0 & 1 & 0 \\ -t & 0 & 0 & 1 \end{pmatrix}, \tag{6.39}$$

i.e. $\alpha = 0, (s_1, s_2) = (1, 0)$, and $O_1 = J$ [see (6.36)] and $O_2 = -\mathbb{1}$.

In the Schrödinger picture a linear time-evolution as in (6.33) transforms the CM γ as

$$\gamma(t) = S(t)\gamma S(t)^T. \tag{6.40}$$

In the next subsection we address the case of very short interaction time, i.e., we consider $S(\delta t)$ for an infinitesimally short time step δt. In this case we obtain

$$S(\delta t) = \mathbb{1} + \delta t M, \tag{6.41}$$

and the correlation matrix $\gamma(t)$ transforms to first order as

$$\gamma(t + \delta t) = \gamma(t) + \delta t[M\gamma(t) + \gamma(t)M^T]. \tag{6.42}$$

Let us in the following write the 4×4 CM of the two-mode Gaussian state as a block matrix as in Eq. (6.6) with 2×2 matrices A, B, C. Then A refers to the first system and is the CM belonging to the reduced density operators of the system 1. Note that for all CMs $\det(\gamma) \geq 1$, and equality holds if and only if (iff) the state is pure. Since our initial state is pure and we consider unitary transformations (and, later, complete Gaussian measurements) this implies that we are only concerned with pure states at all times.

Entanglement and Squeezing of Gaussian States

As one can see in equation (6.7), the single parameter which characterizes the non-local properties of a pure state is the two-mode squeezing parameter r. This automatically implies that any monotonic function of this parameter can be used to quantify the entanglement of pure Gaussian two-mode states and we are free to choose the most convenient measure. Here however we are interested in maximizing the *rate* at which entanglement changes and it is not clear from the outset, that any choice will yield the same result. To see that this is in deed the case, note that the canonical measure of entanglement for pure states is the entropy of entanglement E, i.e., the von Neumann entropy of the reduced state. For pure Gaussian states it is $E(|\psi\rangle) = \cosh(r)^2 \log[\cosh(r)^2] - \sinh(r)^2 \log[\sinh(r)^2]$, where $r = [\mathrm{acosh}(\sqrt{\det A})]/2$, with A the CM of the reduced state [128]. Consider now any function $f(r)$ such that $E(f)$ is a monotonic function of f. The maximization of the rate of E with respect to the evolution is then equivalent to the maximization of the rate of f. The reason for this is that $\max_H \left(\frac{dE}{dt}\right)\big|_{t_0} = \max_H[\left(\frac{dE}{df}\right)\Big|_{t_0} \left(\frac{df}{dt}\right)\big|_{t_0}] = \left(\frac{dE}{df}\right)\Big|_{t_0} \max_H \left(\frac{df}{dt}\right)\big|_{t_0}$. Since E is a monotonic function we have that $\left(\frac{dE}{df}\right)\Big|_{t_0} > 0$, which implies that maximizing $\left(\frac{dE}{dt}\right)\big|_{t_0}$ with respect to the evolution is equivalent to maximize $\left(\frac{df}{dt}\right)\big|_{t_0}$.

One such quantity is $E_p(\gamma) = \det A = \cosh(r)^2$, the determinant of the CM corresponding to the reduced density. It is related to the *purity* of the reduced density matrix. In general the purity is not a measure of entanglement, but for pure states, $|\psi\rangle$ the purity $\mathrm{tr}_2(\rho_{red}^2)$, where $\rho_{red} = \mathrm{tr}_1(|\psi\rangle\langle\psi|)$, decreases the more entangled $|\psi\rangle$ is. Therefore we may use, e.g., the inverse square of purity, i.e., $\mathcal{P}(|\psi\rangle) = [\mathrm{tr}(\rho_{\mathrm{red}}^2)]^{-2}$ to quantify how entangled a given pure state is. For a general two–mode Gaussian state with CM γ as in Eq. (6.6) tracing over the second system yields a reduced density matrix which is Gaussian with CM $\gamma_{\mathrm{red}} = A$. The purity of the reduced state is therefore given by $\det(A)$ as [129] $\mathcal{P}(\gamma) = \{\mathrm{tr}[\rho_{\mathrm{red}}(\gamma)^2]\}^{-2} = \det A$. As mentioned before, the determinant of a CM is one, iff the state is pure, which implies that $E_p(\gamma) = 1$ iff the state is not entangled, i.e., iff $r = 0$.

For the last part of this section another measure of entanglement, namely the *negativity* $\mathcal{N}$ introduced in Ref. [124] is most convenient to use. For a 1×1 Gaussian state with CM γ the negativity is given by the inverse of the smallest symplectic eigenvalue of the partially transposed CM $\tilde{\gamma} = \Lambda\gamma\Lambda$, which can easily be calculated [124] as

$$\mathcal{N}(\gamma) = \left[\min\{\mathrm{sing.val.}\left(J_2^T\tilde{\gamma}J_2\tilde{\gamma}\right)\}\right]^{-1/2}. \tag{6.43}$$

Here Λ is the 4×4 diagonal matrix $\mathrm{diag}(1,1,1,-1)$ (which implements partial

transposition, see [98]) and $J_2 = J \oplus J$ is the symplectic matrix for two modes.

The other interesting quantity that characterizes Gaussian states besides the entanglement is the *squeezing* inherent in the state, i.e., by how much the variance of some (passive-linearly transformed) quadrature is reduced below the standard quantum limit. The reduced variance is given by the smallest eigenvalue $\lambda_{\min}(\gamma)$ of γ and we define the squeezing of a state with CM γ as the inverse of $\lambda_{\min}(\gamma)$

$$\mathcal{S}(\gamma) = \min\{\mathrm{eig}(\gamma)\}^{-1} = [\lambda_{\min}(\gamma)]^{-1}. \tag{6.44}$$

In a situation like the one we consider here where only orthogonal operations are freely available, the squeezing of a state represents a valuable resource which can be used, e.g., for the creation of entanglement [119] and which should be created as efficiently as possible.

Optimal Entanglement/Squeezing Rates

The goal of this section is to determine the optimal strategy for the generation of entanglement [squeezing] in an (infinitesimally) small time step δt. That is, given a pure Gaussian state ρ with CM γ and an interaction Hamiltonian H as in Eq. (6.1) we look for the best choice of the local rotations $V \otimes W$ such that $e^{-iH\delta t}(V \otimes W)\rho(V \otimes W)^\dagger e^{iH\delta t}$ is as entangled [squeezed] as possible. Stating this problem mathematically: We maximize the *entanglement [squeezing] rate*, that is the time-derivative of the chosen entanglement [squeezing] measures E [$\mathcal{S}$] under the time-evolutions obtainable in the given setting.

Maximizing the Entanglement Rate

As measure of entanglement we use E_0, where $E_0(\gamma)$ is the two-mode squeezing parameter r defined in (6.7). The entanglement rate is then simply given by

$$\Gamma_E = \left.\frac{dE_0}{dt}\right|_{t=0} = \lim_{\delta t \to 0} \frac{r(\delta t) - r}{\delta t}, \tag{6.45}$$

where $r \equiv r(0)$ is the entanglement of the initial CM γ.

In order to determine Γ_E we use, following Eq. (6.13), the formula $\Gamma_{E_p} = \sinh(2r)\Gamma_E = 2\sqrt{-\det(A)\det(C)}\Gamma_E$, where Γ_{E_p} denotes the entanglement rate corresponding to the purity-related measure E_p.

Let H as in Eq. (6.8) be the given Hamiltonian. It generates an evolution given by the symplectic transformation $\bar{S}(\delta t)$, which we write in its standard form (6.38) as $\bar{S}(\delta t) := (\bar{O}_1 \oplus \bar{O}_2)S(\delta t)(\bar{O}_1 \oplus \bar{O}_2)^T$. Since local operations

cannot increase the entanglement the only way in which the local control operations may help is to rotate the state by $\tilde{O}_1 \oplus \tilde{O}_2$ before applying H. Thus the best strategy yields a $\gamma(\delta t)$ that can be written as

$$\gamma(\delta t) = S(\delta t)(O_1 \oplus O_2)\gamma(O_1 \oplus O_2)^T S(\delta t)^T, \tag{6.46}$$

where we defined $O_i := \bar{O}_i^T \tilde{O}_i$ and omitted the irrelevant final local rotations coming from $\bar{S}(\delta t)$. Writing $\gamma(\delta t)$ in the form (6.6) and using Eq. (6.42) it is straight forward to determine the CM corresponding to the reduced state,

$$A(\delta t) = O_1 A O_1^T + \delta t(L_0 O_2 C^T O_1^T + \text{H.c.}), \tag{6.47}$$

where $L_0 = \text{diag}(s_2, -s_1)$ is determined by the Hamiltonian H, cf. Eq. (6.38) and Eq. (6.34). One quickly sees that

$$\det[A(\delta t)] = \det(A)[1 + 2\delta t \,\text{tr}(L_0 O_2 C^T A^{-1} O_1^T)],$$

where we used the simple relation for 2×2 matrices: $\det(X + \delta t Y) = \det(X)[1 + \delta t \,\text{tr}(X^{-1}Y)] + o(\delta t^2)$ and the fact that A is symmetric and invertible.

For the entanglement rate corresponding to E_p we obtain

$$\Gamma_{E_p} = 2 \det(A) \text{tr}(L_0 O_2 C^T A^{-1} O_1^T).$$

As mentioned before we can from this easily determine the rate Γ_E corresponding to the two-mode squeezing parameter namely we have

$$\Gamma_E = \sqrt{\frac{\det(A)}{-\det(C)}} \text{tr}(L_0 O_2 C^T A^{-1} O_1^T) = \text{tr}(L_0 O_2 Y O_1^T), \tag{6.48}$$

where we have defined $Y := \sqrt{\det(A)/[-\det(C)]} C^T A^{-1}$.

Our aim is to maximize this expression with respect to the special orthogonal matrices O_1 and O_2. Note that $\det Y = -1$, which can be easily verified using Eq. (6.7). Therefore Y has the restricted singular values $e^l, -e^{-l}, l \geq 0$. Using that L_0 is diagonal it is straight forward to verify that the maximum of Eq. (6.48) is achieved when choosing O_1, O_2 such that they diagonalize Y such that $O_2 Y O_1^T = \text{diag}(e^l, -e^{-l})$. Then the optimal choice for $\tilde{O}_i$ is

$$\tilde{O}_{i,\text{opt}} = \bar{O}_i O_i, \tag{6.49}$$

with $\bar{O}_i$ given by $\bar{S}(\delta t)$. The best state to let H act on is thus $\gamma_{\text{opt}} = (\tilde{O}_{1,\text{opt}} \oplus \tilde{O}_{2,\text{opt}})\gamma(\tilde{O}_{1,\text{opt}} \oplus \tilde{O}_{2,\text{opt}})^T$. Note that l which determines the singular values of Y can be easily determined by Eq. (6.15).

In summary, given an interaction Hamiltonian H corresponding to a matrix K and an initial state with CM γ the optimal state preparation by local rotations (before letting H act) can be understood as a two-step procedure. First transform γ locally such that $C^T A^{-1}$ is diagonal [restricted singular value decomposition, cf. Eq. (6.21)]. If K was already in its restricted singular value decomposition, we are done. Otherwise the second step of the state preparation can be viewed (in the Heisenberg picture) as the restricted singular value decomposition of K. Then the optimal entanglement rate (entanglement is measured by E_0) is given by Eq. (6.14) in terms of the singular values s_k of the Hamiltonian matrix K and the local squeezing parameter l of the given state γ.

In the Fig. 6.2 we compare the entanglement rates and the entanglement obtained for different strategies using the "natural Hamiltonian" H_0. As initial state we consider the product of the vacuum state in the first system and the squeezed vacuum in the second system, i.e.,

$$\gamma_{\text{in}} = \mathbb{1}_2 \oplus \begin{pmatrix} e^{-r} & 0 \\ 0 & e^{r} \end{pmatrix}, \tag{6.50}$$

with squeezing parameter $r = 2.5$. We compare the strategy in which the rate of entanglement creation is optimized at each time to two simpler ones, namely to just apply the natural Hamiltonian H_0 or to simulate the two-mode squeezing Hamiltonian $H_{\text{tms}} = X_1 X_2 - P_1 P_2$ using the optimal scheme of Sec. 6.2. The rate-optimization strategy leads in fact to combination of the other two: one applies first the natural Hamiltonian for a finite time and then (when the "local squeezing" l has all been converted to two-mode squeezing) one simulates H_{tms}. Having initially local squeezing available clearly helps with entanglement generation: for an initial unsqueezed state the optimal rate is constant $\Gamma_E = 1$.

Fig. 6.2b shows that the optimization strategy can lead to noticeably more entanglement in the resulting state after finite time: when the entanglement rate is optimized at each point, more entanglement is produced than, e.g., with the interactions H_0 or H_{tms}. However, optimizing the rate is in general not the best strategy for the creation of entanglement, see Fig. 6.3.

Maximizing the squeezing rate

As in the previous section we are given an interaction Hamiltonian of the form (6.1), an initial Gaussian state with CM γ, and we consider the case of infinitesimal interactions. Our goal is here to determine for each H and γ the strategy which maximizes the squeezing rate. We measure squeezing

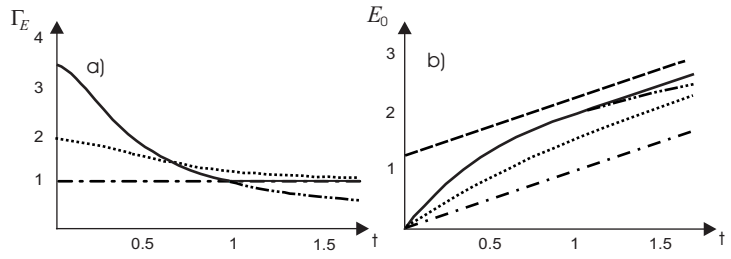

Figure 6.2: (a) The entanglement rate obtained for the squeezed state $\gamma_{\rm in}$ (6.50) as initial state and various strategies. The solid line represents the optimal-rate strategy derived in this section; the dotted line represents the rate obtained by simulating the two-mode squeezing Hamiltonian $H_{\rm tms}$; the "dot–dot–dashed" line represents the rate obtained for the natural Hamiltonian $H_0 = X_1 X_2$. For the vacuum state as initial state we obtain the constant rate 1 (dashed line) (b) The entanglement created by the different strategies [same styles as in a) for the different scenarios]. The dashed line represents the upper bound Eq. (6.59).

by $Q(\gamma) = \log[\mathcal{S}(\gamma)]$, where $\mathcal{S}$ was defined in Eq. (6.44) as the inverse of the smallest eigenvalue of γ. The rate we are interested in is

$$\begin{aligned} \Gamma_S &= \frac{d}{dt} \log \mathcal{S}[\gamma(t)]\Big|_{t=0} \\ &= \frac{-1}{\lambda_{\min}(\gamma)} \lim_{\delta t \to 0} \frac{\lambda_{\min}[\gamma(\delta t)] - \lambda_{\min}(\gamma)}{\delta t}. \end{aligned} \tag{6.51}$$

Note that we use the logarithm of $\mathcal{S}$ instead of $\mathcal{S}$ for convenience. It simplifies the formulas but since log is a monotonic function maximizing the rate of $\log \mathcal{S}$ implies a maximal rate for $\mathcal{S}$ as well.

After applying the general strategy to the input state with CM γ we obtain $\gamma(\delta t)$ as in Eq. (6.42). Doing first order perturbation theory we find that $\lambda_{\min}[\gamma(\delta t)] = \lambda_{\min}(\gamma) + \delta t \hat{x}^T (M^T \gamma + \gamma M) \hat{x} = \lambda_{\min}[1 + \delta t \hat{x}^T (M^T + M)\hat{x}]$, where $\hat{x}$ is the normalized eigenvector corresponding to the smallest eigenvalue $\lambda_{\min}(\gamma)$ of γ. We obtain for the squeezing rate:

$$\Gamma_S = \frac{-1}{\lambda_{\min}(\gamma)} [\hat{x}^T (M^T + M)\hat{x}], \tag{6.52}$$

which is maximized when $-\hat{x}^T (M^T + M)\hat{x}$ is as large as possible. Note that

$$M^T + M \equiv \begin{pmatrix} 0 & N \\ N^T & 0 \end{pmatrix}, \tag{6.53}$$

where $N = \tilde{L}+L^T = J^T K^T + K^T J$, where J is the $SO(2)$–matrix of Eq. (6.36) and we have used the definitions (6.35) and (6.8). One quickly sees that $N = N^T$. Writing K in its restricted singular value decomposition $K = SK_0R$, where $S, R \in SO(2,\mathbb{R})$ and $K_0 = \mathrm{diag}(s_1, s_2)$ as in Eq. (6.21), and using that R, S commute with J we see that $N = R^T(J^T K_0 + K_0 J)S^T = C_S(H)R^T J^T \sigma_z S^T$, where

$$C_S(H) = s_1 - s_2 \tag{6.54}$$

is the *squeezing capability* of the Hamiltonian H. Note that the matrix $\tilde{O} := R^T J^T \sigma_z S^T$ is orthogonal with $\det(\tilde{O}) = -1$ and that we can obtain any such $\tilde{O}$ choosing $R, S \in SO(2,\mathbb{R})$, i.e., by the local operations applied to the initial state. Using the notation $\hat{x}^T = (\vec{x}_1^T, \vec{x}_2^T)$, where $\vec{x}_1, \vec{x}_2 \in \mathbb{R}^2$, we find $\Gamma_S = 2C_S(H)\vec{x}_1^T \tilde{O}\vec{x}_2 \leq 2C_S(H)\mathrm{max}_{\tilde{O}}|\vec{x}_1^T \tilde{O}\vec{x}_2| = 2C_S(H)\|\vec{x}_1\|\|\vec{x}_2\|$, which gives an upper bound

$$\Gamma_S \leq 2C_S(H)\|\vec{x}_1\|\|\vec{x}_2\|$$

for Γ_S. This maximum can be reached for $\tilde{O}_{\mathrm{opt}}$ such that $(-\tilde{O}_{\mathrm{opt}}\vec{x}_2)||\vec{x}_1$. Given γ (i.e., $\vec{x}_1, \vec{x}_2$) we can calculate $\tilde{O}_{\mathrm{opt}}$ with $\det \tilde{O}_{\mathrm{opt}} = -1$ which satisfies this condition. This then determines the optimal choice of $R, S \in SO(2,\mathbb{R})$, i.e. how to transform the initial state with CM γ before letting H act in order to maximize the squeezing rate. One simple choice yielding $\tilde{O} = \tilde{O}_{\mathrm{opt}}$ is $S = \mathbb{1}$, i.e. nothing has to be done on the second system and $R_{\mathrm{opt}} = J^T \sigma_z \tilde{O}_{\mathrm{opt}}^T \in SO(\mathbb{R}, 2)$. Thus, the optimal input state is given by $\gamma_{\mathrm{opt}} = (R_{\mathrm{opt}}^T \oplus \mathbb{1})\gamma(R_{\mathrm{opt}} \oplus \mathbb{1})$.

In summary, we have shown that the maximal squeezing rate is given by Eq. (6.16) as a product of the squeezing capability $C_S(H)$ of the given Hamiltonian and the squeezability $g_S(\gamma)$ of the given state. The optimal CM to let H act on is $\gamma_{\mathrm{opt}} = (R_{\mathrm{opt}}^T \oplus \mathbb{1})\gamma(R_{\mathrm{opt}} \oplus \mathbb{1})$, where

$$R_{\mathrm{opt}} = J^T \sigma_z \tilde{O}^T \tag{6.55}$$

and $-\tilde{O}_{\mathrm{opt}}$ parallelizes $\vec{x}_1$ and $\vec{x}_2$. Note that the fact that $\hat{x}$ is normalized implies that $\Gamma_S \leq C_S(H)$ for any input state. Since we look at the logarithm of the squeezing this implies that $\frac{d\mathcal{S}(\gamma)}{dt} \leq \mathcal{S}(\gamma)C_S(H)$.

Optimal entanglement generation from the vacuum state

In practice, we are interested in creating the largest amount of entanglement when H acts for a *finite* total time t. Optimizing the rate of entanglement creation at each time does lead to a local but not necessarily, as we saw, the global maximum of the entanglement at time t [108].

We now show how to employ the interaction H to create the most entanglement in a given time t. To this end, we make use of the *squeezing* of

γ which was introduced in Eq. (6.44) as the smallest eigenvalue of γ. The squeezing of γ is known [119] to give an upper bound for the amount of entanglement of γ, with $\mathcal{N}(\gamma) \leq \mathcal{S}(\gamma)$. We proceed as follows: First we calculate the strongest squeezing that can be achieved after time t. This also gives an upper bound for the entanglement that can be obtained during this time. Then we point out a strategy that achieves the optimal squeezing and at the same time the strongest entanglement compatible with the given squeezing, thus being optimal on both counts.

The squeezing capability of a symplectic map S, i.e., the factor by which the squeezing in a CM can be increased by the application of S, is given by the inverse square of the smallest singular value of S, since $\mathcal{S}(S\gamma S^T) \leq [\sigma_{\min}(S)]^{-2}\mathcal{S}(\gamma)$. Here and in the following we use that for the smallest singular value of a product AB we have $\sigma_{\min}(AB) \geq \sigma_{\min}(A)\sigma_{\min}(B)$. Now consider the symplectic map $S(t)$ corresponding to the unitary evolution generated by an interaction Hamiltonian H after time t, cf. Eq. (6.37). The singular values of $S(t)$ can easily be calculated analytically. We need them only for small times to first order in t, in which case we find:

$$\sigma_{\pm}[S(t)] = \sqrt{1 \pm \frac{1}{2}(s_1 - s_2)t} + o(t)^2, \tag{6.56}$$

where s_1, s_2 are the restricted singular values of the matrix K [cf. Eq. (6.8)] corresponding to H.

Since $S(t) = S(t/2)S(t/2) = \Pi_{k=1}^{N} S(t/N)$ we see immediately that

$$(\sigma_{\min}[S(t)])^2 \geq e^{-(s_1-s_2)t},$$

which implies that the squeezing capability of $S(t)$ is bounded by $e^{(s_1-s_2)t}$. Now consider a strategy as in Eq. (6.4), alternating the use of H for time t_k with local rotations $V_k \otimes W_k$. Note that the $t_k, k = 1, \ldots, N$, which sum to t, are not assumed to be infinitesimal. The time-evolution effected by this strategy is described by a symplectic map

$$S(t) = \Pi_k \tilde{S}_k, \tag{6.57}$$

where $\tilde{S}_k = O_k S(t_k) O_k'$ and O_k, O_k' are the local rotations corresponding to $V_k \otimes W_k$. Clearly, $\sigma_{\min}[S(t)] \geq \Pi_k e^{-(s_1-s_2)t_k/2} = e^{-(s_1-s_2)t/2}$. Hence $\mathcal{S}[S(t)S(t)^T] \leq e^{(s_1-s_2)t}$, i.e. we have an upper bound to the amount of squeezing that can be produced from an initially unsqueezed pure state by applying H for a total time t.

A strategy to achieve this optimum is the following: we choose the local rotations V_k, W_k as $\pi/2$-rotation in system 1 and $3\pi/2$ in system 2,

the times t_k all equal, and consider the limit $t_k \to 0$. This corresponds to the situation considered in Sec. 6.2 and simulates the Hamiltonian related to $K' = (K + JKJ)/2$. Let $K = O_1 \,\mathrm{diag}(s_1, s_2) O_2$, then we have that $K' = 1/2\, O_1[\mathrm{diag}(s_1, s_2) + \mathrm{diag}(-s_2, -s_1)]O_2$, since rotations commute with J. That is, apart from local rotations the strategy, which simulates the two-mode squeezing Hamiltonian with an efficiency $(s_1 - s_2)/2$, which is the optimal factor according to Eq. (6.27). Letting H_{tms} act for a time $t' = t(s_1 - s_2)/2$ (using up an interaction time t) transforms the vacuum state into the two-mode squeezed state with CM

$$\gamma_{\mathrm{tms}}(t') = \begin{pmatrix} \cosh 2t' \mathbb{1} & \sinh 2t' \sigma_z \\ \sinh 2t' \sigma_z & \cosh 2t' \mathbb{1} \end{pmatrix}. \tag{6.58}$$

which saturates the bounds derived above, since $\mathcal{S}[\gamma_{\mathrm{tms}}(t')] = e^{(s_1 - s_2)t}$.

Now we show that γ_{tms} in Eq. (6.58) is also the most entangled state that can be obtained after letting H act for a total time t. Using Eq. (6.43) for the negativity of a Gaussian state with CM $\gamma = S(t)S(t)^T$ (i.e. an arbitrary strategy applied to the vacuum state) we get

$$\mathcal{N}(\gamma) = [\mathcal{S}(J^T \tilde{\gamma} J \tilde{\gamma})]^{-1/2} \leq \mathcal{S}(\tilde{\gamma}) = \mathcal{S}(\gamma) = e^{(s_1 - s_2)t}.$$

Since $\mathcal{N}[\gamma_{\mathrm{tms}}(t')] = e^{(s_1 - s_2)t}$ the simulation of two-mode squeezing is the optimal strategy for both squeezing and entanglement generation. Note that even a rough approximation of the optimal strategy, i.e., a strategy consisting of just two or three steps already yields a marked improvement in generated squeezing and entanglement.

Up till now we have only considered the unitary evolution of the initial state. There are, however, further tools available in current experiments. There might be additional light modes (ancillas) in the vacuum state on which passive linear optical operations (described by orthogonal and symplectic transformations) as well as complete or partial homodyne measurements can be performed. In principle these might help to increase the entanglement in γ, but in the following we show that this is not the case. We consider the following general set-up: consider system with CM γ, ancilla systems in vacuum state i.e., $\gamma_{\mathrm{anc}} = \mathbb{1}$, linear passive interactions (described by a symplectic and orthogonal matrix O) between the system light mode and the ancillas (e.g. beam splitter between light and ancillary modes), such that the whole system is described by the CM $\gamma' = O^T(\gamma \oplus \gamma_{\mathrm{anc}})O$; clearly, $\mathcal{S}(\gamma') = \mathcal{S}(\gamma)$ and now we show that a Gaussian measurement does not increase $\mathcal{S}(\gamma)$: We write γ' as

$$\gamma' = \begin{pmatrix} A' & C' \\ C'^T & B' \end{pmatrix},$$

where the block matrix B' refers to the ancillary modes to be measured. Then the resulting state is described by the CM $\gamma_{\text{out}} = A' - C'B'^{-1}C'^{T}$ [58]. Using the following characterization of the smallest eigenvalues [130] it is straight forward to see that measurement has reduced the squeezing of the state:

$$\begin{aligned}
\mathcal{S}(\gamma_{out}) &= \min_{x\in\mathbb{C}^n}\left\{\frac{x^\dagger(A'-C'B'^{-1}C'^{T})x}{x^\dagger x}\right\}^{-1} \\
&\leq \min_{x}\left\{\frac{x^\dagger(A'-C'B'^{-1}C'^{T})x}{x^\dagger(\mathbb{1}+C'B'^{-2}C'^{T})x}\right\}^{-1} \\
&= \min_{x}\left\{\frac{y^\dagger\gamma' y}{y^\dagger y} : y=\begin{pmatrix} x \\ -B'^{-1}C'^{T}x\end{pmatrix}\right\}^{-1} \\
&\leq \min_{y\in\mathbb{C}^{2n}}\left\{\frac{y^\dagger\gamma' y}{y^\dagger y}\right\} = \mathcal{S}(\gamma') \quad \blacksquare
\end{aligned}$$

Consequently, unsqueezed ancilla systems and Gaussian measurements are of no help in increasing the squeezing or entanglement in a Gaussian state.

The preceding discussion does not completely solve the problem of optimal entanglement generation with a Hamiltonian H, since only one particular initial state (the vacuum) has been considered. If, e.g., the initial state of the light field is squeezed, we have seen in Sec. 6.3 that better rates can be achieved (see Fig. 6.2), which will translate into larger entanglement after finite times. The methods used above easily yield an upper bound for the entanglement that can be obtained from initially squeezed states: Consider an initial product state with squeezing e^{r_1} and e^{r_2} in systems 1 and 2 and let $r_1 \geq r_2$. By the same arguments as above, after H has acted for a time t the squeezing in the final state and the negativity are bounded by $e^{(s_1-s_2)t+r_1}$. We can find a better bound on the achievable entanglement drawing on results from Ref. [119], where it was shown that the negativity of a two-mode CM γ is bounded by $1/\sqrt{\lambda_1\lambda_2}$, where λ_1, λ_2 are the two smallest eigenvalues of the γ. This implies that

$$\mathcal{N}(\gamma_{\text{out}}) \leq e^{(s_1-s_2)t+(r_1+r_2)/2}, \tag{6.59}$$

which yields the dashed curve in Fig. 6.2b. This bound is most probably not tight for $r_k \neq 0$, not even as $t \to \infty$.

One might think that in order to optimize the entanglement after some finite time t it always suffices to optimize the rate at each time as for the case of a vacuum input. For qubit systems this was indeed shown to be true [107]. In contrast, it does not hold for cv systems as the counterexample depicted in Fig. 6.3 shows: We start with a slightly entangled state with

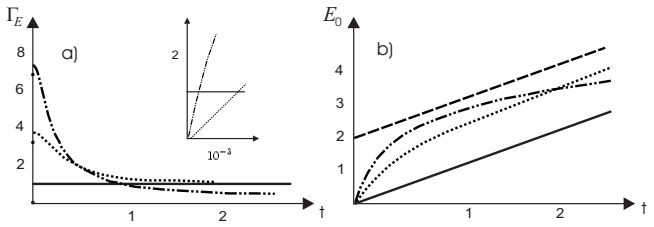

Figure 6.3: (a) The entanglement rate obtained for the initial state $\gamma_{\text{in},2} = S_{r_1,r_2}\gamma_{\text{tms}}(t_0/2)S^T_{r_1,r_2}$, where $S_{r_1,r_2} = \text{diag}(e^{r_1/2}, e^{-r_1/2}, e^{r_2/2}, e^{-r_2/2})$ and $r_1 = r_2 = 2, t_0 = 10^{-3}$. The solid line $\Gamma_E = 1$ is obtained with the strategy that optimizes the entanglement rate at each time; the dotted line represents the rate obtained for optimal simulation of H_{tms}; the "dot–dot–dashed" line represents the rate obtained for the natural Hamiltonian $H_0 = X_1X_2$. The inset shows that one has to "pay" with initial entanglement rates smaller than the optimal value of 1 to reach a state that allows for the large rates later on. (b) The entanglement created by the different strategies [same styles for different scenarios as in a)] and the upper bound Eq. (6.59).

CM $\gamma_{\text{in},2}$ which can be obtained from the two-mode squeezed state $\gamma_{\text{tms}}(t_0/2)$ squeezing both X_1 and X_2 by $r_1 = r_2$. Then the "local squeezing parameter" l is zero and the optimal rate therefore $\Gamma_E = 1$. If t_0 is small and r_1, r_2 large it is possible to sacrifice some entanglement in order to "activate" the local squeezing thus enhancing the rate later on and obtaining significantly more entanglement at time $t \gg t_0$. The difference to the qubit case is related to the fact that in the cv context not all local transformations are available and hence not all equally entangled states are locally equivalent.

We have investigated how a quadratic interaction between two continuous variable systems (as it occurs naturally in certain quantum optical systems) can be optimally used to perform several quantum information tasks when certain simple local control operations (phase space rotations) can be implemented as well. First we have given necessary and sufficient conditions for the simulation of a Hamiltonian evolution given a fixed interaction and fast local rotations. In particular, we have shown that the naturally occurring Hamiltonian Eq. (6.3) allows one to simulate all bilinear Hamiltonians and is in fact of the most versatile kind for this purpose. Moreover we have seen that almost all the Hamiltonians of the form (6.1) (and in particular H_0) allow to generate all symplectic transformations on two modes, i.e., the complete group $SP(2,\mathbb{R})$ can be generated starting from no more than the three Hamiltonians $H_0, H_{\text{loc},1}, H_{\text{loc},2}$.

With these results we have addressed the questions of optimal creation of

entanglement and squeezing for a two–mode Gaussian state using a given interaction of the form (6.1) and local rotations of the form $H_{\mathrm{loc},i} = g(X_i^2+P_i^2)$, both of which are available in current experiments. For the case of small (infinitesimal) interaction times, we have determined the optimal strategy to increase entanglement or squeezing for any input state, i.e, we have derived the maximal entanglement and squeezing rates and determined the strategies which lead to these maxima. For the general case (finite interaction time) we have derived the optimal strategy for the creation of entanglement and squeezing starting with the vacuum state. We have also shown that (in contrast to qubit systems) for continuous variables optimizing the entanglement rate is not necessarily the best way to generate a finite amount of entanglement.

There are several interesting applications of our results for quantum information processing. In particular, we have seen that the beam splitter Hamiltonian $H_{\mathrm{bs}} = X_1P_2 - P_1X_2$ can be simulated with an efficiency factor $1/2$ by H_0. When acting for a time $t = \pi$ the Hamiltonian H_{bs} generates the swap operation between the systems 1 and 2, thus performing the "write-in" and "read-out" operations needed when the atomic ensemble is to be used as a *quantum memory* for the state of the light mode [60].

Another interesting application for atomic ensembles is enabled by the so-called spin-squeezed states [131] which have been prepared experimentally in settings similar to the one described in this chapter [95, 52]. It has been shown that these states allow for a significant increase in the precision of atomic clocks [132]. While the methods presented above show efficient ways to create squeezed atomic states (e.g., by using the interaction to create squeezing or entanglement optimally and then project the atoms into a pure squeezed state by measuring the light), it would also be interesting to find the *optimal* such procedure.

Note that the argument in Sec. 6.3 is easily adapted to similar circumstances. E.g., it was shown in [132] that the interaction between the atoms of a suitably prepared Bose-Einstein–condensate (BEC) can be described by the quadratic Hamiltonian $J_z^2 \approx P^2$, which can be used to drive the BEC into a spin squeezed state. By the same reasoning as in Sec. 6.3 we see that after an interaction time t a squeezing of e^t is the maximum achievable. This shows optimality of the procedure suggested in [132] (which employs effectively the so-called "two-axes counter-twisting" Hamiltonian).

In summary, we have investigated the capabilities of cv interaction Hamiltonians H. We have shown which other Hamiltonians can be simulated with such an H and the available control operations and how to do so efficiently. Then we have derived the optimal entanglement generation rates achievable with this Hamiltonian and given an optimal protocol for the generation of

entanglement between the two modes for finite times.

Chapter 7

Protocols using multiple passes

Quantum networks require an efficient quantum interface between light, which is a natural long distance carrier of quantum information, and atoms, that make a better storage and processing medium. The power of such a device will be intimately connected to its capability of creating high degrees of entanglement in a controlled way, since entanglement represents an all-purpose resource to create conditional dynamics.

Numerous theoretical and experimental works ([60] and references therein) center around the effect of a Kerr interaction between light and atomic ensembles to produce entanglement between continuous light-atom variables. This interspecies entanglement can in turn be converted to atomic spin correlations in form of spin squeezed or spin entangled states between two atomic samples [10] by means of a projection measurement on light. If spontaneous emission is neglected, the degree of squeezing is of the order of $\Delta = 1/(1+\kappa^2)$ where κ is the effective coupling strength between light and atoms, as discussed in section 2.7. Thus, it seems that one can, in principle, produce in this way unlimited atomic squeezing. There are however serious limitations on both, the amount of light atom entanglement as well as the degree of squeezing, which can be achieved from a Kerr interaction. In fact one can express $\kappa^2 = \alpha_0\eta$ where α_0 is the sample's optical (column) density and η is the spontaneous emission probability, c.f. equations (2.40) and (2.43). Thus, decoherence due to spontaneous emission cannot be neglected and a crude estimate for $\eta \ll 1$ leads to an additional contribution, so that $\Delta = 1/(1+\alpha_0\eta) + 2\eta$ ($\Delta = 1$ corresponds to a coherent state). Apparently this expression has a minimum $\Delta_{min} = 2\sqrt{2/\alpha_0}$ corresponding to an optimal spontaneous decay probability $\eta_0 = 1/\sqrt{2\alpha_0}$. In realistic systems the optical density is often limited to values in the range between 1-100, which is true for atomic vapors [13], as well as for cold and trapped atoms. For the optical density of, say, 25, the above estimates lead to the limit on squeezing of the order of $\Delta_{min} \approx 0.5$ (3 dB of

noise reduction) with a single pass QND measurement. The same consideration limits also the amount of light atom entanglement present before the measurement (see Fig.7.1).

But there is still another peculiarity of the Kerr interaction, which limits its performance in creating entanglement: Due to its QND character this interaction conserves certain degrees of freedom, which is reflected in a strict limit on the amount of achievable EPR-type squeezing to $\Delta EPR = 0.5$. Thus, even for an arbitrarily high optical density, the state which originates from a Kerr interaction is never close to a maximally entangled EPR state corresponding to $\Delta EPR \to 0$.

In this Letter we propose experimentally feasible techniques which allow to overcome these limitations and in fact provide an exponential growth in the amount of entanglement and squeezing. Two and three pass protocols have already been proposed in [90, 60]. Taking spontaneous decay into account, we show that passing one and the same pulse of light n times through an atomic ensemble produces an effective optical density of $n\alpha_0$ while the effect of accumulated spontaneous emission noise can be balanced by tuning η to its optimal value for a given number of steps n. Hence, although the coupling strength in a Kerr interaction is directly proportional to the probability of spontaneous decay, this does not pose a fundamental limit on the generation of entanglement or squeezing.

Based on this result we show furthermore that this system provides the realistic possibility to implement the protocols for generating entanglement and squeezing at optimal rates in pure Gaussian continuous variable states, proposed in the preceding chapter. As shown there, in the system under consideration the optimal local operations can be effected simply by $\lambda/4$ plates and mirrors changing the polarization and direction of light propagation in between the passes of the atomic sample. We determine for realistic experimental parameters the optimal spontaneous decay probability for a given number of steps and show thereby that even in the presence of losses the growth of entanglement is still significantly enhanced. In particular, one can in this way engineer a state which is close to an EPR state.

Finally we also suggest a way to convert the entanglement unconditionally into squeezing of the atoms without the use of homodyne detection of light. This method which relies on a certain choice of polarization rotations is as powerful as the QND measurement and it yields in addition a squeezed optical output.

7.1 Single pass

We consider here the setup described in section 2.7, that is a single ensemble interacting with light with no external magnetic field applied. As we want to include atomic decay and absorption losses as they occur in several passes of light through the atomic ensemble, we will have to deal with mixed states of the compound system. It will therefore be convenient to work in the Schrödinger picture. If light and atoms are initially prepared in coherent states, the state will be Gaussian at any time. The state is therefore completely determined by its displacement vector $\vec{d} = \mathrm{tr}\{\vec{R}\rho\}$ and a covariance matrix $\gamma_{i,j} = \mathrm{tr}\{\rho[(\vec{R}_i - \vec{d}_i), (\vec{R}_j - \vec{d}_j)]_+\} \quad (i,\, j = 1, \ldots, 4)$ where $\vec{R} = (X, P, x, p)$ and $[.,.]_+$ denotes the anticommutator. For the given initial states and within the above approximation we have $\vec{d} = \vec{0}$ for all times. Thus, all information about the compound system can be extracted from its covariance matrix.

Taking decay and absorption into account perturbatively, the state after a single pass of a pulse of light through the atomic ensemble is described in terms of input-output relations as

$$\gamma_{out} = \bar{D}(\eta, \epsilon) S(\kappa) \gamma_{in} S(\kappa)^T \bar{D}(\eta, \epsilon) + D(\eta, \epsilon) \gamma_{noise} \tag{7.1}$$

where the scattering matrix

$$S(\kappa) = \begin{pmatrix} 1 & 0 & 0 & \kappa \\ 0 & 1 & 0 & 0 \\ 0 & \kappa & 1 & 0 \\ 0 & 0 & 0 & 1 \end{pmatrix} \tag{7.2}$$

and $D(\eta, \epsilon) = \mathrm{diag}(\eta, \eta, \epsilon, \epsilon)$, $\bar{D}(\eta, \epsilon) = \sqrt{\mathbf{1} - D(\eta, \epsilon)}$, $\gamma_{noise} = \mathrm{diag}(2, 2, 1, 1)$. The output state is a weighted sum of a coherent contribution and a noise component γ_{noise} whose form is due to the fact that the field decay is accompanied by a vacuum noise contribution and the atomic decay both contributes to noise due to the breaking of correlations among the atoms and due to the atoms once decayed being still present in the sample, explaining the factor of 2 in the atomic component of γ_{noise}. Apart from this correction Eq. (7.1) is equivalent to the result derived in [13]. In principle, the noise introduced in atoms increases with the decay of the mean polarization, but this effect is negligible for the example presented (see [133] for a refined model for this interaction using the same formalism).

The coupling constant is given by $\kappa = 2\sqrt{\langle J_x \rangle \langle S_x \rangle}\sigma\Gamma/A\Delta$, the atomic depumping $\eta = N_{ph}\sigma\Gamma^2/A\Delta^2$ and the photonic absorption rate $\epsilon = N_{at}\sigma\Gamma^2/A\Delta^2$ where σ is the cross section on resonance for the probed transition, Γ is the

corresponding spontaneous decay rate, Δ the detuning from resonance and A the cross section of the atomic ensemble illuminated by the pulse. Equation (7.1) is valid for small atomic dephasing and low photon absorption corresponding to $\eta, \epsilon \ll 1$.

A central quantity in this system is the optical density on resonance $\alpha_0 = N_{at}\sigma/A$ which gives the probability for a single photon to get elastically scattered and can be related to the other parameters as $\epsilon = \alpha_0(\Gamma/\Delta)^2$ and $\kappa^2 = \eta\alpha_0$ where we used that initially $\langle J_x\rangle = N_{at}/2$ and $\langle S_x\rangle = N_{ph}/2$. There is an apparent tradeoff between having a large coupling and at the same time low atomic depumping. For a given optical density one can treat ϵ and η as independent parameters tailoring the first by means of the detuning and the last by means of N_{ph}, and there are always optimal values for ϵ and η which maximize the achievable squeezing or entanglement.

We are here especially interested in three quantities characterizing the quantum properties of the state generated: (a) the Gaussian Entanglement of Formation (GEoF) [134], the only available physical Entanglement measure for mixed Gaussian bipartite states, (b) the closely related [56] EPR uncertainty of the combined atom+field system, which indicates how close the state is to a maximally entangled EPR state, given for the present states by $\Delta EPR = \frac{1}{2}[\Delta^2(x_{at} - p_{ph}) + \Delta^2(p_{at} - x_{ph})]$, and finally (c) the atomic (and light) squeezing achievable either by a QND measurement (homodyne detection of light) or by means of a particular disentangling operation at the end of the multi pass protocol.

7.2 Multiple passes

The state created after several passes can be calculated by iterating the map defined by equation (7.1). Note however that the coupling strength depends on the polarizations along x and that these classical variables will decay from pass to pass as $\langle J_x\rangle_{out} = (1-\eta)\langle J_x\rangle_{in}$, $\langle S_x\rangle_{out} = (1-\epsilon)\langle S_x\rangle_{in}$. For the n-th step the remaining coupling strength is hence reduced $\kappa_n = [(1-\eta)(1-\epsilon)]^{n/2}\kappa$. Reflection losses can be taken into account by replacing ϵ by $\zeta = \epsilon + r$ where r is the overall reflectivity of mirrors, cell etc. Equation (7.1) provides then readily a recursion relation

$$\gamma_n = \bar{D}(\eta,\zeta)S(\kappa_n)\gamma_{n-1}S(\kappa_n)^T\bar{D}(\eta,\zeta) + D(\eta,\zeta)\gamma_{noise} \tag{7.3}$$

for the state after n passes which can be solved exactly.

The effect of n consecutive passes is comparable to that of a single pass performed with an n times increased optical density. This is clear from the meaning of α_0 and becomes manifest in the group property $S(\kappa)S(\lambda) =$

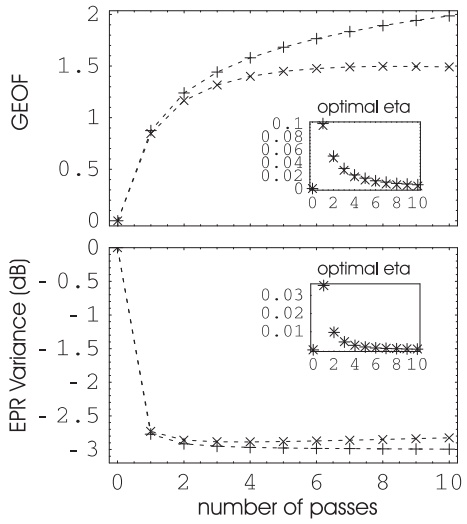

Figure 7.1: GEoF and EPR variance vs. number of passes: For given n both quantities are maximized with respect to η and ζ. The optimal values for η are shown in the inserts. It is always best to have $\zeta = r$ corresponding to $\epsilon \ll \eta$. $+'$es refer to the case $r = 0$, $\times'$es to $r = 2\%$. The optical density is $\alpha_0 = 25$.

$S(\kappa + \lambda)$ of the scattering matrix (7.2). This indicates that the strategy of multiple passes is especially interesting for low optical densities. The dependence of the GEoF and the EPR variance on the number of passes is shown in figure 7.1. In general it can be shown under the assumption of vanishing reflection losses ($r = 0$) that for given optical density and number of steps n there exist optimal choices for η and ϵ such that, taking formally $n \to \infty$, the GEoF tends to infinity. The EPR-variance is limited by 0.5, or 3 dB of squeezing, which is also evident in figure 7.1.

The multipass scheme is capable of improving these features significantly. In particular, applying a unitary operation and its adjoint before and after an interaction changes effectively the type of interaction due to the identity $U^\dagger \exp(-iH)U = \exp(-iU^\dagger HU)$. The transformations which are easy to perform in this system are polarization rotations which change the quadratures as $x \to \cos\phi\, x + \sin\phi\, p$, $p \to \cos\phi\, p - \sin\phi\, x$. In [18] it was shown in a pure state analysis that entanglement and squeezing is created at a maximal rate if one switches from $H \propto p_{at}p_{ph}$ to an interaction $H \propto -x_{at}x_{ph}$ in every second step. The effect of the switching becomes clear if one approximates $\exp(ix_{at}x_{ph}\kappa)\exp(-ip_{at}p_{ph}\kappa) \simeq \exp[-i(p_{at}p_{ph} - x_{at}x_{ph})\kappa + o(\kappa^2)]$. To first order this interaction creates a two-mode squeezed state. In particular

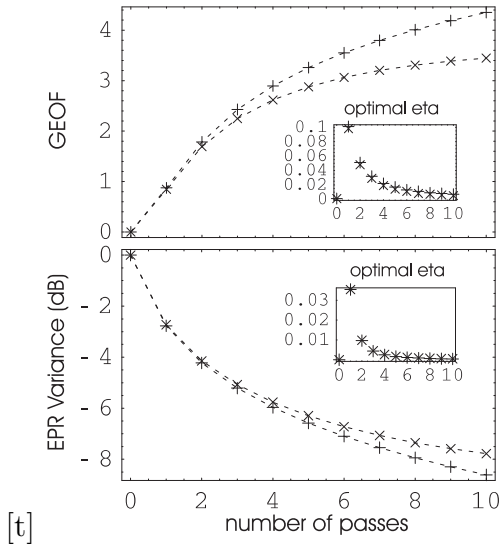

[t]

Figure 7.2: GEoF and EPR variance vs. number of passes including polarization rotations: $+'$es refer to the case $r = 0$, $\times'$es to $r = 2\%$. Optical density $\alpha_0 = 25$.

the growth is linear in n and thus provides an exponential improvement as compared to the scheme without switching. The final state after n passes follows from equation (7.3) by taking the scattering matrix to be $S(\kappa)^T$ - corresponding to an interaction $H \propto -x_{at}x_{ph}$ - in every second step. Figure 7.2 shows how the quantities of interest develop. In comparison with the unswitched case, the GEoF is roughly doubled and the EPR squeezing is no longer limited to 3 dB. In the limit of $n \to \infty$ the resulting state approximates a maximally entangled EPR state which can be used as a resource for continuous variable teleportation. This provides an attractive possibility to establish a quantum memory for light since an unknown quantum state of light can be teleported onto the atoms by performing a joint measurement on the unknown input state and the optical component of the EPR state.

7.3 Disentangling pass and spin squeezing

After multiple passes (with or without switching of polarizations) neither light nor atomic quadratures are squeezed separately. In order to obtain such local squeezing an additional operation has to be carried out. One possibility is to perform a destructive homodyne detection of light, which - in the unswitched scheme - amounts to a QND measurement of the atomic

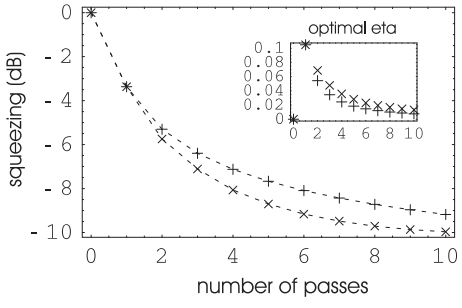

[t]

Figure 7.3: Atomic squeezing after homodyne detection of light: Unswitched scheme (QND measurement) " + " and switched scheme " × ". $\zeta = r = 2\%,\ \alpha_0 = 25$.

p-quadrature and yields a squeezed state of atoms while the light is lost. Performing the same measurement on one half of an EPR state - as it arises in the switched scheme - also leaves the other system in a squeezed state. Figure 7.3 displays the atomic squeezing after a homodyne detection of light for both schemes. The switching provides a small advantage even though the actual interaction has lost its QND character. The tradeoff between squeezing and spontaneous emission noise has also been discussed in [135] for a different type of interaction.

We now show that provided the coupling strength κ can be tuned to a certain value, it is possible to disentangle the state created after several passes by an appropriate last passage of the light pulse through the atomic cloud. The basic mechanism is most clearly seen on the basis of pure states and for the scheme without polarization switching, but it can be easily adapted also for the other case. After n passes the atom and field operators have evolved in the Heisenberg picture as given by $\vec{R}' = S(n\kappa)\vec{R}_{in}$ where $\vec{R}$ is defined as above. By switching to an interaction $H \propto x_{at}x_{ph}$ a single additional pass then yields a state $\vec{R}_{out} = S(-\kappa)^T\vec{R}'$ and thus $p_{at}^{out} = p'_{at} - \kappa x'_{ph} = (1 - n\kappa^2)p_{at}^{in} - \kappa x_{ph}^{in}$. For $0 < n\kappa^2 \leq 1$ this last pass reduces the weight factor of p_{at} indicating the possibility of squeezing but at the same time it feeds light noise into the atomic variance. With initial coherent states one finds $\langle (p_{at}^{out})^2\rangle = [(1 - n\kappa^2)^2 + \kappa^2]/2$. This expression can be minimized with respect to the value of κ, and the optimal value $\kappa_0 = \sqrt{n - 1/2}/n$ leads to a squeezing of $\langle (p_{at}^{out})^2\rangle / \langle (p_{at}^{in})^2\rangle = 1/n - 1/4n^2$ in comparison with the value $1/(n + 1/2)$ achievable in a QND measurement with the same coupling strength κ_0. For large n the difference between these two expressions is negligible. An important aspect of the decoupling scheme is that it is not conditioned on a measurement result, and as a side benefit, light is actually

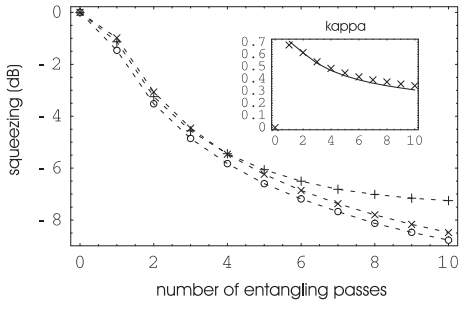

[t]

Figure 7.4: Squeezing of light (" + ") and atomic (" × ") quadrature after n entangling and a single disentangling step. Result from a comparable QND measurement on the atomic system " ∘ ". $\zeta = r = 2\%$, $\alpha_0 = 25$. Insert: Optimal value for coupling $\kappa_{opt} = \alpha_0 \eta_{opt}$ and theoretical magical value $\kappa_0 = \sqrt{n - 1/2}/n$ (solid line). Atomic depumping η decreases with κ while light suffers a constant loss of 2% per pass. Therefore the asymmetry in squeezing of light an atomic variables.

simultaneously squeezed. Figure 7.4 shows the squeezing of both light and atomic quadratures after such a disentangling step as well as the result of a comparable QND measurement with identical coupling κ.

The experimental feasibility of the proposal is illustrated with the following example. Consider an ensemble of cold 87Rb atoms with two ground magnetic states, $F = 1$, $m_F = \pm 1$, forming the atomic two-level spin system. The light is coupled to these states via D1 transition (HWHM natural linewidth 2.5 MHz). Assuming a cylindrical atomic sample with the diameter 100 microns and the length of 500 microns containing 2×10^6 atoms corresponding to a typical dipole trap density of $5 \times 10^{11} cm^{-3}$, a resonant optical density of 25 can be achieved with the atomic dipole crossection $\sigma = 10^{-9} cm^2$. To meet the optimal condition of light absorption being much less than the spontaneous emission probability, $\epsilon \ll \eta$, we choose the light detuning greater than 100 MHz. Then ϵ is reduced to less than 1.5×10^{-3}. Since $\eta/\epsilon = N_{ph}/N_{at}$, we can now adjust the optimal value for η found from theoretical graphs in Fig. 1-4 by choosing the optimal number of photons per pulse. For η in the range of $0.01 - 0.1$ the optimal photon number per pulse is $10^7 - 10^8$. This number of photons is close to optimal for shot noise limited balanced detection. In order to fit the experiment on a table top the physical length of light pulses should not exceed a few meters, since the "tail" of the pulse should clear through the sample before its "head" enters the sample in the next pass. A 3m pulse length corresponds to about 30 MHz Fourier limited bandwidth which fits well with the detuning somewhat

greater than 100 MHz. Switching of the interaction from X-type to P-type for light can be achieved simply by passing the light through a $\lambda/4$ plate in between the passes. For atoms this switching can be achieved by changing the propagation direction of light by 90 degrees.

In summary, we have proposed a quantum interface between light and atoms capable of performing valuable tasks in quantum information processing. By means of several interaction steps and local operations it is possible to efficiently create entangled and squeezed states. In particular one can engineer an EPR state which can act as a resource for a quantum memory for light. Furthermore we showed that without performing any measurement our multipass scheme allows one to create at the same time spin squeezed atoms and quadrature squeezed light.

Appendix A

Effective interaction

A.1 Step up and down components of the dipole operator

We discuss here the decomposition of the dipole operator used in section 2.2. The calculation is done for a $F \to F'$ transition with arbitrary spins F, F'. In the spherical basis, defined by

$$\boldsymbol{\epsilon}_{\pm 1} = \mp(\boldsymbol{\epsilon}_x \pm i\boldsymbol{\epsilon}_y)/\sqrt{2},\ \boldsymbol{\epsilon}_0 = \boldsymbol{\epsilon}_z,$$

the dipole operator can be expanded as

$$\mathbf{d} = \sum_{q=-1}^{+1} d_q \boldsymbol{\epsilon}_q^*.$$

The step up component of $\mathbf{d}$ for a $F \to F'$ transition can thus be expressed as

$$\begin{aligned} \mathbf{d}^+_{F'F} &= \pi^{F'} \mathbf{d} \pi^F \\ &= \sum_{q=-1}^{+1} \sum_{m'=-F'}^{F'} \sum_{m=-F}^{F} \langle F'm'|d_q|Fm\rangle |F'm'\rangle\langle Fm|. \end{aligned}$$

In the convention of Brink and Satchler [136] the Wigner-Eckart theorem states for the matrix elements

$$\langle F'm'|d_q|Fm\rangle = d_{F'} \langle 1q\, Fm|F'm'\rangle$$

where $\langle 1q\, Fm|F'm'\rangle$ is a Clebsch-Gordan coefficient and

$$d_{F'} = -e_0 \langle IJ'F'||r^{\mathrm{el}}||IJF\rangle$$

is the reduced matrix element of the transition and the expression in round brackets is a $3j$-symbol. Altogether we find for

$$\begin{aligned}\boldsymbol{\sigma}^{+}_{F'F} &= \mathbf{d}^{+}_{F'F}/d_{F'} \\ &= \sum_{q}\sum_{m',m}\langle 1q\,Fm|F'm'\rangle|F'm'\rangle\langle Fm|\boldsymbol{\epsilon}^{*}_{q} \\ &= \sqrt{2F'+1}\sum_{q}\sum_{m',m}(-)^{1-F+m'}\begin{pmatrix}1 & F & F'\\ q & m & -m'\end{pmatrix}|F'm'\rangle\langle Fm|\boldsymbol{\epsilon}^{*}_{q}, \end{aligned} \tag{A.1}$$

where the expression in round brackets is a Wigner $3j$-symbol. Occasionally the second form for $\boldsymbol{\sigma}^{+}_{F'F}$ is more convenient. The adjoint is denoted as $\boldsymbol{\sigma}^{-}_{FF'} = (\boldsymbol{\sigma}^{+}_{F'F})^{\dagger}$. A useful property of these operators is

$$\begin{aligned}\boldsymbol{\sigma}^{+}_{F''F}\cdot\boldsymbol{\sigma}^{-}_{FF'} &= \sum_{m'',m'}\left[\sum_{q,m}\langle 1q\,Fm|F''m''\rangle\langle 1q\,Fm|F'm'\rangle\right]|F''m''\rangle\langle F'm'| \\ &= \sum_{m'',m'}\delta_{F',F''}\delta_{m'',m'}|F'm''\rangle\langle F'm'| = \delta_{F',F''}\pi_{F'} \end{aligned} \tag{A.2}$$

where we used the completeness relation of the Clebsch-Gordan coefficients.

A.2 Elimination of spontaneous emission modes

In order to eliminate the modes, which are only populated in spontaneous emission events, we need to evaluate

$$\widetilde{\mathbf{E}}^{-}_{\mathrm{se}}(\mathbf{r}) = \sum_{\lambda}\int_{\bar{b}} d^3k\;\rho\;a^{\dagger}_{\mathbf{k}\lambda}e^{-i(\mathbf{kr}+\omega_c t)}\boldsymbol{\epsilon}_{\mathbf{k}\lambda} \tag{A.3}$$

at the position of each atom. The Equation of motion for modes in $\bar{b}$ is

$$\dot{a}^{\dagger}_{\mathbf{k}\lambda} = i\omega a^{\dagger}_{\mathbf{k}\lambda} + \frac{i\rho d}{\hbar}\sum_{i}\boldsymbol{\epsilon}_{\mathbf{k}\lambda}\cdot\widetilde{\boldsymbol{\sigma}}^{+}_{i}e^{i(\mathbf{kr}_i+\omega_c t)},$$

as follows from (2.7a), and the formal solution to this equation is

$$a^{\dagger}_{\mathbf{k}\lambda}(t) = a^{\dagger}_{\mathbf{k}\lambda}(0)e^{i\omega t} + \frac{i\rho d}{\hbar}\sum_{i}e^{i(\mathbf{kr}_i+\omega t)}\int_0^t dt'\boldsymbol{\epsilon}_{\mathbf{k}\lambda}\cdot\widetilde{\boldsymbol{\sigma}}^{+}_{i}(t')e^{-i(\omega-\omega_c)t'}. \tag{A.4}$$

Inserting this solution into (A.3) and taking the field at position $\mathbf{r}_j$ of the jth atom, one finds

$$\widetilde{\mathbf{E}}^-_{\rm se}(\mathbf{r}_j,t) = \sum_\lambda \int_{\bar{b}} d^3k\, \rho\; a^\dagger_{\mathbf{k}\lambda}(0) e^{-i[\mathbf{k}\mathbf{r}_j-(\omega-\omega_c)t]}\boldsymbol{\epsilon}_{\mathbf{k}\lambda} + \sum_i \int_0^t dt' \sum_\lambda \int_{\bar{b}} d^3k \frac{i\rho^2 d}{\hbar} e^{-i\mathbf{k}(\mathbf{r}_i-\mathbf{r}_j)} e^{i(\omega-\omega_c)(t-t')} \boldsymbol{\epsilon}_{\mathbf{k}\lambda}\boldsymbol{\epsilon}_{\mathbf{k}\lambda}\cdot \widetilde{\boldsymbol{\sigma}}^+_i(t')$$

The first line is the free evolving field, which we will denote by $\mathbf{E}^-_{\rm se,free}$. The second line is the field created by atoms at position $\mathbf{r}_j$. According to assumption (2.1) all terms for $i \neq j$ will have a fast oscillating phase $\exp[-i\mathbf{k}(\mathbf{r}_i-\mathbf{r}_j)]$, such that they will make a negligible contribution. Physically, this amounts to the assumption, that the sample is dilute enough, such that any spontaneously emitted excitation will leave the volume occupied by atoms, before it can get absorbed by a neighboring atom. We thus keep only the term $i=j$, corresponding to the radiation back action of the atom on itself. Moreover, only field modes around ω_c will be populated, and for these modes we assume a flat coupling to atoms. The result is

$$\widetilde{\mathbf{E}}^-_{\rm se}(\mathbf{r}_j,t) = \mathbf{E}^-_{\rm se,free}(\mathbf{r}_j,t) + \frac{i\rho^2 d\omega_c^2}{\hbar c^3} \sum_\lambda \int d\Omega \boldsymbol{\epsilon}_{\mathbf{k}\lambda}\otimes\boldsymbol{\epsilon}_{\mathbf{k}\lambda} \int_0^t dt' \int d\omega e^{i(\omega-\omega_c)(t-t')} \widetilde{\boldsymbol{\sigma}}^+_j(t') \quad \text{(A.5)}$$

In the last line we used the notation $\mathbf{w}\cdot\mathbf{x}\,\mathbf{y}\cdot\mathbf{z} = \mathbf{w}\,\mathbf{x}\otimes\mathbf{y}\,\mathbf{z}$ for the Cartesian tensor product of vectors. Neglecting Lamb shifts, the integral over time and frequencies yields

$$\int_0^t dt' \int d\omega e^{i(\omega-\omega_c)(t-t')} \widetilde{\boldsymbol{\sigma}}^+_j(t') = \pi \widetilde{\boldsymbol{\sigma}}^+_j(t).$$

In the integral over angles in Equ. (A.5) one should bear in mind that it does in principle not enclose a small cone of angle θ around $\mathbf{k}_c$. However, it is easily checked that

$$\sum_\lambda \int_{\bar{b}} d\Omega \boldsymbol{\epsilon}_{\mathbf{k}\lambda}\otimes\boldsymbol{\epsilon}_{\mathbf{k}\lambda} = \frac{8\pi}{3}\mathbb{1} - \mathcal{O}(\theta^2) \simeq \frac{8\pi}{3}\mathbb{1},$$

i.e. the anisotropy introduced by "cutting out" the forward scattering modes enters only in second order of θ, the opening angle for scattering modes, such that we can neglect it. We find for the field at the position of atom j

$$\mathbf{E}^-_{\rm se}(\mathbf{r}_j) = \mathbf{E}^-_{\rm se,free}(\mathbf{r}_j) + \frac{id\omega_c^3}{6\pi\epsilon_0 c^3}\widetilde{\boldsymbol{\sigma}}^+_j, \quad \text{(A.6)}$$

where we used $\rho = \sqrt{\hbar\omega/2\epsilon_0(2\pi)^3}$.

Finally, if we use that - under the very same assumptions used above - the two point correlation function of the vacuum field is given by

$$\langle \mathbf{E}^-_{\mathrm{se,free}}(\mathbf{r}_i,t) \otimes \mathbf{E}^+_{\mathrm{se,free}}(\mathbf{r}_j,t')\rangle \simeq \frac{\omega_c^3\hbar}{6\pi\epsilon_0 c^3}\delta_{i,j}\delta(t-t')\mathbb{1}$$

it is justified to introduce the Langevin operators

$$\mathbf{f}^+_j(t) = \frac{d}{\hbar\sqrt{\gamma}}\mathbf{E}^-_{\mathrm{se,free}}(\mathbf{r}_j,t),$$

where we used the spontaneous emission rate γ defined in (2.13). Combining the last equations we end up with (2.12) and (2.14).

A.3 Decomposition of atomic polarizability operator

In this section we derive the decomposition of the atomic polarizability tensor operator into its scalar, vector and tensor part. Starting point is expression 2.22, $\overleftrightarrow{\alpha} = \sum_{F'}(d^2_{F'}/\hbar\Delta_{F'})\,\boldsymbol{\sigma}^-_{j,FF'}\otimes\boldsymbol{\sigma}^+_{j,F'F}$. First, by means of (A.1) and the adjoint relation we have

$$\boldsymbol{\sigma}^-_{j,FF'}\otimes\boldsymbol{\sigma}^+_{j,F'F} = (2F'+1)\sum_{p,q}\sum_{n,m}\sum_{m'}(-)^{2(F-m')}\begin{pmatrix}1 & F & F'\\ p & n & -m'\end{pmatrix} \times \begin{pmatrix}1 & F & F'\\ q & m & F'\end{pmatrix}|Fn\rangle\langle Fm|\boldsymbol{\epsilon}_p\otimes\boldsymbol{\epsilon}^*_q.$$

This expression can now be split into its operator and tensor part by inserting the identity

$$\sum_{k=0}^{2}\sum_{l=-k}^{k}(2k+1)\begin{pmatrix}1 & 1 & k\\ -q & p & l\end{pmatrix}\begin{pmatrix}1 & 1 & k\\ -\bar{q} & \bar{p} & l\end{pmatrix} = \delta_{p,\bar{p}}\delta_{q,\bar{q}}.$$

such that

$$\boldsymbol{\sigma}^-_{j,FF'}\otimes\boldsymbol{\sigma}^+_{j,F'F} = (2F'+1)(-)^{F-F'}\sum_{k,l}(2k+1)\left[\sum_{\bar{p},\bar{q}}(-)^{\bar{q}}\begin{pmatrix}1 & 1 & k\\ -\bar{q} & \bar{p} & l\end{pmatrix}\boldsymbol{\epsilon}_{\bar{p}}\otimes\boldsymbol{\epsilon}^*_{\bar{q}}\right]$$
$$\times\left[\sum_{n,m}(-)^{F-n}\sum_{q,p,m'}(-)^{F'+2-p-m'-q}\begin{pmatrix}F' & 1 & F\\ -m' & q & m\end{pmatrix}\begin{pmatrix}1 & 1 & k\\ -q & p & l\end{pmatrix}\begin{pmatrix}1 & F' & F\\ -p & m' & -n\end{pmatrix}|Fn\rangle\langle Fm|\right]$$

The expression for the operator part, second line, can be further simplified by means of the identity

$$\sum_{\mu_1,\mu_2,\mu_3} (-)^{l_1+l_2+l_3-\mu_1-\mu_2-\mu_3} \begin{pmatrix} l_2 & l_3 & j_1 \\ -\mu_2 & \mu_3 & m_1 \end{pmatrix} \begin{pmatrix} l_3 & l_1 & j_2 \\ -\mu_3 & \mu_1 & m_2 \end{pmatrix} \begin{pmatrix} l_1 & l_2 & j_3 \\ -\mu_1 & \mu_2 & m_3 \end{pmatrix} = \begin{pmatrix} j_1 & j_2 & j_3 \\ m_1 & m_2 & m_3 \end{pmatrix} \begin{Bmatrix} j_1 & j_2 & j_3 \\ l_1 & l_2 & l_3 \end{Bmatrix}.$$

Changing $3j$-symbols into Clebsch-Gordan coefficients we get

$$\begin{aligned} \boldsymbol{\sigma}^{-}_{j,FF'} \otimes \boldsymbol{\sigma}^{+}_{j,F'F} = (2F'+1) \frac{(-)^{F'-F-1}}{\sqrt{3(2F+1)}} \sum_{k=0}^{2} (2k+1) \begin{Bmatrix} F & k & F \\ 1 & F' & 1 \end{Bmatrix} \\ \times \sum_{l=-k}^{k} \left[\sum_{n,m=-F}^{F} \langle Fmkl|Fn\rangle |Fn\rangle\langle Fm| \right] \left[\sum_{p,q=-1}^{1} \langle 1\bar{p}\, kl|1q\rangle \boldsymbol{\epsilon}_p \otimes \boldsymbol{\epsilon}^*_q \right] \end{aligned} \tag{A.7}$$

The operators in the second line are irreducible tensor operators of rank $0, 1$ and 2. As is well known, they can in turn be related to angular momentum operators such that the whole expression can be written as

$$\boldsymbol{\sigma}^{-}_{j,FF'} \otimes \boldsymbol{\sigma}^{+}_{j,F'F} = \frac{(-)^{F'-F-1}}{\sqrt{3(2F+1)}} \sum_{k} (2k+1) \begin{Bmatrix} F & k & F \\ 1 & F' & 1 \end{Bmatrix} c_k \overleftrightarrow{T}_k \tag{A.8}$$

where

$$c_0 = 1, \quad c_1 = \frac{1}{\sqrt{2F(F+1)}}, \quad c_2 = -\frac{3}{\sqrt{10F(F+1)(2F-1)(2F+3)}}$$

and, in Cartesian coordinates,

$$\begin{aligned} \overleftrightarrow{T}_0 &= \begin{pmatrix} \mathbb{1} & 0 & 0 \\ 0 & \mathbb{1} & 0 \\ 0 & 0 & \mathbb{1} \end{pmatrix} = \overleftrightarrow{\mathbb{1}}, \\ \overleftrightarrow{T}_1 &= i \begin{pmatrix} 0 & -F_z & F_y \\ F_z & 0 & -F_x \\ -F_y & F_x & 0 \end{pmatrix} = i\, \mathbf{F} \times ., \\ \overleftrightarrow{T}_2 &= -\begin{pmatrix} 2F_x^2 - 2\mathbf{F}^2/3 & 2F_xF_y - iF_z & 2F_xF_z + iF_y \\ 2F_yF_x + iF_z & 2F_y^2 - 2\mathbf{F}^2/3 & 2F_yF_z - iF_x \\ 2F_zF_x - iF_y & 2F_zF_y + iF_x & 2F_z^2 - 2\mathbf{F}^2/3. \end{pmatrix} \\ &= -2\mathbf{F} \otimes \mathbf{F} - i\mathbf{F} \times . + 2F(F+1)/3 \overleftrightarrow{\mathbb{1}}. \end{aligned}$$

Equality of expressions (A.7) and (A.8) can be easily verified by comparing matrix elements. If, in addition, we use that

$$d^2_{F'} = |\langle J'IF'||d||JIF\rangle|^2 = (2F+1) \begin{Bmatrix} J' & F' & I \\ F & J & 1 \end{Bmatrix}^2 |\langle J'||d||J\rangle|^2 \tag{A.9}$$

and

$$\frac{1}{\Delta_{F'}} = \frac{1}{\Delta_{F+1}} \frac{\omega_{F+1} - \omega_c}{\omega_{F+1} - \omega_c - (\omega_{F+1} - \omega_{F'})} = \frac{1}{\Delta} \frac{\Delta}{\Delta - \delta_{F'}},$$

where we abbreviated $\Delta = \Delta_{F+1}$ and $\delta_{F'} = \omega_{F+1} - \omega_{F'}$, the overall polarizability can be written as

$$\overleftrightarrow{\alpha} = \frac{|\langle J'||d||J\rangle|^2}{\hbar\Delta} \sum_{k=0}^{2} a_k(\Delta) \overleftrightarrow{T}_k,$$

which is Equ. 2.24. The coefficients are given by

$$a_k(\Delta) = -(-)^F c_k(2k+1)\sqrt{\frac{2F+1}{3}} \left[\sum_{F'} \frac{\Delta(-)^{F'}}{\Delta - \delta_{F'}} (2F'+1) \left\{ \begin{smallmatrix} J' & F' & I \\ F & J & 1 \end{smallmatrix} \right\}^2 \left\{ \begin{smallmatrix} F & k & F \\ 1 & F' & 1 \end{smallmatrix} \right\} \right]. \tag{A.10}$$

In the asymptotic limit of large (blue) detuning, $-\Delta \gg \delta_{F'}$, the sum in square brackets can be simplified by means of

$$\sum_{F'=F-1}^{F+1} (-)^{F'} (2F'+1) \left\{ \begin{smallmatrix} J' & F' & I \\ F & J & 1 \end{smallmatrix} \right\}^2 \left\{ \begin{smallmatrix} F & k & F \\ 1 & F' & 1 \end{smallmatrix} \right\} = (-)^{-(2J+2F+J'+I+k)} \left\{ \begin{smallmatrix} J & I & F \\ F & k & J \end{smallmatrix} \right\} \left\{ \begin{smallmatrix} J & J & k \\ 1 & 1 & J' \end{smallmatrix} \right\}$$

to get

$$\begin{aligned} a_k &= \lim_{\Delta \to -\infty} a_k(\Delta) \\ &= -(-)^{-(2J+F+J'+I+k)} c_k(2k+1) \sqrt{\frac{2F+1}{3}} \left\{ \begin{smallmatrix} J & I & F \\ F & k & J \end{smallmatrix} \right\} \left\{ \begin{smallmatrix} J & J & k \\ 1 & 1 & J' \end{smallmatrix} \right\}. \end{aligned} \tag{A.11}$$

From this expression it is evident that a_2 has to vanish because the triple $\{J, J, k\} = \{1/2, 1/2, 2\}$ does not satisfy the triangle inequality. For the particular case of the cesium ($I = 7/2$) D_2-line at $F = 4 \to F' = 3, 4, 5$ the asymptotic values of the non-vanishing coefficients are

$$a_0 = 1/6, \quad a_1 = 1/48.$$

Bibliography

[1] M. Nielsen and I. Chuang, *Quantum Computation and Qauntum Information* (Cambridge University Press, Cambridge, 2000).

[2] P. Zoller, T. Beth, D. Binosi, R. Blatt, H. Briegel, D. Bruss, T. Calarco, J. I. Cirac, D. Deutsch, J. Eisert, A. Ekert, C. Fabre, N. Gisin, P. Grangiere, M. Grassl, S. Haroche, A. Imamoglu, A. Karlson, J. Kempe, L. Kouwenhoven, S. Kröll, G. Leuchs, M. Lewenstein, D. Loss, N. Lütkenhaus, S. Massar, J. E. Mooij, M. B. Plenio, E. Polzik, S. Popescu, G. Rempe, A. Sergienko, D. Suter, J. Twamley, G. Wendin, R. Werner, A. Winter, J. Wrachtrup, and A. Zeilinger, Eur. Phys. J. **36**, 203 (2005).

[3] P. W. Shor, SIAM J. Comp. **26**, 1484 (1997).

[4] R. P. Feynman, Int. J. Theor. Phys. **21**, 462 (1982).

[5] N. Gisin, G. G. Ribordy, W. Tittel, and H. Zbinden, Rev. Mod. Phys. **74**, 145 (2002).

[6] L.-M. Duan, J. Cirac, M. Lukin, and P. Zoller, Nature **414**, 413 (2001).

[7] H. J. Briegel, W. Dr, J. I. Cirac, and P. Zoller, Phys. Rev. Lett. **81**, 5932 (1998).

[8] J. Cirac, P. Zoller, H. Kimble, and H. Mabuchi, Phys. Rev. Lett. **78**, 3221 (1997).

[9] H. Mabuchi, M. Armen, B. Lev, M. Loncar, J. Vuckovic, H. J. Kimble, J. Preskill, M. Roukes, and A. Scherer, Quant. Inf. Comp. **1**, 7 (2001).

[10] B. Julsgaard, A. Kozhekin, and E. S. Polzik, Nature **413**, 400 (2001).

[11] B. Julsgaard, J. Sherson, J. Cirac, J. Fiurasek, and E. Polzik, Nature **432**, 482 (2004).

[12] W. Happer, Rev. Mod. Phys. **44**, 169 (1972).

[13] L.-M. Duan, J. Cirac, P. Zoller, and E. Polzik, Phys. Rev. Lett. **85**, 5643 (2000).

[14] B. Julsgaard, Ph.D. thesis, University of Aarhus, 2003.

[15] K. Hammerer, E. S. Polzik, and J. I. Cirac, Phys. Rev. A **72**, 052313 (2005).

[16] K. Hammerer, M. M. Wolf, E. S. Polzik, and J. I. Cirac, Phys. Rev. Lett. **94**, 150503 (2005).

[17] C. A. Muschik, K. Hammerer, E. S. Polzik, and J. I. Cirac, quant-ph/0512226.

[18] B. Kraus, K. Hammerer, G. Giedke, and J. I. Cirac, Phys. Rev. A **67**, 42314 (2003).

[19] K. Hammerer, K. Molmer, E. S. Polzik, and J. I. Cirac, Phys. Rev. A **70**, 044304 (2004).

[20] L.-M. Duan, J. Cirac, and P. Zoller, Phys. Rev. A **66**, 23818 (2002).

[21] M. G. Raymer, I. A. Walmsley, J. Mostowski, and B. Sobolewska, Phys. Rev. A **32**, 332 (1985).

[22] K. Blow, R. Loudon, S. Phoenix, and T. Shepherd, Phys. Rev. A **42**, 4102 (1990).

[23] C. Cohen-Tannoudji, in *Proceedings of the International School of Physics Enrico Fermi*, edited by E. Arimondo, W. Phillips, and F. Stumia (North-Holland, Amsterdam, 1992), Vol. CXVIII, p. 99.

[24] E. Inonu and E. Wigner, Proceedings of the National Academy of Science of the United States of America **39**, 510 (1953).

[25] F. Arecchi, H. Thomas, R. Gilmore, and E. Courtens, Phys. Rev. A **6**, 2211 (1972).

[26] T. Holstein and H. Primakoff, Phys. Rev. **58**, 1098 (1940).

[27] J. Geremia, J. Stockton, and H. Mabuchi, Science **304**, 270 (2004).

[28] A. Kuzmich, N. Bigelow, and L. Mandel, Europhys. Lett. **42**, 481 (1998).

[29] P. Grangier, J. Levenson, and J. Poizat, Nature **396**, 537 (1998).

[30] B. Schumaker and C. Caves, Phys. Rev. A **31**, 3093 (1985).

[31] C. Caves and B. Schumaker, Phys. Rev. A **31**, 3068 (1985).

[32] G. Giedke, L.-M. Duan, P. Zoller, and J. Cirac, Quant. Inform. Comp. **1**, 79 (2001).

[33] D. Bouwmeester, J. Pan, K. Mattle, M. Eibl, H. Weinfurter, and A. Zeilinger, Nature **390**, 575 (1997).

[34] D. Fattal, E. Diamanti, K. Inoue, and Y. Yamamoto, Phys. Rev. Lett. **92**, 37904 (2004).

[35] I. Marcikic, H. de Riedmatten, W. Tittel, H. Zbinden, and N. Gisin, Nature **421**, 509 (2003).

[36] Y.-H. Kim, S. Kulik, and Y. Shih, Phys. Rev. Lett. **86**, 1370 (2001).

[37] D. Boschi, S. Branca, F. D. Martini, L. Hardy, and S. Popescu, Phys. Rev. Lett. **80**, 1121 (1998).

[38] R. Ursin, T. Jennewein, M. Aspelmeyer, R. Kaltenbaek, M. Lindenthal, P. Walther, and A. Zeilinger, Nature **430**, 849 (2004).

[39] J.-W. Pan, M. Daniell, S. Gasparoni, G. Weihs, and A. Zeilinger, Phys. Rev. Lett. **86**, 4435 (2001).

[40] A. Furusawa, J. Sorensen, S. Braunstein, C. Fuchs, H. Kimble, and E. Polzik, Science **282**, 706 (1998).

[41] T. Zhang, K. Goh, C. Chou, P. Lodahl, and H. Kimble, Phys. Rev. A **67**, 33802 (2003).

[42] W. Bowen, N. Treps, B. Buchler, R. Schnabel, T. Ralph, H.-A. Bachor, T. Symul, and P. K. Lam, Phys. Rev. A **67**, 32302 (2003).

[43] H. Yonezawa, T. Aoki, and A. Furusawa, Nature **431**, 430 (2004).

[44] N. Takei, H. Yonezawa, T. Aoki, and A. Furusawa, Phys. Rev. Lett. **94**, 220502 (2005).

[45] M. Riebe, H. Haffner, C. Roos, W. Hansel, J. Benhelm, G. Lancaster, T. Korber, C. Becher, F. Schmidt-Kaler, D. James, and R. B. R, Nature **429**, 724 (2004).

[46] M. Barrett, J. Chiaverini, T. Schaetz, J. Britton, W. Itano, J. Jost, E. Knill, C. Langer, D. Leibfried, R. Ozeri, and D. Wineland, Nature **429**, 737 (2004).

[47] S. Braunstein and A. Pati, *Quantum Information with Continuous Variables* (Kluwer, New York, 2003).

[48] M. Holland, M. Collett, D. Walls, and M. Levenson, Phys. Rev. A **42**, 2995 (1990).

[49] J. Poizat, J. Roch, and P. Grangier, Ann. Phys. Fr. **19**, 256 (1994).

[50] L. Vaidman, Phys. Rev. A **49**, 1473 (1994).

[51] S. Braunstein and H. Kimble, Phys. Rev. Lett. **80**, 869 (1998).

[52] A. Kuzmich, L. Mandel, and N. Bigelow, Phys. Rev. Lett. **85**, 1594 (2000).

[53] T. Opartny and J. Fiurasek, Phys. Rev. Lett. **95**, 53602 (2005).

[54] L. Mista and R. Filip, Phys. Rev. A **71**, 32342 (2005).

[55] G. Giedke, B. Kraus, M. Lewenstein, and J. Cirac, Phys. Rev. A **87**, 167904 (2001).

[56] G. Giedke, M. Wolf, O. Krüger, R. Werner, and J. Cirac, Phys. Rev. Lett. **91**, 107901 (2003).

[57] S. Braunstein, H. Kimble, and C. Fuchs, J. Mod. Opt. **47**, 267 (2000).

[58] G. Giedke and J. Cirac, Phys. Rev. A **66**, 32316 (2002).

[59] C. Bennett, G. Brassard, C. Crpeau, R. Jozsa, A. Peres, and W. Wootters, Phys. Rev. Lett. **70**, 1895 (1993).

[60] A. E. Kozhekin, K. Molmer, and E. Polzik, Phys. Rev. A **62**, 33809 (2000).

[61] C. Schori, B. Julsgaard, J. Sørensen, and E. Polzik, Phys. Rev. Lett. **89**, 57903 (2002).

[62] M. Fleischhauer and M. Lukin, Phys. Rev. Lett. **84**, 5094 (2000).

[63] M. Fleischhauer and M. Lukin, Phys. Rev. A **65**, 22314 (2002).

[64] C. Liu, Z. Dutton, C. Behroozi, and L. Hau, Nature **409**, 490 (2001).

[65] M. Bajcsy, A. Zibrov, and M. Lukin, Nature **426**, 638 (2003).

[66] A. Dantan and M. Pinard, Phys. Rev. A **69**, 43810 (2004).

[67] D. Dieks, Phys. Lett. A **92**, 271 (1982).

[68] W. Wootters and W. Zurek, Nature **299**, 802 (1982).

[69] R. Werner, Quantum Information and Quantum Computing, lecture Notes, http://www.imaph.tu-bs.de/qi/qi.html.

[70] S. Popescu, Phys. Rev. Lett. **72**, 797 (1994).

[71] S. Massar and S. Popescu, Phys. Rev. Lett. **74**, 1259 (1995).

[72] R. Derka, V. Buzek, and A. K. Ekert, Phys. Rev. Lett. **80**, 1571 (1998).

[73] D. Bruss, A. Ekert, and C. Macchiavello, Phys. Rev. Lett. **81**, 2598 (1998).

[74] K. Audenaert, C. Fuchs, C. King, and A. Winter, Quantum Inform. Comput. **4**, 1 (2004).

[75] A. Holevo, *Probabilistic and Statistical Aspects of Quantum Theory* (North-Holland, Amsterdam, 1982).

[76] C. Helstrom, *Quantum Detection and Estimation Theory* (Academic, New York, 1976).

[77] H. Yuen and M. Lax, IEEE Trans. Inform. Theory **19**, 740 (1973).

[78] H. Yuen, R. Kennedy, and M. Lax, IEEE Trans. Inform. Theory **21**, 125 (1975).

[79] V. Giovannetti, S. Lloyd, L. Maccone, J. Shapiro, and B. Yen, Phys. Rev. A **70**, 22328 (2004).

[80] P. Davis, *Circulant matrices* (Wiley, New York, 1979).

[81] N. Cerf, O. Krueger, P. Navez, R. Werner, and M. Wolf, Phys. Rev. Lett. **95**, 70501 (2005).

[82] N. Cerf, A. Ipe, and X. Rottenberg, Phys. Rev. Lett. **85**, 1754 (2000).

[83] F. Grosshans and P. Grangier, Phys. Rev. A **64**, 10301 (2001).

[84] C. Caves and K. Wodkiewicz, Phys. Rev. Lett. **93**, 40506 (2004).

[85] S. Braunstein, C. Fuchs, H. Kimble, and P. van Loock, Phys. Rev. A **64**, 22321 (2001).

[86] C. Chou, H. de Riedmatten, D. Felinto, S. Polyakov, S. van Enk, and H. Kimble, Nature **438**, 828 (2005).

[87] T. Chanelire, D. Matsukevich, S. Jenkins, S.-Y. Lan, T. Kennedy, and A. Kuzmich, Nature **438**, 833 (2005).

[88] M. Eisaman, A. Andre, F. Massou, M. Fleischhauer, A. Zibrov, and M. D. Lukin, Nature **438**, 837 (2005).

[89] A. Kuzmich and E. S. Polzik, in *Quantum Infomation with Continuous Variables*, edited by S. Braunstein and A. Pati (Kluwer, Dordrecht, 2003), p. 231.

[90] J. Fiurasek, Phys. Rev. A **68**, 22304 (2003).

[91] J. Sherson, A. Sørensen, J. Fiurasek, K. Molmer, and E. Polzik, quant-ph/0505170.

[92] J. Fiurasek, J. Sherson, T. Opatrny, and E. Polzik, quant-ph/0510099.

[93] A. Parkins, E. Solano, and J. Cirac, quant-ph/0510173.

[94] A. Dantan, J. Cviklinski, M. Pinard, and P. Grangier, quant-ph/0512175.

[95] J. Hald, J. Sørensen, C. Schori, and E. Polzik, Phys. Rev. Lett. **83**, 1319 (1999).

[96] A. Kuzmich and E. Polzik, Phys. Rev. Lett. **85**, 5639 (2000).

[97] L.-M. Duan, G. Giedke, J. Cirac, and P. Zoller, Phys. Rev. Lett. **84**, 2722 (2000).

[98] R. Simon, Phys. Rev. Lett. **84**, 2726 (2000).

[99] R. Werner and M. Wolf, Phys. Rev. Lett. **86**, 3659 (2000).

[100] G. Giedke, B. Kraus, M. Lewenstein, and J. Cirac, Phys. Rev. A **64**, 52303 (2001).

[101] J. Eisert, S. Scheel, and M. Plenio, Phys. Rev. Lett. **89**, 137903 (2002).

[102] J. Fiurasek, Phys. Rev. Lett. **89**, 137904 (2002).

[103] L. Thomsen, S. Mancini, and H. Wiseman, Phys. Rev. A **65**, 61801 (2002).

[104] I. Bouchoule and K. Mølmer, Phys. Rev. A **66**, 43811 (2002).

[105] A. D. Lisi and K. Mølmer, Phys. Rev. A **66**, 52303 (2002).

[106] D. Berry and B. Sanders, Phys. Rev. A **66**, 12313 (2002).

[107] W. Dür, G. Vidal, J. Cirac, N. Linden, and S. Popescu, Phys. Rev. Lett. **87**, 137901 (2001).

[108] B. Kraus and J. Cirac, Phys. Rev. A **63**, 62309 (2001).

[109] P. Zanardi and L. F. C. Zalka, Phys. Rev. A **62**, 30301 (2000).

[110] J. Dodd, M. Nielsen, M. Bremner, and R. Thew, Phys. Rev. A **65**, 40301 (2002).

[111] C. Bennett, A. Harrow, D. Leung, and J. Smolin, IEEE Trans. Inform. Theory **49**, 1895 (2003).

[112] M. Leifer, L. Henderson, and N. Linden, Phys. Rev. A **67**, 12306 (2003).

[113] P. Wocjan, M. Rötteler, D. Janzing, and T. Beth, J. Quant. Inform. Comp. **2**, 133 (2002).

[114] M. Nielsen, M. Bremner, J. Dodd, A. Childs, and C. Dawson, Phys. Rev. A **66**, 22317 (2002).

[115] G. Vidal and J. Cirac, Phys. Rev. A **66**, 22315 (2002).

[116] C. Bennett, J. Cirac, M. Leifer, N. Leung, N. Linden, S. Popescu, and G. Vidal, Phys. Rev. A **66**, 12305 (200).

[117] G. Vidal, K. Hammerer, and J. I. Cirac, Phys. Rev. Lett. **88**, 237902 (2002).

[118] K. Hammerer, G. Vidal, and J. I. Cirac, Phys. Rev. A **66**, 62321 (2002).

[119] M. Wolf, J. Eisert, and M. Plenio, Phys. Rev. Lett. **90**, 47904 (2003).

[120] K. Mølmer, Eur. Phys. J. D **5**, 301 (199).

[121] E. Polzik, Phys. Rev. A **59**, 4202 (1999).

[122] R. Simon, N. Mukunda, and B. Dutta, Phys. Rev. A **49**, 1567 (1994).

[123] S. Lloyd and S. Braunstein, Phys. Rev. Lett. **82**, 1784 (1999).

[124] G. Vidal and R. Werner, Phys. Rev. A **65**, 32314 (2002).

[125] R. Horn and C. Johnson, *Topics in Matrix Analysis* (Cambridge University Press, Camebridge, 1994).

[126] L.-M. Duan, A. Sørensen, J. Cirac, and P. Zoller, Phys. Rev. Lett. **85**, 3991 (2000).

[127] S. Braunstein, Phys. Rev. A **71**, 55801 (2005).

[128] S. van Enk, Phys. Rev. A **60**, 5095 (1999).

[129] H. Scutaru, J. Math. Phys. **39**, 6403 (1998).

[130] R. Horn and C. Johnson, *Matrix Analysis* (Cambridge University Press, Camebridge, 1987).

[131] M. Kitagawa and M. Ueda, Phys. Rev. A **47**, 5138 (1993).

[132] A. Sørensen, L.-M. Duan, J. Cirac, and P. Zoller, Nature **409**, 63 (2001).

[133] L. Madsen and K. Molmer, Phys. Rev. A **70**, 52324 (2004).

[134] M. Wolf, G. Giedke, O. Krüger, R. Werner, and J. Cirac, Phys. Rev. A **69**, 52320 (2004).

[135] A. Andre and M. Lukin, Phys. Rev. A **65**, 53819 (2002).

[136] D. Brink and G. Satchler, *Angular Momentum* (Clarendon Press, Oxford, 1979).